ENCLOSURE 1 TO TXX-94325

CPSES FUEL STORAGE

LICENSING REPORT

Comanche Peak Steam Electric Station (CPSES)

Expansion of Spent Fuel Storage Capacity

Revision 0

December 9, 1994

TABLE OF CONTENTS

LIST OF FIGURES

LIST OF TABLES

LIST OF ACRONYMS/DEFINITIONS

ACI	American Concrete Institute
AISC	American Institute of Steel Construction
ANS	American Nuclear Society
ASME	American Society of Mechanical Engineers
CCW	Component Cooling Water
CPSES	Comanche Peak Steam Electric Station
DBA	Design Basis Accident
DDOF	Dynamic Degrees of Freedom
DOE	Department of Energy
FSAR	Final Safety Analysis Report
High density (1/4)	A storage pattern within the high density racks utilizing administrative controls to position spent fuel in a 1 out of 4 expanded checker board configuration. The racks are free standing and the center to center spacing between cell locations is a nominal 9 inch (the center to center spacing of the spent fuel assemblies is a nominal 18 inch). See Figure 3-2.
High density (2/4)	A storage pattern within the high density racks utilizing administrative controls to position spent fuel in a 2 out of 4 checker board configuration. The racks are free standing and the center to center spacing between cell locations is a nominal 9 inch (the center to center spacing of the spent fuel assemblies is a nominal 18 inch within the same row and a nominal 12.7 inch diagonally). See Figure 3-2.
HEPA	High-efficiency particulate air
HX	Heat Exchanger
k_{eff}	Effective multiplication factor
LOCA	Loss of Coolant Accident
Low density	The licensed racks which have no restrictions on the placement of spent fuel assemblies. Storage locations are a nominal 16 inch center to center and the racks are bolted to pool floor.

LWR	Light Water Reactor
MDA	Minimum Detectable Activity
OBE	Operational Basis Earthquake
OFA	Optimized Fuel Assembly
RMWS	Reactor Makeup Water System
RWST	Refueling Water Storage Tank
Seismic Category I	Those structures, systems, and components, including their foundations and supports, designed to withstand the effects of the Safe Shutdown Earthquake and remain functional
SFP	Spent Fuel Pool
SFP1	Spent Fuel Pool Number 1
SFP2	Spent Fuel Pool Number 2
SRP	Standard Review Plan
SSE	Safe Shutdown Earthquake
SSI	Safe Shutdown Impoundment
SSW	Service Water System
TEDE	Total Effective Dose Equivalent
w/o	Weight percent
ZPA	Zero period acceleration

1.0 INTRODUCTION

Comanche Peak Steam Electric Station (CPSES) is serviced by a common Fuel Building which contains Spent Fuel Pool Number 1 (SFP1) and Spent Fuel Pool Number 2 (SFP2). The total licensed spent fuel storage capacity of CPSES SFP1 and SFP2 is 1116 storage locations. SFP1 is filled to capacity with storage racks providing a total installed capacity of 556 locations. The storage cell spacing is a nominal 16 inch center to center, and no special neutron absorbing material is utilized in the design of these racks. The racks installed in SFP1 have no restrictions on the placement of fuel assemblies and will be referred to as "low density racks" within this report.

SFP2 is designed and licensed to contain storage racks of the same design as those in SFP1 with a design capacity of 560 locations. SFP2 contains no spent fuel racks and has never been used to store spent fuel.

TU Electric plans to install high density racks fabricated by Westinghouse Electric Corporation in SFP2. The low density racks in SFP1 will not be modified. The purpose of the new high density racks in SFP2 is to increase the total amount of licensed spent fuel storage locations in SFP1 and SFP2 from 1116 to 1291. The cell spacing in the high density racks is a nominal 9 inch center to center, and the racks contain no special neutron absorbing material. The spent fuel assemblies will be stored in either a one (1) out of four (4) configuration, referred to in this report as high density (1/4), or a two (2) out of four (4) configuration, referred to in this report as high density (2/4). Actual storage will depend on the discharge burnup and the initial U235 enrichment. Report references to high density racks apply to both the high density (1/4) and the high density (2/4) storage configurations.

This report describes the design, fabrication, and analysis of the high density racks. This report supports the TU Electric request that a License Amendment be issued to CPSES Unit 1 Facility Operating License NPF-87 [Ref. 1] and Unit 2 Facility Operating License NPF-89 [Ref. 2] to include use of high density racks in SFP2 that meet the criteria contained within this report.

1.1 PRESENT FACILITY DESCRIPTION

The present spent fuel storage for CPSES is described in detail in the Final Safety Analysis Report (FSAR) [Ref. 3] in Section 9.1. CPSES is serviced by a common Fuel Building which houses facilities for storage and transfer of new and spent fuel. The Fuel Building is a controlled leakage building designed to seismic Category I requirements. Two pools are provided for CPSES spent fuel storage. Each pool may be used to store fuel from either or both of the CPSES units. The two reinforced concrete pools are stainless-steel lined and are an integral part of the Fuel Building. A separate wet cask pit is provided as a loading area for spent fuel shipping casks. The SFP1, SFP2, and the wet cask pit are connected with a common fuel transfer canal. Connections between the transfer canal and each spent fuel pool (SFP) can be closed using a hinged swing gate. The wet cask pit and sections of the fuel transfer canal can be isolated by using a removable lift gate. (See Figure 1-1).

The designed and licensed storage capacity for spent fuel at CPSES is 1116 fuel assemblies of which 2 spaces may be used for failed fuel. Presently, all spent fuel assemblies are stored in SFP1 in low density racks. As currently installed, CPSES has a storage capacity of 556 spent fuel assemblies in SFP1. SFP1 has no physical or administrative controls to limit use of the available storage locations. SFP2 contains no spent fuel storage racks and has never been utilized to store spent fuel.

SFP1 utilizes water of the same boron concentration as that of the Refueling Water Storage Tank (RWST). Borated makeup water is supplied either from the Boron Recycle system by way of the recycle evaporator feed pumps or from the RWST. Normal makeup water to compensate for evaporation losses is taken from the demineralized water supply. A redundant makeup water source is provided from the reactor makeup system. This system is a seismic Category I system.

The SFP cooling and clean-up system consists of two cooling loops, two purification loops, and one surface skimmer loop. Each cooling loop includes a pump, heat exchanger, and associated piping, valves, and instrumentation. This system is a seismic Category I system.

As currently operated, one SFP cooling water pump takes suction from SFP1 and discharges through the tubes inside of the SFP heat exchangers and back to the pool. The second pump is in standby. Either SFP cooling water pump with either SFP heat exchanger (HX) can be used to cool SFP1 in the event that one pump or HX is out of service.

1.2 PROPOSED MODIFICATION

The existing 556 available spent fuel storage locations in SFP1 provide sufficient storage capacity to meet CPSES storage needs through Unit 1 Refueling Outage 4 in the spring of 1995. Additional storage capacity is required prior to Unit 2 Refueling Outage 2 (Spring 1996).

To increase the storage capacity, TU Electric plans to install free standing high density racks in SFP2. The high density racks will expand the available storage to a total of 1291 locations. Administrative controls will be in place governing the use of the fuel storage locations in SFP2 based on initial enrichment and burnup considerations. This installation of the high density racks will extend the anticipated storage capability for CPSES to approximately the year 2000.

As described later in this report, the SFP cooling and cleanup systems, and heating, ventilation and air conditioning (HVAC) systems will be modified to support the use of high density racks. The fuel building structure, SFP makeup systems, and building radiation monitoring will remain unchanged.

1.3 SUMMARY OF REPORT

This report follows the guidance of the NRC Position Paper entitled, "OT Position for Review and Acceptance of Spent Fuel Storage and Handling Applications," dated April 14, 1978, as amended by the NRC letter dated January 18, 1979 [Ref. 5]. Sections 3.0 through 5.0 of this report are consistent with the section format and content of the NRC OT Position Paper, Sections III through IV. Some analyses have assumed the use of storage configurations which are more conservative than requested as part of the licensing submittal. Details of these conservative and bounding assumptions are provided in discussions of the specific analyses within this report.

Section 1.0 provides an introduction and basic description of the high density rack modification.

Section 2.0 provides a summary description of the features of the existing low density and new high density racks.

Section 3.0 addresses nuclear and thermal-hydraulic concerns of normal storage and handling of spent fuel and postulated accidents with respect to criticality and the ability of the SFP cooling system to maintain sufficient cooling.

Section 4.0 describes the mechanical, material, and structural aspects of the high density racks. It contains information concerning the capability of the high density racks and SFPs to withstand the effects of natural phenomena and other design loading conditions.

Section 5.0 concerns environmental aspects of the use of high density racks relating to thermal and radiological releases from the facility under normal and accident conditions. This section also addresses occupational radiation exposures resulting from the use of the high density racks, generation of radioactive waste, need for expansion, commitment of material and non-material resources, and a cost/benefit assessment.

Section 6.0 provides a listing of references used throughout this report.

1.4 INTERFACES WITH OTHER ORGANIZATIONS

Westinghouse has performed the mechanical design, seismic/structural analysis, thermal-hydraulic analysis, nuclear criticality analysis, related calculations, and the hardware fabrication of the free standing high density racks. TU Electric has performed the balance of the design analyses for the installation and use of the high density racks. TU Electric is responsible for implementation of the modification.

1.5 CONCLUSIONS

On the basis of the information and evaluations presented in this report, TU Electric concludes that the use of high density racks will provide safe fuel storage. The modification is in conformance with NRC requirements. The installation and use of high density racks as described in this report will provide reasonable assurance that the health and safety of the general public will not be endangered.

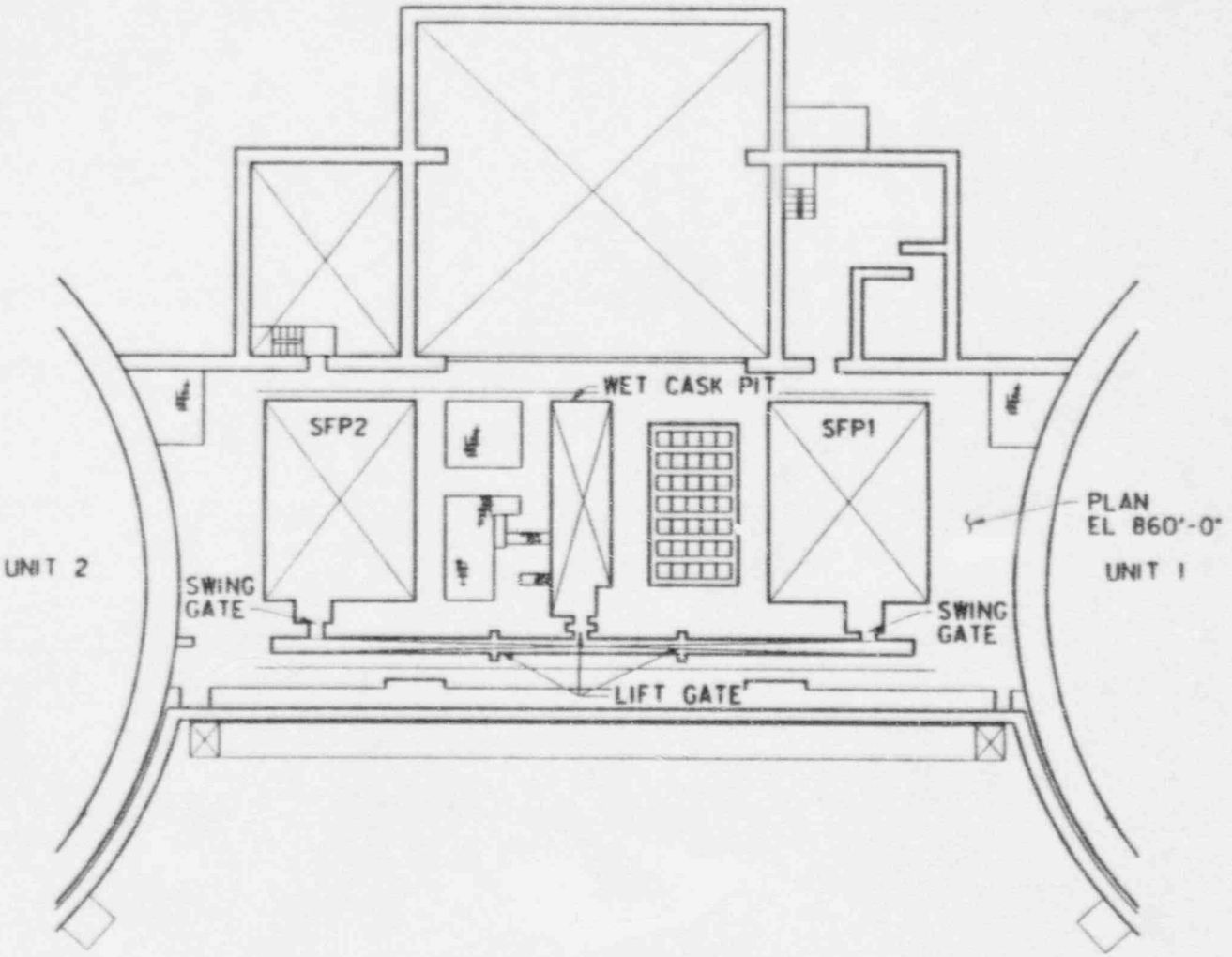

THIS DRAWING CREATED ELECTRONICALLY

TU ELECTRIC CPSES GLEN ROSE, TEXAS
FUEL BUILDING LAYOUT PLAN AT EL 860'-0"
FIGURE 1-1

DS1394036

2.0 SUMMARY OF RACK DESIGN

2.1 EXISTING LOW DENSITY RACK DESIGN

The two SFPs are designed and licensed to contain low density racks that have a total capacity of 1116 spent fuel assemblies with nominal 16 inch center to center spacing. Low density racks are composed of individual vertical cells fastened together to form a module which is firmly bolted to anchors in the floor of the SFP. The low density racks maintain a separation between spent fuel assemblies sufficient to maintain a subcritical array with the effective multiplication factor (k_{eff}) $\leq$ 0.95. Surfaces that come into contact with fuel assemblies are made of annealed austenitic stainless steel which is resistant to corrosion during normal and emergency water quality conditions. Currently, these racks are only installed in SFP1.

Low density racks are designed to withstand shipping, handling, normal operating loads (dead loads of fuel assemblies), as well as Safe Shutdown Earthquake (SSE) loads. These racks meet American Nuclear Society (ANS) Safety Class 3 and American Society of Mechanical Engineers (ASME) Boiler and Pressure Vessel Code Section III, Appendix XVII [Ref. 4] requirements. The low density racks are also designed to meet the seismic Category I requirements of Reg. Guide 1.29, Revision 2, February 1976 [Ref. 6].

The low density racks have adequate energy absorption capabilities to withstand the impact of a dropped spent fuel assembly from a maximum lift height of 3.5 feet above the top of the rack. Cranes capable of carrying loads heavier than a spent fuel assembly are prevented by interlocks or administrative controls, or both, from traveling over the spent fuel storage areas.

The low density racks can withstand an uplift force equal to the uplift force of the fuel handling bridge crane.

SFP1 will continue to utilize the low density racks without any changes.

2.2 HIGH DENSITY RACK DESIGN

2.2.1 HIGH DENSITY RACK DESIGN CRITERIA

TU Electric intends to install high density racks in SFP2. See Figure 2-1 for the high density rack arrangement for SFP2. Some analyses have assumed the installation and use of storage configurations that are more conservative than that shown in Figure 2-1. Details of these conservative and bounding assumptions are provided in discussions of the specific analyses within this report.

A list of design criteria for the high density racks is given below:

1. The high density racks are designed to meet the nuclear requirements of ANS-57.2-1983 [Ref. 7]. The k_{eff} in the SFP is less than or equal to 0.95, including uncertainties.

2. The high density racks are designed to allow coolant flow such that boiling in the water channels between the fuel rods of the assemblies in the rack does not occur.

3. The high density racks are designed to seismic Category I requirements, and are classified as American Nuclear Society (ANS) Safety Class 3 and ASME Code Class 3 Component Support structures. The structural evaluation and seismic analyses are performed using the specified loads and load combinations in Section 4.3.2

4. The high density racks are designed to withstand loads which may result from fuel handling accidents and from the maximum uplift force of the fuel handling bridge crane without deformation that would result in a violation of the criticality acceptance criterion.

5. Each storage position in the high density racks is designed to support and guide the fuel assembly in a manner that will reduce the possibility of application of excessive lateral, axial and bending loads to fuel assemblies during fuel assembly handling and storage.

6. The materials used in construction of the high density racks are compatible with the SFP environment and the fuel assemblies. The high density racks are free standing, self-supporting, and fabricated from ASME SA-479 or SA-240 type 304 material complying with NF-2000, Class 3, Subsection NF, Section III, ASME B & PV Code [Ref.4]. The only exceptions are the leveling screws which are type 17-4 pH stainless steel.

7. The high density racks use two storage configurations based on initial fuel enrichment and burnup considerations. The configurations are defined as follows:

   High density (2/4) - A checkerboard loading pattern where 2 out of 4 available storage locations are used to store spent fuel. See Figure 3-2.

   High density (1/4) - An expanded checkerboard loading pattern where 1 out of 4 available storage locations are used to store spent fuel. See Figure 3-2.

   See Section 3.4.4 for a detailed description and discussion of the use of these fuel storage configurations. Placement of fuel assemblies in the proper location will be subject to administrative controls.

8. Potential locations for gas traps in the high density racks have openings, such as machined flow holes in the base plates of the racks, at every storage location.

2.2.2 DESCRIPTION OF HIGH DENSITY RACKS FOR SFP2

The high density rack arrangement for SFP2 is shown in Figure 2-1. High density rack design data is shown in Table 2-1. The racks are not anchored to the floor nor braced to the pool walls.

The high density racks originally contained Boraflex as a neutron absorber. The Boraflex has been removed, and the wrapper for the Boraflex has been replaced with a spacer plate to satisfy structural requirements.

Placement of fuel in the high density racks in SFP2 is controlled administratively. All new and spent fuel with initial enrichments up to 5.0 w/o may be placed in the high density 1 out of 4 expanded checkerboard arrangement. Fuel which meets the initial enrichment and minimum burnup requirements of Figure 3-3 may be placed in the high density 2 out of 4 checkerboard arrangement. Figure 3-2 illustrates these configurations. Vacant spaces surrounding the assembly will be controlled administratively to prevent inadvertent fuel assembly insertion.

The high density racks consist of stainless steel cells welded together to produce a matrix structure as shown in Figure 2-2. The fuel rack assembly consists of two major sections which are the cell assembly and the base support assembly. Figures 2-3 and 2-4 illustrate these sections.

The major components of the cell assembly are the fuel assembly cell and the spacer plate. The spacer plate is attached to the outside of the cell by spot welding along its length. The spacer plate contributes to the structural integrity and fuel spacing requirements of the high density rack. The cells are welded to the baseplate and to one another to form an integral structure without the use of a supporting grid structure.

The major components of the baseplate assembly are the leveling pad assembly, the leveling pad screw, and the support block. The top of the support block is welded to the high density rack baseplate. The leveling pad assemblies transmit the loads to the pool floor via bridge plates and provide a sliding contact. The leveling pad screws permit the leveling adjustment of the high density rack at the time of installation.

TABLE 2-1

HIGH DENSITY RACK DESIGN DATA

Number of Available Storage Locations	*735
Number of Racks	three 11x14 array six 12x14 array
Center to Center Spacing of Cells	9.0 inch nominal
Cell Inside Width	8.8 inch nominal
Rack Assembly Dimensions	11x14 array- 100"x127"x174" 12x14 array- 109"x127"x174"
Dry Weights Per Rack Assembly	11x14 array- 18,900 lbs. nominal 12x14 array- 20,600 lbs. nominal

* There are 1470 total storage cell locations. The indicated 735 locations assumes 2 out of 4 loading configuration.

FIGURE 2-1

HIGH DENSITY RACK ARRANGEMENT FOR SFP2

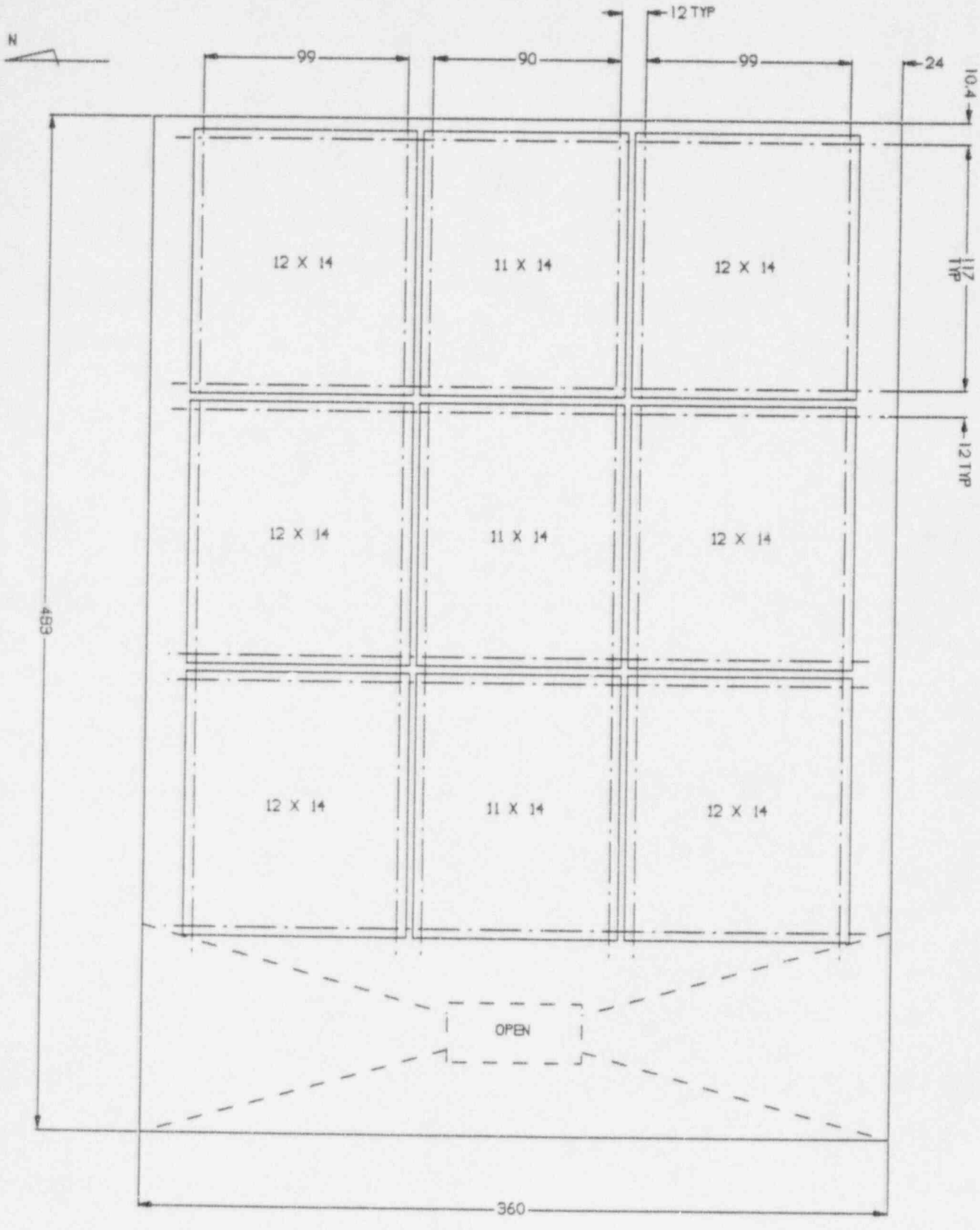

ALL DIMENSIONS ARE NOMINAL INCHES

FIGURE 2-2

HIGH DENSITY RACK

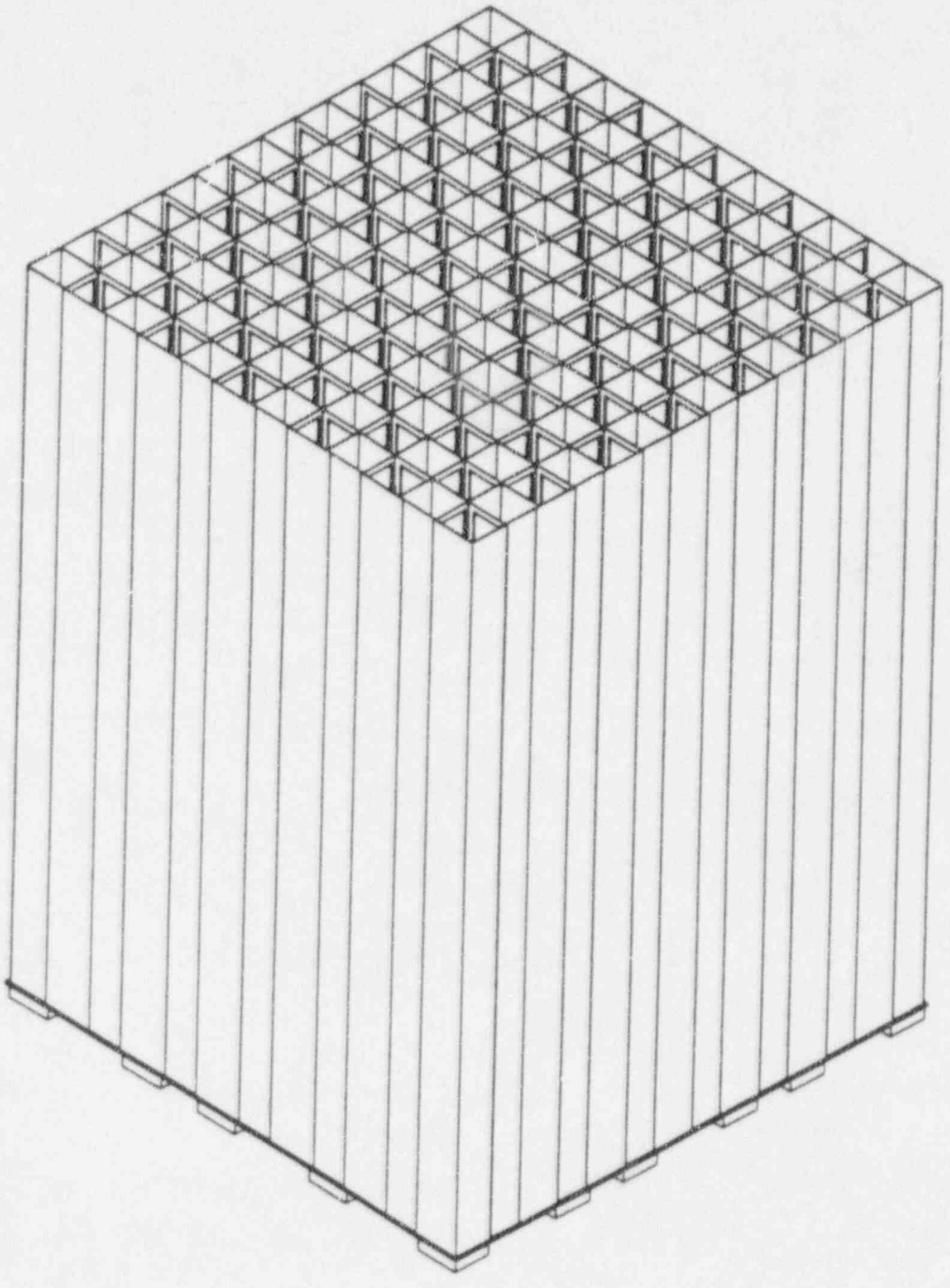

FIGURE 2-3

HIGH DENSITY RACK CROSS SECTION

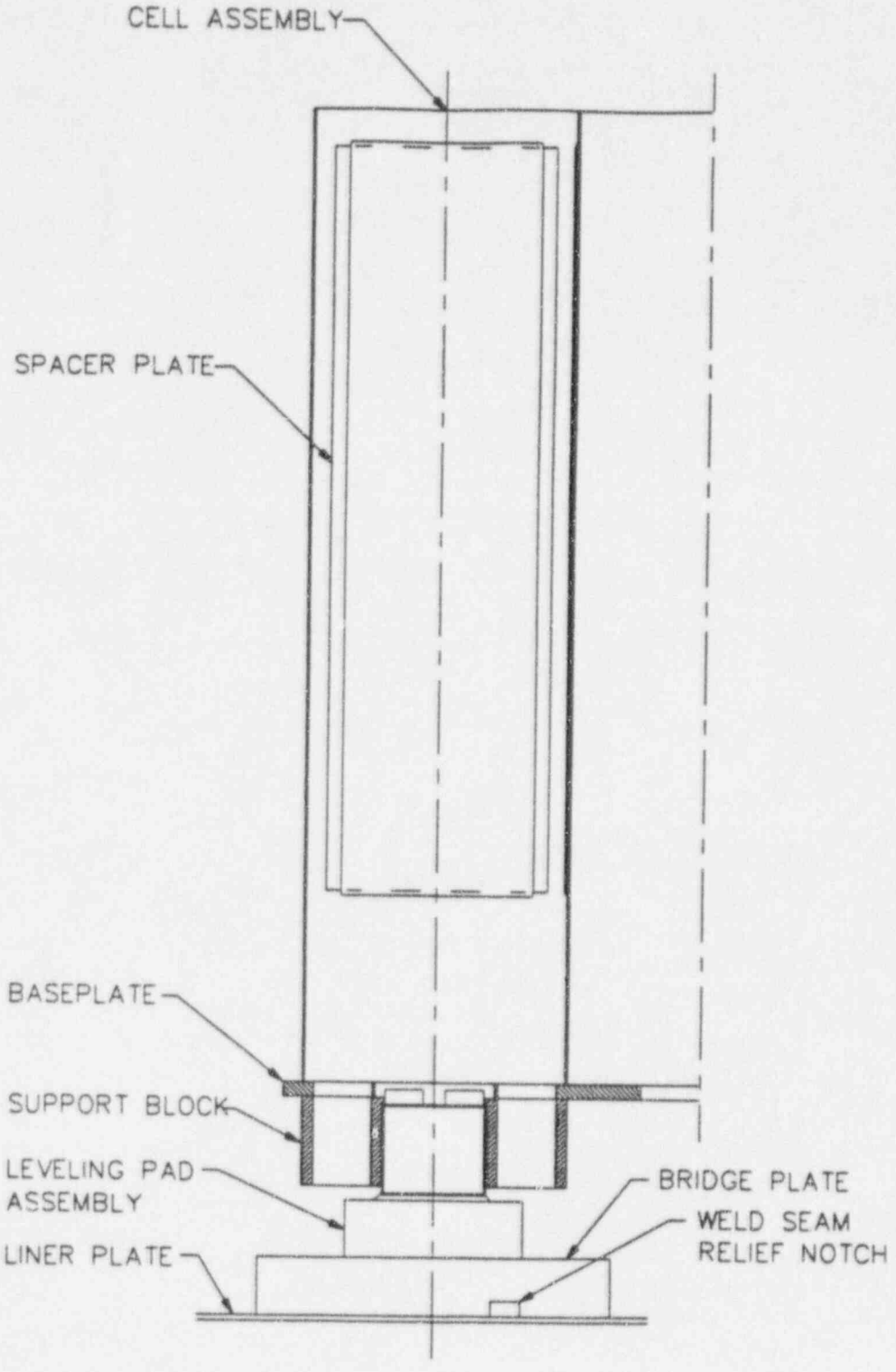

FIGURE 2-4

HIGH DENSITY RACK TOP VIEW

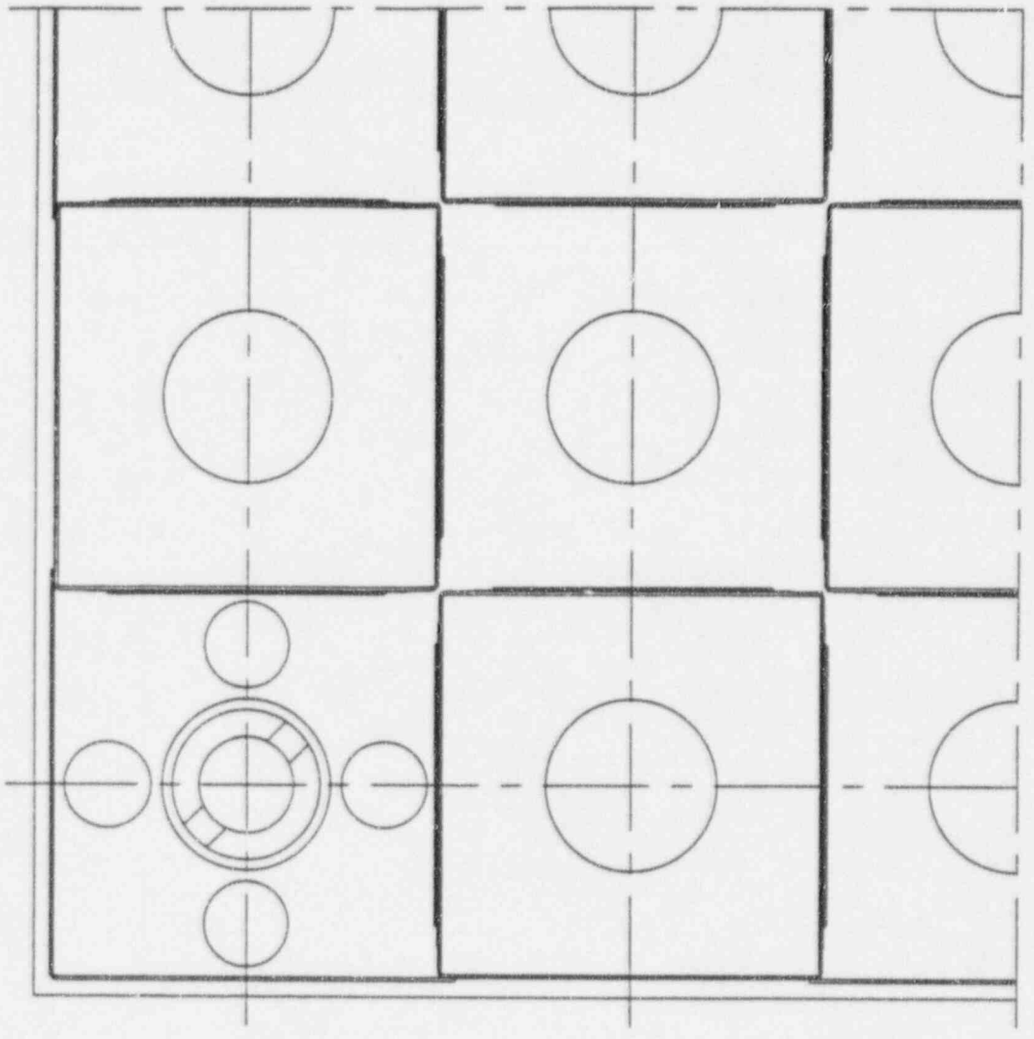

3.0 NUCLEAR AND THERMAL-HYDRAULIC CONSIDERATIONS

3.1 NEUTRON MULTIPLICATION FACTOR

The CPSES high density rack criticality analyses are based on maintaining $k_{eff} \leq 0.95$ including biases and uncertainties for storage of 17x17 fuel assemblies under full water density conditions.

The high density rack cell is depicted in Figure 3-1, with nominal dimensions provided.

The following storage configurations and enrichment limits are considered in this analysis:

High Density (2/4) Storage of 17x17 fuel assemblies in a high density (2/4) checkerboard arrangement with empty cells. A high density (2/4) checkerboard with empty cells means that no two fuel assemblies may be stored face adjacent. Fuel assemblies may be stored corner adjacent. Fuel assemblies must have an initial enrichment no greater than 2.9 w/o U235 (nominal) or satisfy a minimum burnup requirement.

High Density (1/4) Storage of 17x17 fuel assemblies in a high density (1/4) checkerboard arrangement with empty cells. A high density (1/4) checkerboard with empty cells means that no two fuel assemblies may be stored face adjacent or corner adjacent. Fuel assemblies may have an enrichment no greater than 5.0 w/o U235 (nominal) with no requirement on minimum burnup.

The analytical methods employed herein conform with ANSI N18.2-1973 [Ref. 21], ANSI 57.2-1983 [Ref. 7], and ANSI N16.9-1975, [Ref. 44].

3.1.1 NORMAL STORAGE

The high density racks for CPSES are designed to assure that, including uncertainties, there is a 95 percent probability at a 95 percent confidence level that the effective neutron multiplication factor (k_{eff}) of the fuel assembly array will be less than or equal to 0.95. This design basis satisfies the criteria in ANS-57.2-1983 [Ref. 7] and in OT Position for Review and Acceptance of Spent Fuel Storage and Handling Applications [Ref. 5].

3.1.2 POSTULATED ACCIDENTS

The following accident conditions have been evaluated to assure that the criticality acceptance criterion ($k_{eff} \leq 0.95$, including uncertainties) is satisfied:

1. An assembly is inadvertently dropped and comes to rest horizontally on top of the racks.
2. An assembly is inadvertently dropped and comes to rest vertically on top of the racks in an already loaded storage cell.
3. A fuel assembly is misloaded within the racks or adjacent to but outside the racks.
4. The spent fuel pool temperature increases or decreases outside the normal operating range.

For occurrences of any postulated accident, the double contingency principle of ANSI/ANS 8.1-1983 [Ref. 9] is applied. This principle states that one is not required to assume two unlikely independent concurrent events to ensure protection against a criticality accident. Thus, for these postulated accident conditions, the presence of soluble boron in the storage pool water can be assumed as a realistic initial condition since not assuming its presence would be a second unlikely event.

3.1.3 CRITICALITY CALCULATION METHODOLOGY

3.1.3.1 ANALYTICAL METHODS

The criticality calculation method and cross-section values are verified by comparison with critical experiment data for fuel assemblies similar to those for which the racks are designed. This benchmarking data is sufficiently diverse to establish that the method bias and uncertainty will apply to rack conditions which include strong neutron absorbers, large water gaps and low moderator densities.

The design method which ensures the criticality safety of the CPSES high density racks uses NITAWL-II [Ref. 10] and XSDRNPM-S [Ref. 42] for cross-section generation and KENO-Va [Ref. 11] for reactivity determination.

The 227 energy group cross-section library that is the common starting point for all cross-sections used for the benchmarks of KENO-Va and the KENO-Va storage rack calculations is generated from ENDF/B-V [Ref. 12] data. The NITAWL-II program includes, in this library, the self-shielded resonance cross-sections that are appropriate for each particular geometry. The Nordheim Integral Treatment is used. Energy and spatial weighting of cross-sections is performed by the XSDRNPM-S program which is a one-dimensional discrete ordinates transport theory code. These multigroup cross-section sets are then used as input to KENO-Va which is a Monte Carlo theory program designed for reactivity calculations.

KENO-Va Monte Carlo calculations are performed with sufficient neutron histories to assure convergence. A typical KENO-Va Monte Carlo calculation involves more than 60,000 neutron histories.

A set of 32 critical experiments [Ref. 17,18,19,20] has been analyzed using the above method to demonstrate its applicability to criticality analysis and to establish the method bias and uncertainty. The benchmark experiments cover a wide range of geometries, materials, and enrichments, including relatively low enriched (2.35, 2.46, and 4.31 w/o), water moderated, oxide fuel arrays separated by various materials (B4C, aluminum, steel, water, etc.) that simulate LWR fuel shipping and storage conditions. Comparison with these experiments demonstrates the wide range of applicability of the method. Table 3-1 summarizes these experiments.

The 32 experiments result in an average KENO-Va k_{eff} of 0.9930. Comparison with the average measured experimental k_{eff} of 1.0007 results in a method bias of 0.0077 Δk. The standard deviation of the bias value is 0.00136 Δk. The 95/95 one-sided tolerance limit factor for 32 values is 2.20 [Ref. 43]. Thus, there is a 95 percent probability with a 95 percent confidence level that the uncertainty in reactivity, due to the method, is not greater than 0.0030 Δk.

Material and construction tolerance reactivity effects and reactivity sensitivities are determined using the transport theory computer code, PHOENIX-P [Ref. 23]. PHOENIX-P is a depletable, two-dimensional, multigroup, discrete ordinates, transport theory code which utilizes a 42 energy group nuclear data library.

PHOENIX-P has been used to demonstrate its predictive capability in a series of comparisons against direct experimental data from critical experiments and against isotopic measurements. These comparisons provide a good assessment of the code's ability to predict key physics parameters over a wide range of lattice variations. Reactivity comparisons are accomplished by comparing appropriate predictions to Strawbridge and Barry's 101 criticals [Ref. 13] and the Babcock and Wilcox (B&W) cores XI-1,2,7,8,9 and cores XIV-1,6 spatial criticals [Ref. 14, 15, 16]. Isotopic comparisons are discussed in Section 3.1.3.2.

The range of lattice parameters of the 101 criticals is given in Table 3-2. The resulting mean PHOENIX-P k_{eff} for all 101 criticals is 1.00222 with a standard deviation of 0.00809. This shows PHOENIX-P results to be in excellent agreement with experimental data for all dependent parameters, with no significant bias or trends as a function of lattice parameters.

The core loadings and compositions studied in the seven B&W core spatial criticals are given in Table 3-3. The resulting mean k_{eff} of the seven critical experiments was 1.00151 with a standard deviation of 0.00098. The overall mean core k_{eff} for this set of critical experiments with diverse lattice configurations is in very good agreement with expected experimental values. The overall standard deviation indicates excellent stability of the PHOENIX-P library and methodology.

3.1.3.2 REACTIVITY EQUIVALENCING FOR BURNUP

Increased flexibility for the storage of spent fuel assemblies is achievable by means of the concept of reactivity equivalencing. Reactivity equivalencing is predicated upon the reactivity decrease associated with fuel depletion. A series of reactivity calculations is performed to generate a set of enrichment-burnup ordered pairs which yield an equivalent k_{eff} for fuel stored in the CPSES high density racks. The data points on the reactivity equivalence curve are generated with the transport theory computer code, PHOENIX-P.

A study was done to examine fuel reactivity as a function of time following reactor shutdown. Fission product decay was accounted for using CINDER [Ref. 24]. CINDER is a point-depletion computer code used to determine fission product activities. The fission products were permitted to decay for 30 years after shutdown. The fuel reactivity was found to reach a maximum at approximately 100 hours after shutdown. At this time, the major fission product poison, Xe-135, has nearly completely decayed away. Furthermore, the fuel reactivity was found to decrease continuously from 100 hours to 30 years following shutdown. Therefore, the most reactive time for a fuel assembly after shutdown of the reactor is conservatively approximated by removing the Xe-135.

The PHOENIX-P code has been validated by comparisons with experiments where the isotopic fuel composition has been examined following reactor shutdown. In addition, an extensive set of benchmark critical experiments has been analyzed with PHOENIX-P. Comparisons between measured and predicted uranium and plutonium isotopic fuel compositions are shown in Table 3-4. The measurements were made on fuel discharged from Yankee Core 5 [Ref. 22]. The PHOENIX-P predictions agree quite well with measurements for all measured isotopes throughout the burnup range.

Uncertainties associated with the burnup dependent reactivities computed with PHOENIX-P are accounted for in the development of the individual reactivity equivalence limits. For burnup credit, an uncertainty is applied to the PHOENIX-P calculational results which starts at zero for zero burnup and increases linearly with burnup, passing through 0.01 Δk at 30,000 MWD/MTU. This bias is very conservative and is based on consideration of the good agreement between PHOENIX-P predictions and measurements and on conservative estimates of fuel assembly reactivity variances with depletion history.

3.1.4 CRITICALITY ANALYSIS

3.1.4.1 HIGH DENSITY (1/4) RACKS - NORMAL STORAGE

This section describes the analytical techniques and models employed to perform the criticality analysis for the CPSES high density (1/4) checkerboard arrangement.

Section 3.1.4.1.1 describes the reactivity calculations performed for high density (1/4) checkerboarding with a nominal enrichment of 5.0 w/o U235. Section 3.1.4.1.2 presents the results of calculations performed to show the reactivity sensitivity of variations in enrichment, center to center spacing, and cell wall thickness. The worth of soluble boron in the spent fuel racks is also discussed in Section 3.1.4.1.2.

3.1.4.1.1 REACTIVITY CALCULATIONS

To show that storage of 17x17 fuel assemblies in the high density (1/4) checkerboard arrangement in spent fuel racks satisfies the 0.95 k_{eff} criticality acceptance criteron, KENO-Va is used to establish a nominal reference reactivity and PHOENIX-P is used to assess the effects of material and construction tolerance variations. The normal temperature range of 50°F to 150°F is considered in the analysis. A final 95/95 k_{eff} is developed by statistically combining the individual tolerance impacts with the calculational and methodology uncertainties and summing this term with the nominal KENO-Va reference reactivity.

The following assumptions are used to develop the nominal case KENO-Va model for storage of fuel assemblies in the CPSES racks in a high density (1/4) checkerboard arrangement:

1. The fuel assembly parameters relevant to the criticality analysis are based on the Westinghouse 17x17 OFA design. Calculations show that, for the enrichment considered here, the Westinghouse 17x17 OFA design is the most reactive fuel assembly.

2. All fuel assemblies contain uranium dioxide at a nominal enrichment of 5.0 w/o over the entire length of each rod.

3. The fuel pellets are modeled assuming nominal values for theoretical density and dishing fraction.

4. No credit is taken for any natural or reduced enrichment axial blankets.

5. No credit is taken for any U234 or U236 in the fuel, nor is any credit taken for the buildup of fission product poison material.

6. No credit is taken for any spacer grids or spacer sleeves.

7. No credit is taken for any burnable absorber in the fuel rods.

8. The moderator is pure water (no boron) at a temperature of 68°F. A value of 1.0 g/cm^3 is used for the density of the spent fuel pool water.

9. The array is infinite in lateral (x and y) extent and axial (vertical) extent. This prevents neutron leakage outside the array.

10. Fuel storage cells are loaded with fuel assemblies in a high density (1/4) checkerboard arrangement as shown in Figure 3-2. No two fuel assemblies are allowed to be face adjacent or corner adjacent.

11. The rack spacer material made of stainless steel used in the high density racks is not modeled. This is conservative since stainless steel will act as a neutron absorber.

With the above assumptions, the KENO-Va calculation for the nominal case results in a k_{eff} of 0.9243 with a 95 percent probability/95 percent confidence level uncertainty of 0.0029 Δk.

Calculational and methodology biases must be considered in the final k_{eff} summation prior to comparing against the 0.95 k_{eff} limit. The following biases are included:

Methodology: As discussed in Section 3.1.3.1 of this report, benchmarking of the Westinghouse KENO-Va methodology resulted in a method bias of 0.0077 Δk.

Water Temperature: To account for the effect of the normal range of spent fuel pool water temperatures (50°F to 150°F), a reactivity bias of 0.0005 Δk is applied. The water temperature bias is calculated with PHOENIX-P due to thermal scattering kernel limitations in NITAWL-II.

To evaluate the reactivity effects of possible variations in material characteristics and mechanical/construction dimensions, PHOENIX-P perturbation calculations are performed. For the Comanche Peak high density (1/4) checkerboard arrangement, UO_2 material tolerances are considered along with construction tolerances related to the cell I.D., cell pitch, and cell wall thickness. Uncertainties associated with calculation and methodology accuracy are also considered in the statistical summation of uncertainty components.

The following tolerance and uncertainty components are considered in the total uncertainty statistical summation:

U235 Enrichment: The standard DOE enrichment tolerance of 0.05 w/o U235 about the nominal 5.0 w/o U235 reference enrichment was evaluated with PHOENIX-P and resulted in a reactivity increase of 0.0015 Δk.

UO_2 Density: A 2.0% variation about the nominal 95% reference theoretical density was evaluated with PHOENIX-P and resulted in a reactivity increase of 0.0024 Δk.

Fuel Pellet Dishing: A variation in fuel pellet dishing fraction from 0.0% to 2.0% (the nominal reference value is 1.211%) was evaluated with PHOENIX-P and resulted in a reactivity increase of 0.0014 Δk.

Storage Cell I.D.: The 0.05 inch tolerance about the nominal 8.83 inch reference cell I.D.was evaluated with PHOENIX-P and resulted in a reactivity increase of 0.0001 Δk.

Storage Cell Pitch : The 0.06 inch tolerance about the nominal 9.00 inch reference cell pitch was evaluated with PHOENIX-P and resulted in a reactivity increase of 0.0006 Δk.

Stainless Steel Wall Thickness: The 0.004 inch tolerance about the nominal 0.075 inch reference stainless steel wall thickness was evaluated with PHOENIX-P and resulted in a reactivity increase of 0.0010 Δk.

Assembly Position: The KENO-Va reference reactivity calculation assumes fuel assemblies are symmetrically positioned within the storage cells since experience has shown that centered fuel assemblies yield equal or more conservative results in rack k_{eff} than non-centered (asymmetric) positioning. Therefore, no reactivity uncertainty needs to be applied for this tolerance since the most reactive configuration is considered in the calculation of the reference k_{eff}.

Calculation Uncertainty: The KENO-Va calculation for the nominal reference reactivity resulted in a k_{eff} with a 95 percent probability/95 percent confidence level uncertainty of 0.0029 Δk.

Methodology Uncertainty: As discussed in Section 3.1.3.1 of this report, comparison against benchmark experiments showed that the 95 percent probability/95 percent confidence uncertainty in reactivity, due to method, is not greater than 0.0030 Δk.

The maximum k_{eff} for the Comanche Peak high density (1/4) checkerboard arrangement is developed by adding the calculational and methodology biases and the statistical sum of independent uncertainties to the KENO-Va reference reactivity. The summation is shown in Table 3-5 and results in a maximum k_{eff} of 0.9379.

Since k_{eff} is less than 0.95 including uncertainties at a 95/95 probability/confidence level, the acceptance criterion for criticality is met for storage of 17x17 fuel assemblies with nominal enrichment up to 5.0 w/o U235 in the Comanche Peak high density (1/4) checkerboard arrangement spent fuel racks.

3.1.4.1.2 SENSITIVITY ANALYSIS AND SOLUBLE BORON WORTH

To show the dependence of k_{eff} on fuel and storage cells parameters, as requested in the OT Position for Review and Acceptance of Spent Fuel Storage and Handling Applications [Ref. 5], the variation of the k_{eff} with respect to the following parameters was developed using the PHOENIX-P computer code:

1. Fuel enrichment, with a 0.50 w/o U235 variation about the nominal case enrichment.

2. Center to center spacing of storage cells, with a 0.50 inch variation about the nominal case center to center spacing.

3. Cell wall thickness, with a 0.05 inch variation about the nominal case cell wall thickness.

Results of the sensitivity analysis are shown in Figure 3-4.

PHOENIX-P calculations were also performed to evaluate the reactivity benefits of soluble boron for the high density (1/4) checkerboard spent fuel storage configuration. Results of these calculations are provided in Figure 3-5. As the curve shows, the presence of soluble boron in the Comanche Peak spent fuel pool provides substantial reactivity margin.

3.1.4.2 HIGH DENSITY (2/4) RACKS - NORMAL STORAGE

This section describes the analytical techniques and models employed to perform the criticality analysis and reactivity equivalencing evaluations for the Comanche Peak high density (2/4) spent fuel storage rack checkerboard arrangement.

Section 3.1.4.2.1 describes the reactivity calculations performed for the high density (2/4) checkerboard with a nominal fresh fuel (no burnup) enrichment of 2.90 w/o U235. Section 3.1.4.2.2 describes the analysis which allows for storage of assemblies with nominal enrichments above 2.90 w/o U235 and up to 5.0 w/o U235 by taking credit for accumulated fuel burnup. Finally, Section 3.1.4.2.3 presents the results of calculations performed to show the reactivity sensitivity of variations in enrichment, center to center spacing, and cell wall thickness. The worth of soluble boron in the spent fuel pools is also discussed in this section.

3.1.4.2.1 REACTIVITY CALCULATIONS

To show that storage of 17x17 fuel assemblies in a high density (2/4) checkerboard arrangement satisfies the 0.95 k_{eff} criticality acceptance criterion, KENO-Va is used to establish a nominal reference reactivity, and PHOENIX-P is used to assess the effects of material and construction tolerance variations. The normal temperature range of 50°F to 150°F is considered in the analysis. A final 95/95 k_{eff} is developed by statistically combining the individual tolerance impacts with the calculational and methodology uncertainties and summing this term with the nominal KENO-Va reference reactivity.

The following assumptions are used to develop the nominal case KENO-Va model for storage of fuel assemblies in the CPSES racks in a high density (2/4) checkerboard arrangement:

1. The fuel assembly parameters relevant to the criticality analysis are based on the Westinghouse 17x17 OFA design. Calculations show that for the enrichment considered here, the Westinghouse 17x17 OFA design is the most reactive fuel assembly.

2. All fuel assemblies contain uranium dioxide at a nominal enrichment of 2.90 w/o over the entire length of each rod.

3. The fuel pellets are modeled assuming nominal values for theoretical density and dishing fraction.

4. No credit is taken for any natural or reduced enrichment axial blankets.

5. No credit is taken for any U234 or U236 in the fuel, nor is any credit taken for the buildup of fission product poison material.

6. No credit is taken for any spacer grids or spacer sleeves.

7. No credit is taken for any burnable absorber in the fuel rods.

8. The moderator is pure water (no boron) at a temperature of 68°F. A limiting value of 1.0 g/cm^3 is used for the density of the spent fuel pool water.

9. The array is infinite in lateral (x and y) extent and axial (vertical) extent. This prevents neutron leakage outside the array.

10. Fuel storage cells are loaded with fuel assemblies in a high density (2/4) checkerboard arrangement as shown in Figure 3-2. No two fuel assemblies are allowed to be face adjacent. Fuel assemblies may be stored corner adjacent.

11. The rack spacer material made of stainless steel used in the high density racks is not modeled. This is conservative since stainless steel will act as a neutron absorber.

With the above assumptions, the KENO-Va calculation for the nominal case results in a k_{eff} of 0.9266 with a 95 percent probability/95 percent confidence level uncertainty of 0.0025 Δk.

Calculational and methodology biases must be considered in the final k_{eff} summation prior to comparing against the 0.95 k_{eff} limit. The following biases are included:

Methodology: As discussed in Section 3.1.3.1 of this report, benchmarking of the Westinghouse KENO-Va methodology resulted in a method bias of 0.0077 Δk.

Water Temperature: To account for the effect of the normal range of spent fuel pool water temperatures (50°F to 150°F), a reactivity bias of 0.0036 Δk is applied. The water temperature bias is calculated with PHOENIX-P due to thermal scattering kernel limitations in NITAWL-II.

To evaluate the reactivity effects of possible variations in material characteristics and mechanical/construction dimensions, PHOENIX-P perturbation calculations are performed. For the Comanche Peak high density (2/4) checkerboard arrangement, UO_2 material tolerances are considered as are construction tolerances related to the cell I.D., cell pitch, and cell wall thickness. Uncertainties associated with calculation and methodology accuracy are also considered in the statistical summation of uncertainty components.

The following tolerance and uncertainty components are considered in the total uncertainty statistical summation:

U235 Enrichment: The standard DOE enrichment tolerance of 0.05 w/o U235 about the nominal 2.90 w/o U235 reference enrichment was evaluated with PHOENIX-P and resulted in a reactivity increase of 0.0038 Δk.

UO_2 Density: A 2.0% variation about the nominal 95% reference theoretical density was evaluated with PHOENIX-P and resulted in a reactivity increase of 0.0027 Δk.

Fuel Pellet Dishing: A variation in fuel pellet dishing fraction from 0.0% to 2.0% (the nominal reference value is 1.211%) was evaluated with PHOENIX-P and resulted in a reactivity increase of 0.0016 Δk.

Storage Cell I.D.: The 0.05 inch tolerance about the nominal 8.83 inch reference cell I.D. was evaluated with PHOENIX-P and resulted in no reactivity increase.

Storage Cell Pitch : The 0.06 inch tolerance about the nominal 9.00 inch reference cell pitch was evaluated with PHOENIX-P and resulted in a reactivity increase of 0.0032 Δk.

Stainless Steel Wall Thickness: The 0.004 inch tolerance about the nominal 0.075 inch reference stainless steel wall thickness was evaluated with PHOENIX-P and resulted in a reactivity increase of 0.0016 Δk.

Assembly Position: The KENO-Va reference reactivity calculation assumes fuel assemblies are symmetrically positioned within the storage cells. Experience has shown that centered fuel assemblies yield equal or more conservative results in rack k_{eff} than non-centered (asymmetric) positioning. Therefore, no reactivity uncertainty needs to be applied for this tolerance since the most reactive configuration is considered in the calculation of the reference k_{eff}.

Calculation Uncertainty: The KENO-Va calculation for the nominal reference reactivity resulted in a k_{eff} with a 95 percent probability/95 percent confidence level uncertainty of 0.0025 Δk.

Methodology Uncertainty: As discussed in Section 3.1.3.1 of this report, comparison against benchmark experiments showed that the 95 percent probability/95 percent confidence uncertainty in reactivity, due to method, is not greater than 0.0030 Δk.

The maximum k_{eff} for the Comanche Peak high density (2/4) checkerboard arrangement is developed by adding the calculational and methodology biases and the statistical sum of independent uncertainties to the KENO-Va reference reactivity. The summation is shown in Table 3-6 and results in a maximum k_{eff} of 0.9451.

Since k_{eff} is less than 0.95 including uncertainties at a 95/95 probability/confidence level, the acceptance criterion for criticality is met for storage of fresh (no burnup) 17x17 fuel assemblies with nominal enrichment up to 2.90 w/o U235 in the Comanche Peak high density (2/4) checkerboard arrangement.

3.1.4.2.2 BURNUP CREDIT REACTIVITY EQUIVALENCING

Increased flexibility for storage of burned fuel assemblies in the CPSES racks in a high density (2/4) checkerboard arrangement is achievable by means of the concept of reactivity equivalencing. The concept of reactivity equivalencing is predicated upon the reactivity decrease associated with fuel depletion. For burnup credit, a series of reactivity calculations are performed to generate a set of enrichment-fuel assembly discharge burnup ordered pairs which yield an equivalent k_{eff} for storage in the spent fuel storage racks.

Figure 3-3 shows the constant k_{eff} contour generated for the CPSES racks in a high density (2/4) checkerboard arrangement. This curve represents combinations of fuel enrichment and discharge burnup which yield the same rack multiplication factor (k_{eff}) as the rack loaded with Westinghouse 17x17 OFA fresh fuel (zero burnup) at 2.90 w/o U235. Calculations were performed to show that the Westinghouse 17x17 OFA fuel assembly yields the highest reactivity at burned conditions of all 17x17 fuel assembly types considered.

As shown in Figure 3-3, the endpoints are 0 MWD/MTU where the fuel assembly enrichment is 2.90 w/o, and 16500 MWD/MTU where the fuel assembly enrichment is 5.0 w/o. The interpretation of the endpoint data is as follows: the reactivity of the spent fuel rack containing 5.0 w/o fuel at 16500 MWD/MTU is equivalent to the reactivity of the rack containing 2.90 w/o fresh fuel. Reactivity uncertainty is applied to all points on Figure 3-3 consistent with the methodology described in Section 3.1.3.2.

The curve in Figure 3-3 is based on calculations of constant rack reactivity. In this way, the environment of the storage rack and its influence on assembly reactivity is implicitly considered. The data from Figure 3-3 is also provided in Table 3-7. Use of linear interpolation between the tabulated values is acceptable since the curve shown in Figure 3-3 is linear in between the tabulated points.

The effect of axial burnup distribution on assembly reactivity has been considered in the development of the Comanche Peak high density (2/4) checkerboard burnup credit limit. Westinghouse evaluations have been performed to quantify axial burnup reactivity effects and to confirm that the reactivity equivalencing methodology described in Section 2.2 results in calculations of conservative burnup credit limits. The evaluations show that axial burnup effects can cause assembly reactivity to increase only at burnup-enrichment combinations which are well beyond those calculated for the CPSES high density (2/4) checkerboard burnup credit limit. Therefore, additional accounting of axial burnup distribution effects in the Comanche Peak high density (2/4) burnup credit limit is not necessary.

3.1.4.2.3 SENSITIVITY ANALYSIS AND SCLUBLE BORON WORTH

To show the dependence of k_{eff} on fuel and storage cells parameters, the variation of the k_{eff} with respect to the following parameters was developed using the PHOENIX-P computer code:

1. Fuel enrichment, with a 0.50 w/o U235 variation about the nominal case enrichment.

2. Center to center spacing of storage cells, with a 0.50 inch variation about the nominal case center to center spacing

3. Cell wall thickness, with a 0.05 inch variation about the nominal case cell wall thickness.

Results of the sensitivity analysis are shown in Figure 3-6.

PHOENIX-P calculations were also performed to evaluate the reactivity benefits of soluble boron for the high density (2/4) checkerboard spent fuel storage configuration. Results of these calculations are provided in Figure 3-5. As the curve shows, the presence of soluble boron in the Comanche Peak spent fuel pool provides substantial reactivity margin.

3.1.4.3 POSTULATED ACCIDENTS

Most accident conditions will not result in an increase in k_{eff} of the rack. Examples are:

Fuel assembly drop on top of rack - Horizontal	The rack structure pertinent for criticality is not excessively deformed, and the dropped assembly which comes to rest horizontally on top of the rack has sufficient water separating it from the active fuel height of stored assemblies to preclude neutronic interaction.
Fuel assembly drop on top of rack - Vertical	The calculations have been performed excluding axial features, therefore dropping a fuel assembly into an already loaded cell does not increase reactivity relative to the analyzed configuration for normal storage.

However, two accidents can be postulated in each storage configuration which would increase reactivity beyond the analyzed normal storage condition.

Fuel assembly misloaded into a fully loaded rack	A fuel assembly misloaded into a fully loaded rack would include a fuel assembly loaded into an excluded cell, dropped against the outer edge of a fuel rack module or dropped between the rack module and the spent fuel pool wall. Of these three conditions, the misloaded fuel assembly in an excluded cell will bound the reactivity increase of all three.
Fuel Pool Water Temperature Change	A temperature increase or decrease outside of the normal operating range (50°F to 150°F) can increase the reactivity of the spent fuel racks.

These accidents will be discussed below for each storage configuration.

To evaluate the reactivity impact of a misloaded assembly in an excluded cell in the high density (2/4) checkerboard, the impact of loading a fresh assembly at 5.0 w/o U235 in an array of spent fuel rack cells with fresh assemblies at 2.90 w/o U235 stored in a 2-out-of-4 checkerboard arrangement was determined. The reactivity increase associated with this misloading is 0.243 Δk.

To evaluate the reactivity impacts of a misloaded assembly in an excluded cell in the 1-out-of-4 checkerboard, the impact of loading a fresh assembly at 5.0 w/o U235 in an array of spent fuel rack cells with fresh assemblies at 5.0 w/o U235 stored in a 1-out-of-4 checkerboard arrangement was determined. The reactivity increase associated with this misloading is 0.173 Δk.

In the high density (2/4) checkerboard arrangement, an increase in reactivity could result from a heatup event during which the pool temperature would increase to greater than 150°F. Since the fuel assemblies located in the high density (2/4) racks are overmoderated at 68°F, a reactivity increase results from the reduction in moderator density due to a temperature increase. Calculations show that if the spent fuel pool water temperature was to increase from 150°F to 212°F, reactivity would increase by 0.0018 Δk.

In the high density (1/4) checkerboard arrangement, an increase in reactivity could result from a "cooldown" event during which the pool temperature would drop below 50°F. Since the fuel assemblies located in the high density (1/4) racks are essentially isolated from one another and a single fuel assembly in water is undermoderated at 68°F, a reactivity increase results from an increase in moderator density due to a temperature decrease. Calculations show that if the spent fuel pool water temperature was to decrease from 50°F to 32°F, reactivity would increase by 0.0005 Δk.

For occurrences of any of the above postulated accidents, the double contingency principle of ANSI/ANS 8.1-1983 [Ref. 9] can be applied. This states that one is not required to assume two unlikely, independent, concurrent events to ensure protection against a criticality accident. Thus, for these postulated accident conditions, the presence of soluble boron in the storage pool water can be assumed as a realistic initial condition since not assuming its presence would be a second unlikely event.

From the above accident calculations, the highest reactivity increases for the high density (1/4) and (2/4) checkerboard arrangements are 0.173 and 0.243 Δk, respectively. The soluble boron concentration in the spent fuel pool needed to offset these reactivity increases and maintain k_{eff} below 0.95 was calculated by KENO-Va to be 1500 ppm for 2-out-of-4 checkerboard storage and 1200 ppm for 1-out-of-4 storage. The normal boron concentration in the SFPs is at least 2400 ppm, well above the minimum needed.

TABLE 3-1
BENCHMARK CRITICAL EXPERIMENTS FOR KENO-Va

Critical Number	General Description	Enrichment (U235w/o)	Reflector	Separating Material	Soluble Boron (ppm)	Measured k_{eff}	(k_{eff} +/- One Sigma)
1	UO2 Rod Lattice	2.46	water	water	0	1.0002	0.99347 +/- 0.00234
2	UO2 Rod Lattice	2.46	water	water	1037	1.0001	0.99361 +/- 0.00193
3	UO2 Rod Lattice	2.46	water	water	764	1.0000	0.99459 +/- 0.00194
4	UO2 Rod Lattice	2.46	water	B4C pins	0	0.9999	0.98766 +/- 0.00217
5	UO2 Rod Lattice	2.46	water	B4C pins	0	1.0000	0.98838 +/- 0.00221
6	UO2 Rod Lattice	2.46	water	B4C pins	0	1.0097	1.00132 +/- 0.00221
7	UO2 Rod Lattice	2.46	water	B4C pins	0	0.9998	0.99570 +/- 0.00225
8	UO2 Rod Lattice	2.46	water	B4C pins	0	1.0083	0.99905 +/- 0.00210
9	UO2 Rod Lattice	2.46	water	water	0	1.0030	0.99660 +/- 0.00299
10	UO2 Rod Lattice	2.46	water	water	143	1.0001	0.99707 +/- 0.00199
11	UO2 Rod Lattice	2.46	water	stainless steel	514	1.0000	0.99862 +/- 0.00203
12	UO2 Rod Lattice	2.46	water	stainless steel	217	1.0000	0.99411 +/- 0.00207
13	UO2 Rod Lattice	2.46	water	borated aluminum	15	1.0000	0.99229 +/- 0.00218
14	UO2 Rod Lattice	2.46	water	borated aluminum	92	1.0001	0.98847 +/- 0.00208
15	UO2 Rod Lattice	2.46	water	borated aluminum	395	0.9998	0.98424 +/- 0.00205
16	UO2 Rod Lattice	2.46	water	borated aluminum	121	1.0001	0.98468 +/- 0.00209
17	UO2 Rod Lattice	2.46	water	borated aluminum	487	1.0000	0.98521 +/- 0.00195
18	UO2 Rod Lattice	2.46	water	borated aluminum	197	1.0002	0.99203 +/- 0.00211
19	UO2 Rod Lattice	2.46	water	borated aluminum	634	1.0002	0.98924 +/- 0.00201
20	UO2 Rod Lattice	2.46	water	borated aluminum	320	1.0003	0.99461 +/- 0.00197
21	UO2 Rod Lattice	2.46	water	borated aluminum	72	0.9997	0.98770 +/- 0.00220
22	UO2 Rod Lattice	2.35	water	borated aluminum	0	1.0000	0.99347 +/- 0.00128
23	UO2 Rod Lattice	2.35	water	stainless steel	0	1.0000	0.99566 +/- 0.00116
24	UO2 Rod Lattice	2.35	water	water	0	1.0000	0.99785 +/- 0.00239
25	UO2 Rod Lattice	2.35	water	stainless steel	0	1.0000	0.98964 +/- 0.00240
26	UO2 Rod Lattice	2.35	water	borated aluminum	0	1.0000	0.98841 +/- 0.00234
27	UO2 Rod Lattice	2.35	water	B4C	0	1.0000	0.99015 +/- 0.00231
28	UO2 Rod Lattice	4.31	water	stainless steel	0	1.0000	0.99063 +/- 0.00247
29	UO2 Rod Lattice	4.31	water	water	0	1.0000	0.98986 +/- 0.00228
30	UO2 Rod Lattice	4.31	water	stainless steel	0	1.0000	1.00011 +/- 0.00248
31	UO2 Rod Lattice	4.31	water	borated aluminum	0	1.0000	1.00070 +/- 0.00254
32	UO2 Rod Lattice	4.31	water	borated aluminum	0	1.0000	1.00088 +/- 0.00253

TABLE 3-2

SUMMARY OF LATTICE PARAMETERS FOR

STRAWBRIDGE AND BARRY 101 CRITICALS

Lattice Parameter	Range
Enrichment (w/o)	1.04 to 4.07
Boron Concentration (ppm)	0 to 3392
Water to uranium ratio	1.0 to 11.96
Pellet diameter	0.44 to 2.35
Lattice pitch (cm)	0.95 to 4.95
Clad material	none, aluminum, and stainless steel
Lattice Type	square and hexagonal
Fuel density (g/cm^3)	7.5 to 18.9

TABLE 3-3

B&W CORE LOADING AND COMPOSITIONS STUDIED

Core Loading		Number of Fuel Rods	Number of Water-Filled Positions	Number of Pyrex Rods	Soluble Boron (ppm)
XI	1	4961	0	0	1511
	2	4808	153	0	1334
	7	4808	81	72	1031
	8	4808	9	144	794
	9	4808	9	144	779
XIV	1	4736	225	0	1289
	6	4736	201	24	1179

TABLE 3-4

COMPARISON OF PHOENIX ISOTOPIC PREDICTION

TO YANKEE CORE 5 MEASUREMENTS

Quantity (Atom Ratio)	% Difference
U-235/U	-0.8
U-236/U	-1.5
U-238/U	0.0
Pu-239/Pu	+1.1
Pu-240/Pu	-2.8
Pu-241/Pu	-3.8
Pu-242/Pu	-3.0
Pu-239/U-238	+0.1
U-235/U-238	-0.8

Percent difference is average difference of ten comparisons for each isotope.

TABLE 3-5

HIGH DENSITY (1/4) k_{eff} SUMMARY

	Δk	k_{eff}
Nominal KENO-Va Reference Reactivity:		0.9243
Calculational & Methodology Biases:		
Methodology (Benchmark) Bias	+0.0077	
Pool Temperature Bias (50°F - 150°F)	+0.0005	
TOTAL Bias	+0.0082	
Best-Estimate Nominal k_{eff}:		0.9325
Tolerances & Uncertainties:		
UO2 Enrichment Tolerance	+0.0015	
UO2 Density Tolerance	+0.0024	
Fuel Pellet Dishing Variation	+0.0014	
Cell Inner Diameter	+0.0001	
Cell Pitch	+0.0006	
Cell Wall Thickness	+0.0010	
Calculational Uncertainty (95/95)	+0.0029	
Methodology Bias Uncertainty (95/95)	+0.0030	
TOTAL Uncertainty (statistical)	+0.0054	

$$\sqrt{\sum_{i=1}^{8} ((tolerance_i \ldots or \ldots uncertainty_i)^2)} = 0.0054$$

Final k_{eff} Including Uncertainties & Tolerances: 0.9379

TABLE 3-6

HIGH DENSITY (2/4) k_{eff} SUMMARY

	Δk	k_{eff}
Nominal KENO-Va Reference Reactivity:		0.9266
Calculational & Methodology Biases:		
Methodology (Benchmark) Bias	+0.0077	
Pool Temperature Bias (50°F - 150°F)	+0.0036	
TOTAL Bias	+0.0113	
Best-Estimate Nominal k_{eff}:		0.9379
Tolerances & Uncertainties:		
UO2 Enrichment Tolerance	+0.0038	
UO2 Density Tolerance	+0.0027	
Fuel Pellet Dishing Variation	+0.0016	
Cell Pitch	+0.0032	
Cell Wall Thickness	+0.0016	
Calculational Uncertainty (95/95)	+0.0025	
Methodology Bias Uncertainty (95/95)	+0.0030	
TOTAL Uncertainty (statistical)	+0.0072	

$$\sqrt{\sum_{i=1}^{7} \left((tolerance_i \ldots or \ldots uncertainty_i)^2 \right)} = 0.0072$$

Final k_{eff} Including Uncertainties & Tolerances:	0.9451

TABLE 3-7

HIGH DENSITY (2/4) BURNUP REQUIREMENT

Nominal Enrichment (w/o)	Burnup (MWD/MTU)
2.90	0
3.00	800
3.20	2400
3.40	4000
3.60	5600
3.80	7200
4.00	8900
4.20	10400
4.40	12000
4.60	13500
4.80	15100
5.00	16500

FIGURE 3-1

HIGH DENSITY RACK CELL LAYOUT

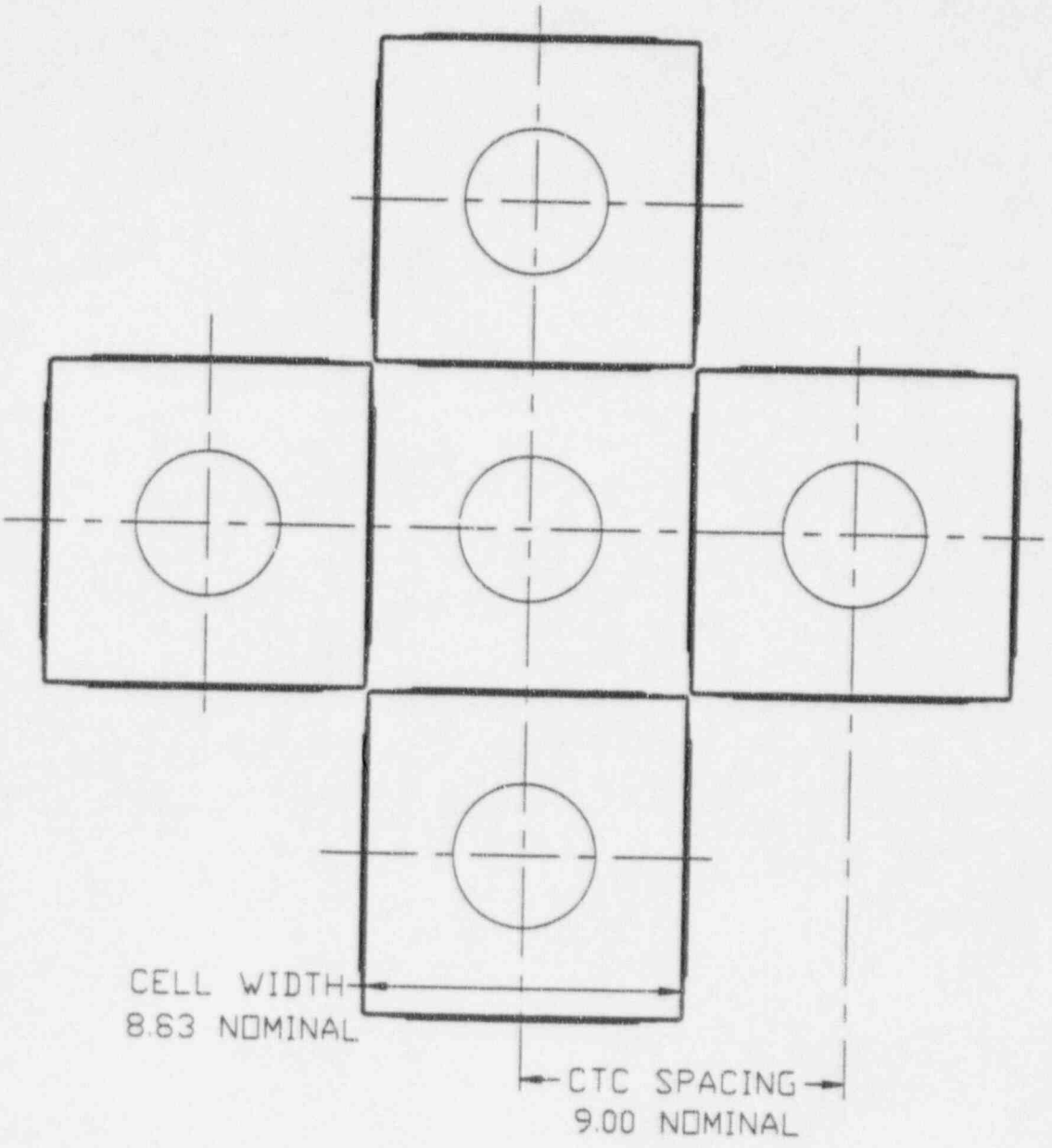

FIGURE 3-2

EXAMPLE CHECKERBOARD LOADING CONFIGURATIONS

FOR HIGH DENSITY RACKS

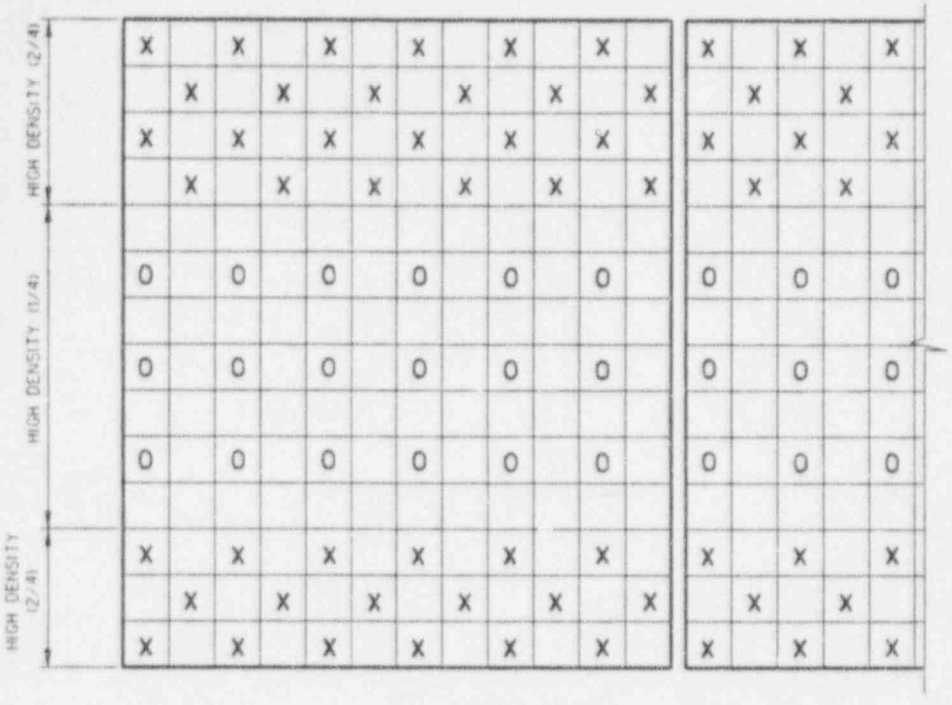

0 ANY NEW OR SPENT FUEL

X FUEL WHICH MEETS INITIAL ENRICHMENT AND MINIMUM BURNUP REQUIREMENT OF FIGURE 3-3

VACANT STORAGE LOCATIONS

NOTE:
THIS FIGURE PROVIDES EXAMPLES OF ACCEPTABLE LOADING CONFIGURATIONS. OTHER ACCEPTABLE CONFIGURATIONS BASED ON (1/4) OR (2/4) LOADING ARE POSSIBLE AND MAY BE USED.

FIGURE 3-3

MINIMUM BURNUP VERSUS INITIAL U235 ENRICHMENT

FOR HIGH DENSITY (2/4) RACKS

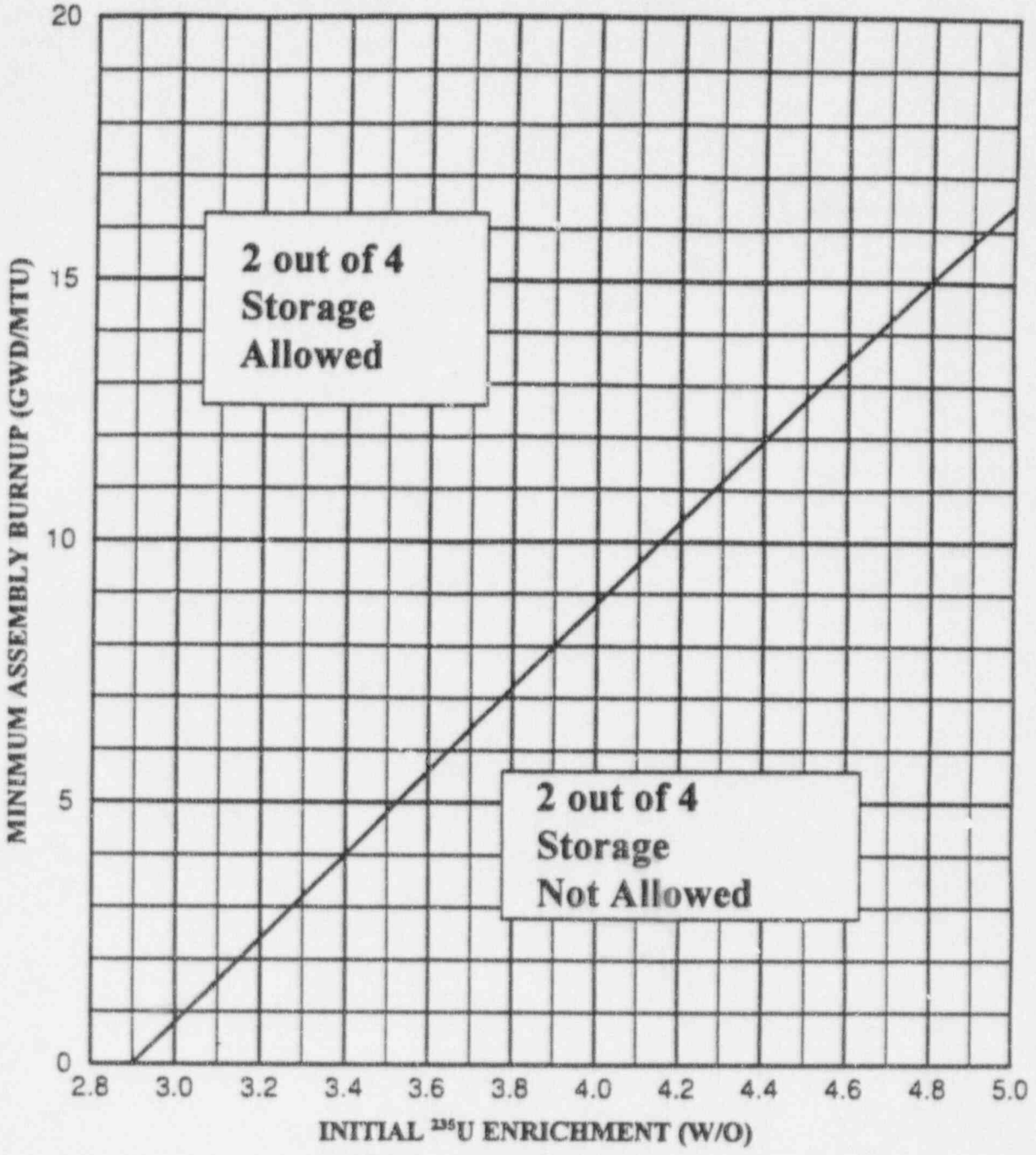

FIGURE 3-4

HIGH DENSITY (1/4) RACK REACTIVITY SENSITIVITIES

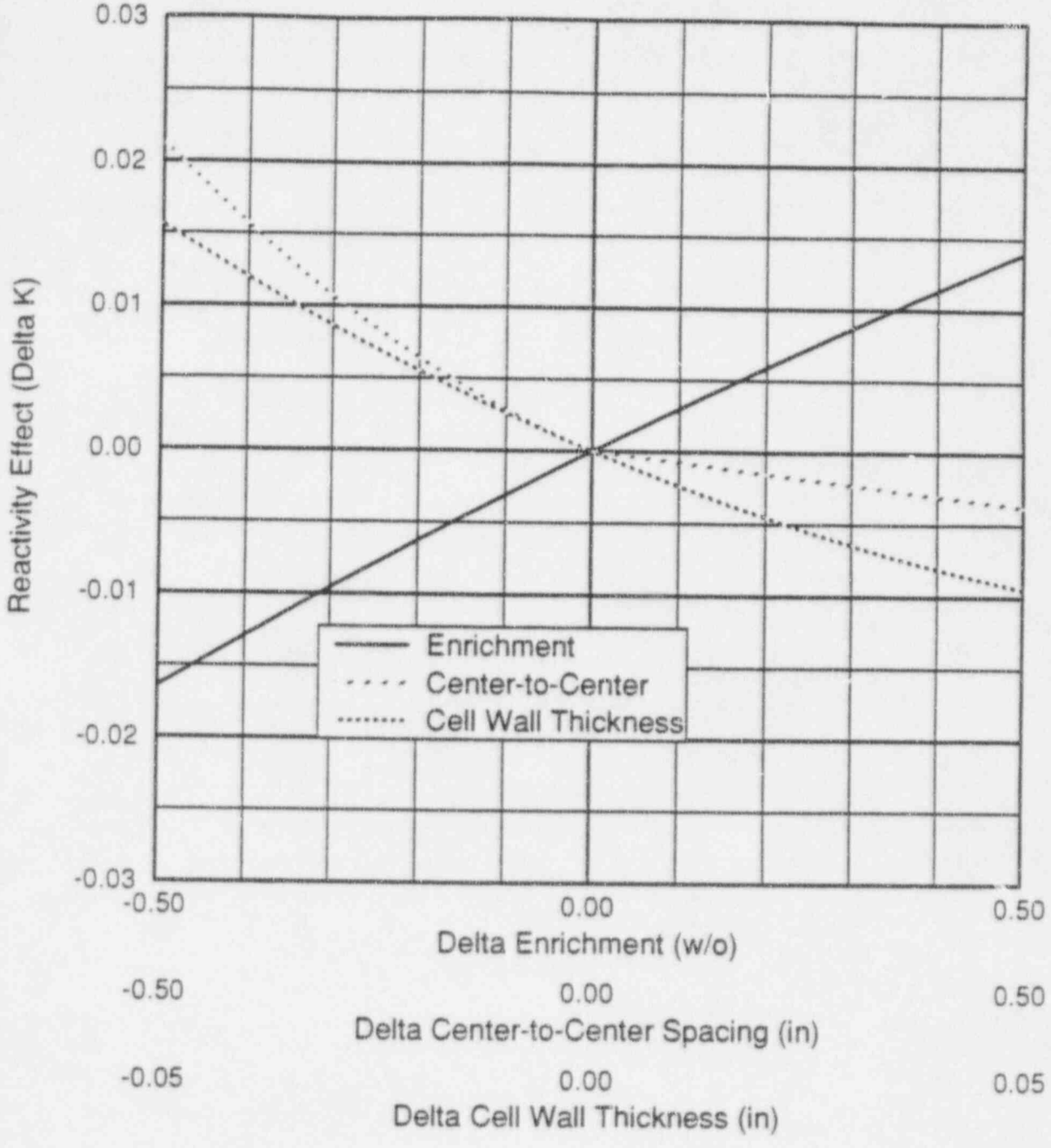

FIGURE 3-5

HIGH DENSITY RACK SOLUBLE BORON WORTH

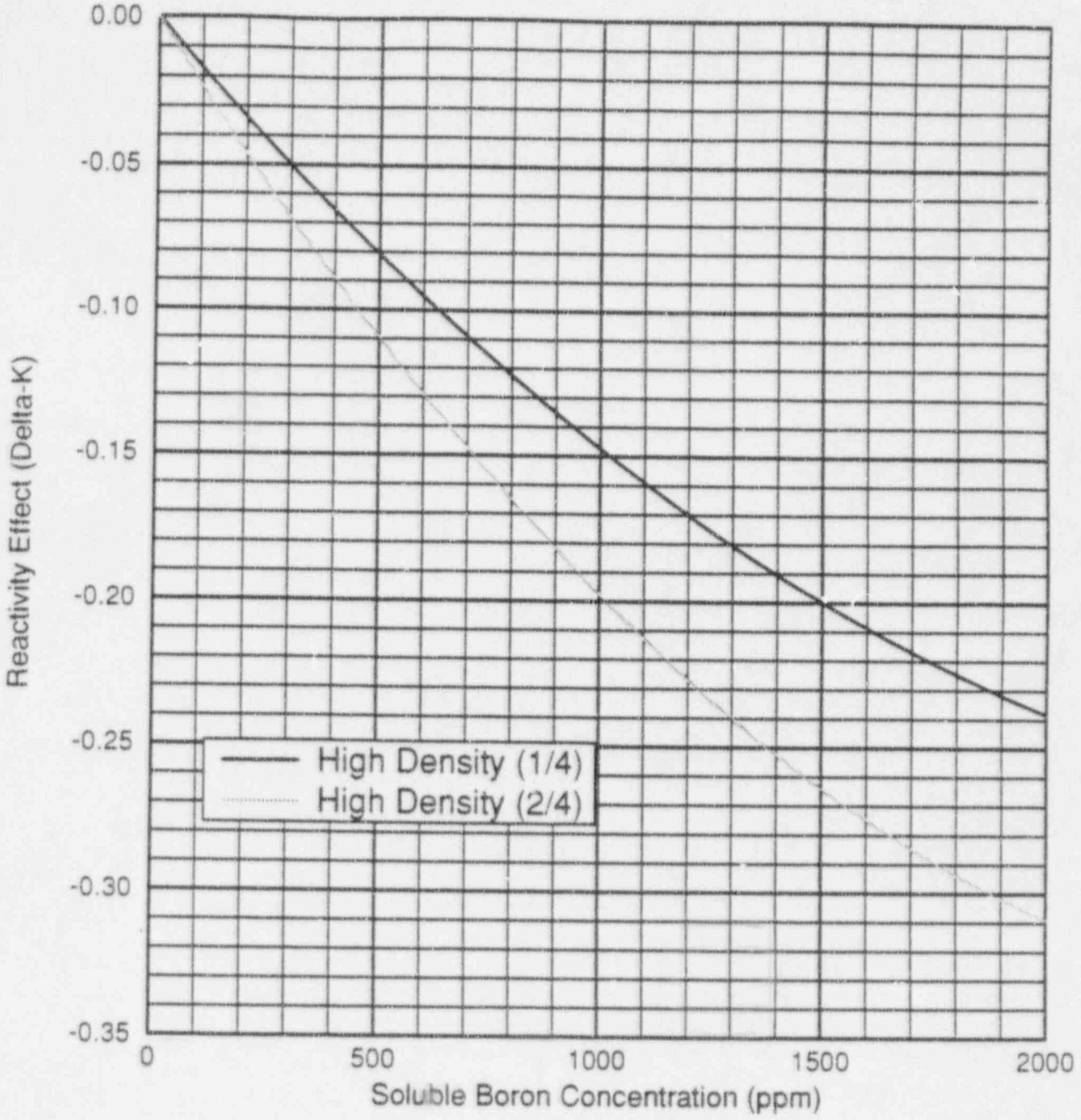

FIGURE 3-6

HIGH DENSITY (2/4) RACK REACTIVITY SENSITIVITIES

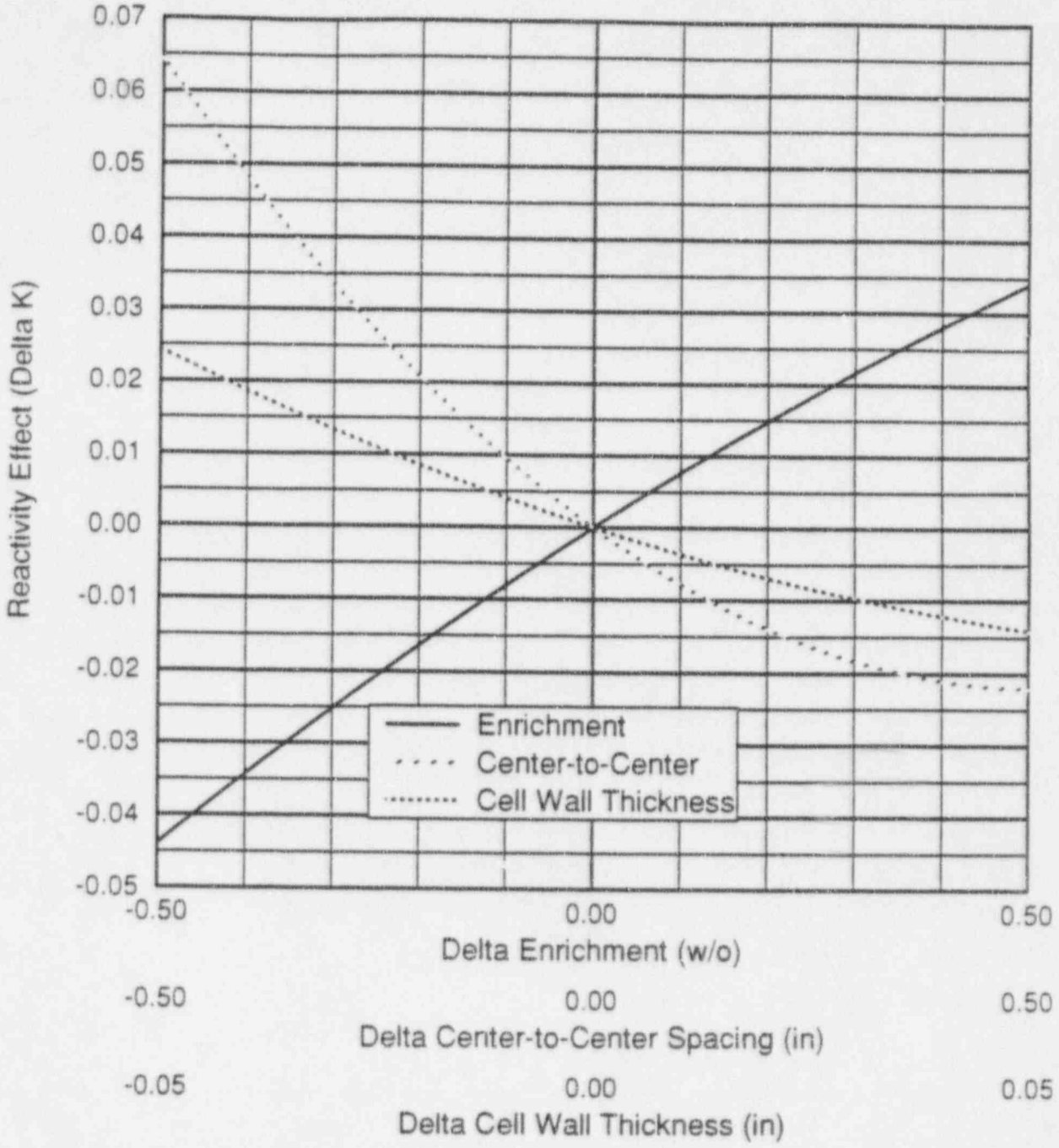

3.2 DECAY HEAT CALCULATIONS FOR THE SPENT FUEL POOL (BULK)

3.2.1 DECAY HEAT ANALYSES

For the proposed installation and use of high density racks, the SFP cooling system's ability to cool the SFPs was evaluated to verify that decay heat can be removed during operating conditions and that acceptable SFP temperatures are maintained. Spent fuel decay heat calculations were performed in accordance with NRC Branch Technical Position ASB 9-2, Residual Decay Energy for Light Water Reactors for Long Term Cooling [Ref. 8].

In accordance with the Updated FSAR for CPSES, the following three conditions were assumed for the purpose of evaluating the spent fuel pool cooling system:

A normal Maximum Design Condition, which corresponds to a normal refueling in one unit while the other unit is operating. Such refuelings occur in the fall (after September 15) or in the spring (before May 31), when Component Cooling Water (CCW), Station Service Water (SSW) and Safe Shutdown Impoundment (SSI) temperatures are relatively low.

A normal Maximum Summer Design Condition, which corresponds to both units operating during the hotter summer months, when CCW, SSW, and SSI temperatures can be relatively high.

An Abnormal Maximum Design Condition, which corresponds to an Emergency Core Offload in one unit while the other unit is operating. This condition is assumed to occur at any time of the year.

Because CPSES has two shared spent fuel pools, the assumed design conditions of Section III.1.h of SRP 9.1.3 [Ref. 8] do not apply. The CPSES design allows for back-to-back refuelings with sharing of the spent fuel storage, which is not accounted for in SRP 9.1.3.

The three design conditions are defined as follows:

Maximum Design Condition

The normal design temperature of the bulk SFP water is less than 150°F for normal operation (and less than 200°F in the event of a single failure in the spent fuel pool cooling system) based on decay heat generation from a normal full core offload at 7 days after shutdown, plus decay heat from the opposite unit's last refueling discharge, plus decay heat from fuel assemblies from a maximum number of previous refuelings in both pools. At least 193 spaces in the spent fuel pools are assumed to remain available to accept one full core in accordance with ANSI N18.2 and ANSI N210. To maximize decay heat loads, outage durations are conservatively assumed to be 30 days for 12 month fuel cycles and 45 days for 18 month fuel cycles. A normal full core offload is conservatively assumed to start at 100 hours after the reactor is subcritical and to be complete at 168 hours (approximately 3 assemblies per hour). Toward the end of the refueling outage, the partially burned assemblies from the last offload are assumed to be reloaded into the core. The number of fuel assemblies from the offload that are retained in the SFPs is assumed to be one-third of a core (either 64 or 65 fuel assemblies) for 12 month cycles and 94 fuel assemblies for 18 month cycles.

The normal design temperature of the SFP heat exchanger (HX) outlet is 140°F to protect the resins in the cleanup system.

The Component Cooling Water (CCW) and Station Service Water (SSW) conditions assumed are representative of one unit operation at full power and one unit shutdown during normal refueling periods.

Maximum Summer Design Conditions

The normal design temperature of the bulk SFP water is less than 150°F for normal operation (and less than 200°F in the event of a single failure in the spent fuel pool cooling system) based on decay heat from the most recent refueling discharge at the end of the outage, plus decay heat from the opposite unit's previous refueling discharge, plus decay heat from a maximum number of previous refuelings in both pools. At least 193 spaces in the spent fuel pools are assumed to remain available to accept one full core in accordance with ANSI N18.2 and ANSI N210.

The normal design temperature of the SFP heat exchanger outlet is 140°F to protect the resins in the cleanup system.

The CCW and SSW conditions are assumed to correspond to both units in MODE 1. The Safe Shutdown Impoundment (SSI) temperature is assumed to be normal maximum (102°F) for two units in MODE 1.

Abnormal Maximum Design Conditions

The SFP water temperatures are maintained at less than 212°F for two loop operation based on an emergency core offload 150 hours after shutdown, plus the most recent refueling discharge 36 days after shutdown, plus the opposite units previous refueling discharge 66 days after shutdown, plus decay heat from a maximum number of previous refuelings in both pools. No failures are assumed coincident with this condition.

The heat removal is assumed to be by one operating unit and one shutdown unit. The SSI temperature is assumed to be normal maximum (102°F).

Table 3-8 shows the assumed SFP loading for the calculation of the decay heat loads for the design conditions which are illustrated in Figure 3-7. Conservative bounding analyses were performed which assumed a total capacity of 3386 spent fuel assemblies. The resulting heat loads bound the use of high density racks in SFP2.

These three design condition heat loads are illustrated on Figure 3-7 for 18 month fuel cycles which is the current Licensing Basis for CPSES. Figure 3-7 shows a 9.2 X 10^6 BTU/hr increase in heat load for an increase in storage capacity from 1116 to 3386 assemblies. Figure 3-7 also shows that 1.0 X 10^6 BTU/hr is added by the change from 1116 to 1291 assemblies. The SFP cooling system was evaluated based on design modifications to the cooling and HVAC systems which will be implemented prior to the use of racks in SFP2. The calculated temperatures satisfy the design requirements for each design condition above. Therefore, the maximum spent fuel bulk temperatures associated with storage of additional spent fuel are acceptable and the SFP cooling system will be adequate for use of high density racks.

TABLE 3-8

SFP LOADING FOR DECAY HEAT LOADS

18 Month Cycles	No. of FA	Heat Load X 10^6 BTU/hr
Emergency Core Offload Reserve	193	0
Full Core Offload (2nd Unit)	193	34.8@168 hours
Refueling Discharge (1st Unit)	94	6.9@52 days
Previous 6 Discharges:		
At 1.5 years	94	1.21
At 2.0 years	94	0.92
At 3.0 years	94	0.67
At 3.5 years	94	0.61
At 4.5 years	94	0.52
At 5.0 years	94	0.50
Subtotal: (1116)	1044	46.3
94 FA at 6.0 years	94	0.49
94 FA at 6.5 years	94	0.47
Subtotal: (1291)	188	0.96
At 7.5 years	94	0.45
At 8.0 years	94	0.45
At 9.0 years	94	0.44
At 9.5 years	94	0.43
At 10.5 year	94	0.43
At 11.0 year	94	0.42
At 12.0 year	94	0.42
At 12.5 year	94	0.41
At 13.5 years	94	0.41
At 14.0 years	94	0.40
At 15.0 years	94	0.39
At 15.5 years	94	0.39
At 16.5 years	94	0.38
At 17.0 years	94	0.38
At 18.0 years	94	0.37
At 18.5 years	94	0.37
At 19.5 years	94	0.36
At 20.0 years	94	0.36
At 21.0 years	94	0.34
At 21.5 years	94	0.33
At 22.5 years	94	0.33
At 23.0 years	94	0.32
Subtotal: Total Rerack	2068	8.55
Spares	86	0
Total (32 Discharges)	3386	55.7

FIGURE 3-7

SPENT FUEL POOL DESIGN HEAT LOADS

18 MONTH FUEL CYCLE

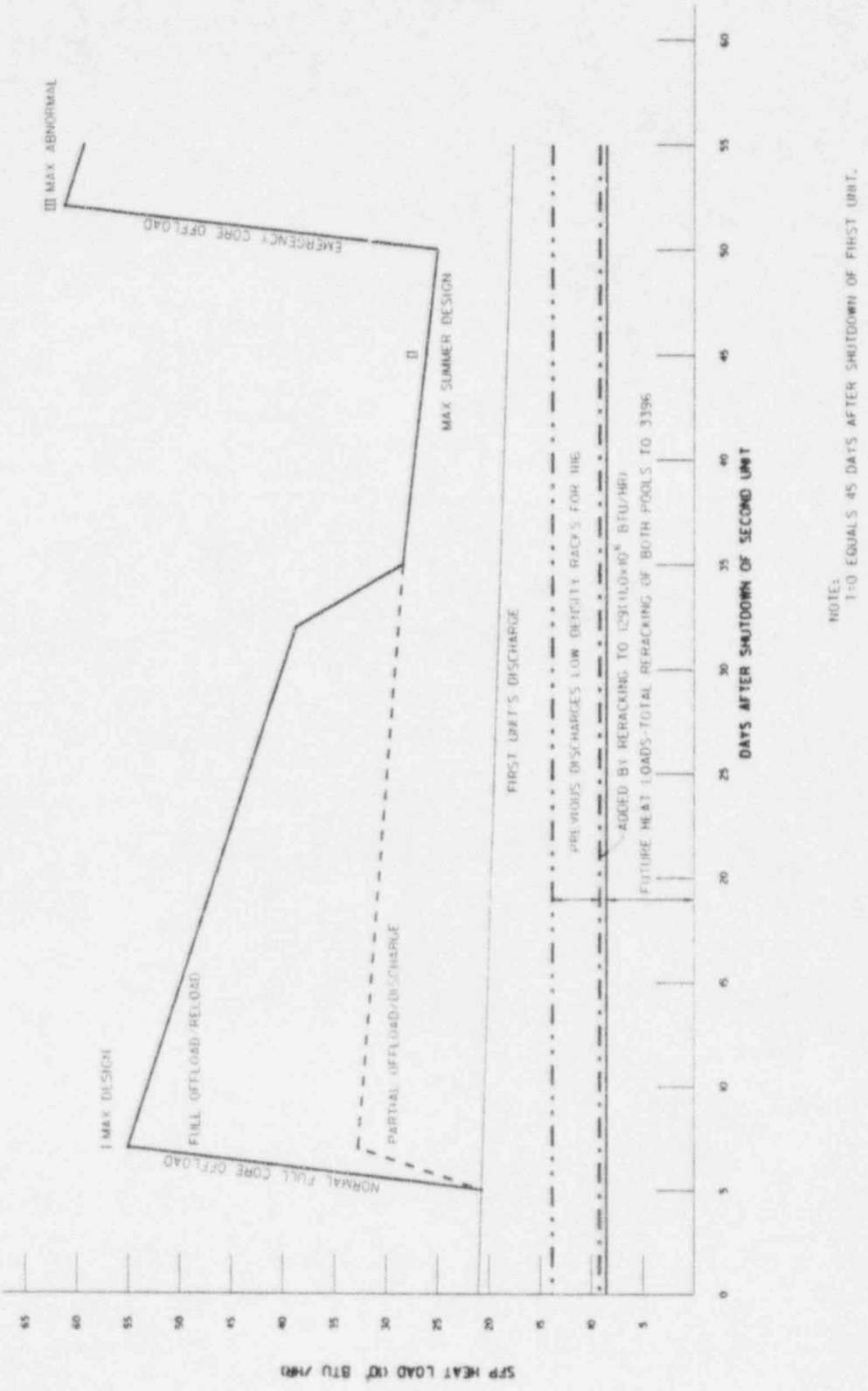

NOTE:
1-0 EQUALS 45 DAYS AFTER SHUTDOWN OF FIRST UNIT.

3.2.2 CHANGES TO THE SFP COOLING SYSTEM DESIGN

The design temperatures of the SFP cooling and cleanup system are in accordance with ANSI N210-1976 [Ref. 27], and the design temperatures of the SFP cleanup system are consistent with the intent of SRP Section 9.1.3.III.1.d [Ref. 8]. Accordingly, the maximum normal design temperature of the SFPs is 150°F based on the ANSI N210 and ACI 318 [Ref. 25] requirements for normal or any other long term period. To satisfy the intent of the SRP, the maximum design temperature of water to the demineralizers is less than 140°F for maximum normal heat loads with normal cooling systems in operation, assuming a single active failure.

SFP cooling is provided by the Spent Fuel Pool Cooling and Cleanup System (see Figure 3-8), which consists of two cooling loops, each with a purification loop downstream of the HX. The suction lines, protected by SFP suction screens, are located approximately four feet below the normal SFP water level. The return lines terminate approximately six feet above the fuel assemblies. An antisiphon hole is provided in the return lines one foot below normal water level. Cleanup is provided by the purification loops and one surface skimmer loop. One cooling loop per pool containing spent fuel is normally in operation to remove decay heat. Heat is transferred via the SFP heat exchangers to the Component Cooling Water (CCW) system for each unit. SFP HX 1 is cooled by Unit 1 CCW and SFP HX 2 is cooled by Unit 2 CCW. CCW heat loads are transferred to the SSI via the associated SSW systems for each unit.

When heat loads are sufficiently low, one SFP cooling loop can cool one SFP. The increase in heat loads due to use of high density racks (i.e. addition of capacity in SFP2) will require both trains of cooling to be capable of sharing the cooling load from the same pool to maintain the temperature within design limits. The current licensing basis of the SFP cooling system does not provide for alignment of both loops to the same pool. Prior to the use of racks in SFP2, design modifications will be implemented to provide the capability of aligning both cooling loops to one pool. Because the SFP cooling pumps are not protected from loss of suction, alignment of both loops to one pool could present a potential common mode failure. Design changes will be implemented to prevent such failures.

In the event of a single failure, one SFP cooling water pump using either heat exchanger is

required for cooling both pools to maintain temperatures below 200°F. Prior to the use of racks in SFP2, design modifications will be implemented to provide the capability of aligning each separate cooling loop to both pools. The design of the SFP cooling system and pool area HVAC exhaust registers do not practically allow connection of a single SFP cooling loop to two pools. The exhaust registers in the side of the pool are too low to accommodate pool level changes which would result from aligning a cooling loop to both pools. Design changes will be implemented to elevate or relocate the exhaust registers in the pool area.

3.2.3 IMPACT ON SFP MAKEUP WATER SYSTEMS

Makeup water requirements for evaporation are less than 2 gpm per pool at the normal maximum temperature of 150°F and are less than 10 gpm per pool at 212°F. Normal makeup water, to compensate for evaporation losses, is supplied from the demineralized water supply system. In the case of a failure or malfunction of the demineralized water supply system, makeup water could be supplied by the Reactor Makeup Water System (RMWS) from either unit.

The minimum time to boiling if cooling to one or both SFPs were lost was evaluated. Following loss of SFP cooling during normal conditions, the minimum time from 150°F to boiling is greater than 3 hours for the normal Maximum Design Condition and greater than 7 hours for the normal Maximum Summer Design Condition. Indication of loss of cooling (i.e., increases above the normal maximum temperature or loss of pool level) is subject to alarms in the control room. Thus, there is sufficient time to detect the loss of cooling and to restore at least one train of the two trains of safety related cooling prior to boiling.

The RMWS, whose associated pumps, piping and valves are designated as seismic Category I and Safety Class 3, are able to supply water at a rate which would allow restoration of cooling and which exceeds the boil-off rates for the maximum design conditions. In the event of a loss of water from a pool to the minimum suction elevation of 854 feet, there is sufficient volume in each seismic Category I RMWS storage tanks to provide makeup to restore and maintain levels until cooling is restored.

If RMWS is not available for SFP makeup water, there is sufficient time to provide an alternate means of makeup from the fire protection system. Fire hose stations in the area of the SFPs are capable of suppiying makeup in excess of the boil-off rates. Since the fire protection system makeup is from the SSI, the supply of fire protection water is essentially unlimited.

Therefore, the SFP makeup water sources are sufficient to restore and maintain the water levels in the SFPs for the duration of a loss of cooling to the pools.

3.2.4 IMPACT ON COMPONENT COOLING WATER SYSTEM

The SFP heat loads for various plant operating modes under the previously discussed conditions were revised along with total heat loads of CCW HX and associated CCW temperatures. The increases in heat loads do not exceed the bounding design of CCW.

Therefore, the increase does not impact existing CCW temperature limits.

3.2.5 IMPACT ON SERVICE WATER SYSTEM

The SSW systems remove the additional SFP heat loads rejected by the CCW heat exchangers to the SSI, which is the plant's ultimate heat sink. The maximum increase in heat rejection to the SSI is 1.0×10^6 BTU/hr for the additional 175 storage locations. The bounding increase in heat rejection for an increase in storage capacity from 1116 to 3386 assemblies is 9.2×10^6 BTU/hr. These increases in heat loads do not exceed the bounding design of SSW and the SSI. Therefore, SSW and the ultimate heat sink will continue to perform their intended safety functions.

3.2.6 IMPACT ON SFP CLEANUP SYSTEM

The impact of the use of high density racks on the CPSES SFP cleanup system was evaluated. The system is designed to respond to varying water purity levels rangir.. from equilibrium conditions of undisturbed fuel storage to transient, relatively high impurity conditions due to refueling activities. The increased spent fuel storage capacity does not affect the design basis or functional requirements of the cleanup system.

In order to protect the resins in the demineralizers, the maximum temperature of the water to the purification loops is 140°F for either one or two pump operation.

Refueling activities involving mixing of pool water with reactor coolant and frequent moves of crud laden fuel present the maximum load for the CPSES cleanup system. Operational experience has demonstrated that SFP waterborne radionuclide concentrations increase following the onset of fuel handling activities and quickly decrease after such activities cease. The increase during fuel handling is the result of the mechanical dislodging or dissolution of corrosion products adhering to the fuel assembly surfaces.

Aged fuel (greater than 5 years) presents a low potential for increasing the waterborne activity in the pool. Fission products within the cladding decay significantly over time, and due to the corrosion resistance of the cladding, the decaying fission products from an assembly should be largely retained within the cladding. Most of the deposited corrosion products on the exterior of the fuel assemblies are dislodged during the initial movements of those assemblies. The remaining exterior particles will decay significantly during long term storage. Therefore, due to the decay of the radioactive sources inside and outside the fuel cladding and the long term stability of the cladding material, the aged assemblies do not contribute significantly to the waterborne activity and the cleanup system load.

Short term increases in the SFP source term are dependent on crud transport, fission product release, or system cross-flow resulting from refueling operations. Since these circumstances are essentially independent of the quantity of spent fuel stored, the cleanup system is negligibly impacted by the increased spent fuel storage capability. The impact of ion exchange resin replacement on the radioactive waste system due to longer fuel storage is discussed in Section 5.2.1.

3.2.7 IMPACT ON HVAC SYSTEM

The Fuel Building HVAC system, which serves the general areas of the SFPs and the spent fuel pool cooling system, is a nonsafety-related system designed to maintain a slight negative pressure with respect to the environs. The environmental design of equipment in general areas of the Fuel Building are based on maximum normal air temperatures of either 104°F or 122°F. As a result, the design requirement for the Fuel Building HVAC system as described in the FSAR [Ref. 3] is to maintain air temperatures in general areas below the environmental design parameters for normal conditions. A preliminary evaluation of the ability of the Fuel Building HVAC to maintain air temperatures within this limit determined that the increase in SFP heat loads will affect the Fuel Building HVAC system during normal operation. Design modifications will be implemented prior to storage of spent fuel in SFP2 to either decrease the heat loads or increase cooling to the areas containing safety related equipment .

During normal conditions, as the SFP water temperature increases, the evaporation rate from the pool increases. For this purpose, mist eliminators are provided in the pool exhaust to remove entrained moisture particles from the exhaust air steam. As discussed in section 3.2.2, the increase in the number of spent fuel assemblies stored in the CPSES SFPs as a result of use of high density racks will not increase the normal pool temperatures past the maximum temperature of 150°F. Fogging will not occur on the operating floor, since maximum humidity is calculated to be less than 100%.

The Fuel Building HVAC exhausts to the Primary Plant Ventilation system which has both ESF Filtration Units for LOCA and Non-ESF Filtration Units for normal operation. There is no credit for either type of filtration in the fuel handling accident analysis. The Non-ESF units will not be affected by the normal operation of the spent fuel pool cooling system. The ESF units contain demisters and heaters to ensure the efficiency of the iodine adsorbers are maintained. Therefore, the PPV Filtration Units will continue to perform their design function.

In the event of a loss of the non-safety ventilation, the temperature and humidity in the Fuel Building will increase due to the storage of spent fuel in SFP2. Preliminary evaluations show that these increased temperatures and humidity can be accommodated by the existing Class 1E equipment in accordance with the FSAR. Prior to the use of racks in SFP2, equipment qualification updates will be implemented to document the qualification.

The pump room coolers are safety-related and designed to maintain air temperatures in the pump rooms below 122°F during normal and accident conditions. Calculations demonstrate adequate margin exists to meet the design requirement for normal conditions. For accident conditions, the evaluation determined that the pump room coolers are acceptable if the piping heat loads are reduced (e.g. insulation added) or flow of safety chilled water to the cooling coils is increased. A design modification to ensure equipment qualification temperatures are maintained will be implemented prior to the storage of spent fuel in SFP2.

Therefore, the design of the Fuel Building and the pump room HVAC systems will be adequate for additional heat loads caused by use of high density racks.

FIGURE 3-8

SPENT FUEL POOL COOLING AND CLEANUP SYSTEM

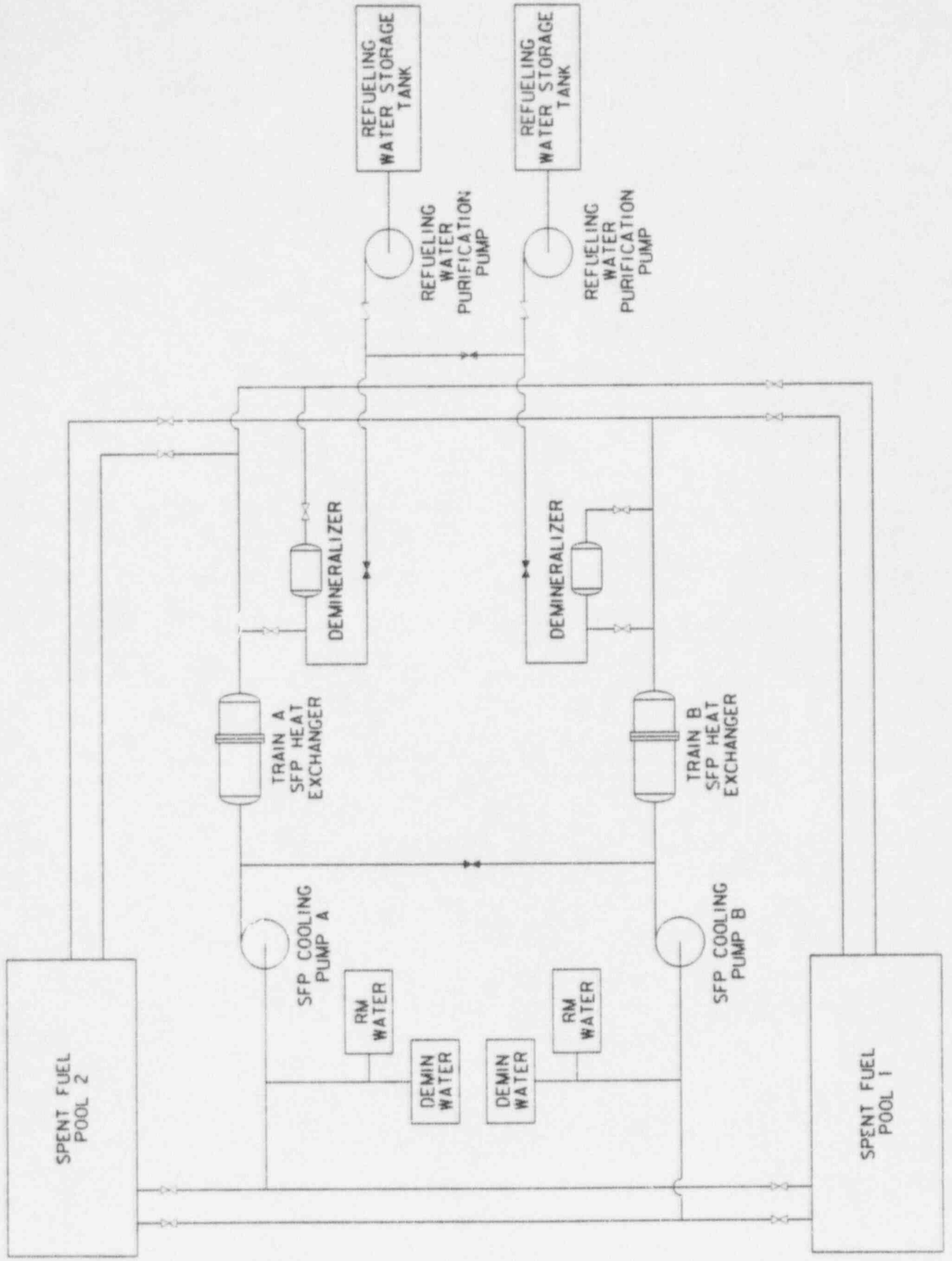

3.3 THERMAL-HYDRAULIC ANALYSIS FOR SPENT FUEL COOLING

Thermal-hydraulic analyses were performed to determine the maximum fuel clad temperatures which may occur as a result of using the high density racks. As discussed below, the results of the analyses of SFP cooling show that the design will be capable of maintaining the design temperatures given in section 3.2.

3.3.1 CRITERIA

The criteria used to determine the acceptability of the design from a thermal-hydraulic viewpoint is summarized as follows:

1. The design must allow adequate cooling by natural circulation and by flow provided by the SFP cooling system. The coolant will remain subcooled at all points within the pool when the cooling system is operational. When the cooling system is postulated to be inoperable, the temperature of the fuel cladding shall be sufficiently low that no structural failures occur and that no safety concerns exist.

2. For normal operations, the maximum pool temperature shall not exceed 150°F. For conservatism, the temperatures of the storage racks and the stored fuel are evaluated assuming that the temperature of the water at the inlet to the storage cells is 150°F during normal operation.

3. The rack design must not allow trapped air or steam.

4. Direct gamma heating of the storage cell walls and the intercell water must be considered.

3.3.2 KEY ASSUMPTIONS

1. All storage cells filled (4/4).

2. The maximum spent fuel assembly decay heat output is 62.23 BTU/sec per assembly following 150 hours decay after shutdown. For conservatism, this value was used for all storage locations.

3. The maximum temperature of the water at the inlet to the storage cells is 150°F when the cooling system is operational.

4. Under postulated accident conditions, when no SFP cooling systems are operational, the maximum temperature at the inlet to the cells is assumed to be equal to the saturation temperature at the top of the SFP (212°F). This number is conservative, since sufficient cold water is constantly being added to the SFP to maintain water level.

3.3.3 ANALYTICAL METHOD AND CALCULATION

A natural circulation calculation is employed to determine the thermal-hydraulic conditions within the spent fuel storage cells. The model used assumes that downflow occurs in the peripheral gap between the pool walls and the outermost storage cells and lateral flow occurs in the space between the bottom of the racks and the bottom of the pool. The effect of flow area blockage in the rack is conservatively accounted for and a multi-channel formulation is used to determine the variation in axial flow velocities through the various storage cells. The hydraulic resistance of the storage cells and the fuel assemblies is conservatively modeled by applying uncertainty factors to loss coefficients obtained from various sources.

The solution is obtained by iteratively solving the conservation equations (mass, momentum and energy) for the natural circulation loops. The flow velocities and fluid temperatures that are obtained are then used to determine the fuel cladding temperatures. An elevation view of a typical model is sketched in Figure 3-9 where the flow paths are indicated by arrows. Note that each cell shown in that sketch actually corresponds to a row of cells that is located at the same distance from the pool walls. This is more clearly shown in a plan view, Figure 3-10.

As shown in Figure 3-10, the lateral flow area underneath the storage cells decreases as the distance from the wall increases. This counteracts the decrease in the total lateral flow that occurs because of flow that branches up and flows into the cells. This is significant because the lateral flow velocity affects both the lateral pressure drop underneath the cells and the turning losses that are experienced as the flow branches up into the cells. These effects are considered in the natural circulation analysis.

The most recently discharged or "hottest" fuel assemblies are assumed to be located in various rows during different calculations in order to ensure that they may be placed anywhere within the pool without violating safety limits. In order to simplify the calculations, each row of the model was composed of storage cells having a uniform decay heat level. This decay heat level may or may not correspond to a specific batch of fuel, but the model is constructed so that the total heat input is correct. The "hottest" fuel assemblies are assumed to be placed in a given row of the model in order to ensure that conservatively accurate results are obtained for those assemblies. In fact, the most conservative analysis that can be performed is to assume that all assemblies in the pool (or rows in the model) have the same maximum decay heat rate. This maximizes the total natural circulation flowrate which leads to conservatively large pressure drops in the downcomer and lateral flow areas which reduces the driving pressure drop across the limiting storage locations.

For the high density racks, the most conservative loading pattern is used. Since the natural circulation velocity strongly affects the temperature rise of the water and the heat transfer coefficient within a storage cell, the hydraulic resistance experienced by the flow is a significant parameter in the evaluation. In order to reduce the resistance, the design of the inlet area of the racks has been chosen to increase this flow area. Each storage cell has one or more flow openings as shown in Figure 3-11. The use of these large or multiple flow holes precludes the possibility that all flow into the inlet of a given cell can be blocked by debris or other foreign material that may get into the pool. In order to determine the impact of a partial blockage on the thermal-hydraulic conditions in the cells, an analysis is also performed for various assumed blockages.

3.3.4 RESULTS

Normal Operation

Assumptions: a) Cooling system operational.

b) 150 hours after shutdown, Decay Heat = 62.23 BTU/second/assembly.

c) Uniform decay heat loading in pool. No credit for lower actual heat input.

d) Peak rod has 60 percent more heat output than average rod.

e) A nominal water level is 24 feet above the top of the fuel storage racks.

Results of the analysis show that no boiling occurs at any point within the storage racks when the normal cooling system is in operation or whenever pool temperature is maintained within its allowable limits.

Flow Blockage Analysis

Assumptions: a) 150 hours after shutdown.

b) Temperature of water at inlet to storage racks = 150°F.

Results of the analysis show that should up to 80% flow blockage occur, there would be no boiling inside the cells. Because of the large or multiple flow openings that are used in the Westinghouse storage racks, it is highly improbable that a complete blockage could occur.

Abnormal Condition

Under postulated accident conditions where all SFP cooling systems become inoperative, makeup water is provided. Although it is highly unlikely that a complete loss of cooling capability could occur, the racks are analyzed to this condition.

Assumptions: a) It is conservatively assumed that temperature of water at the inlet to spent fuel racks is 212°F which corresponds to the saturation temperature at the top of the pool.

b) A nominal water level of 20 feet above the top of the racks is maintained.

c) The assemblies that are evaluated are at 150 hours after shutdown.

d) The peak rods are assumed to have 60 percent greater heat output than average rods.

e) All storage cells are filled (4/4) and all downflow occurs in the peripheral gap.

Results of this analysis show that due to the effects of natural circulation, the fuel cladding temperatures are sufficiently low to preclude structural failures.

FIGURE 3-9

TYPICAL SFP NATURAL CIRCULATION MODEL

(ELEVATION VIEW)

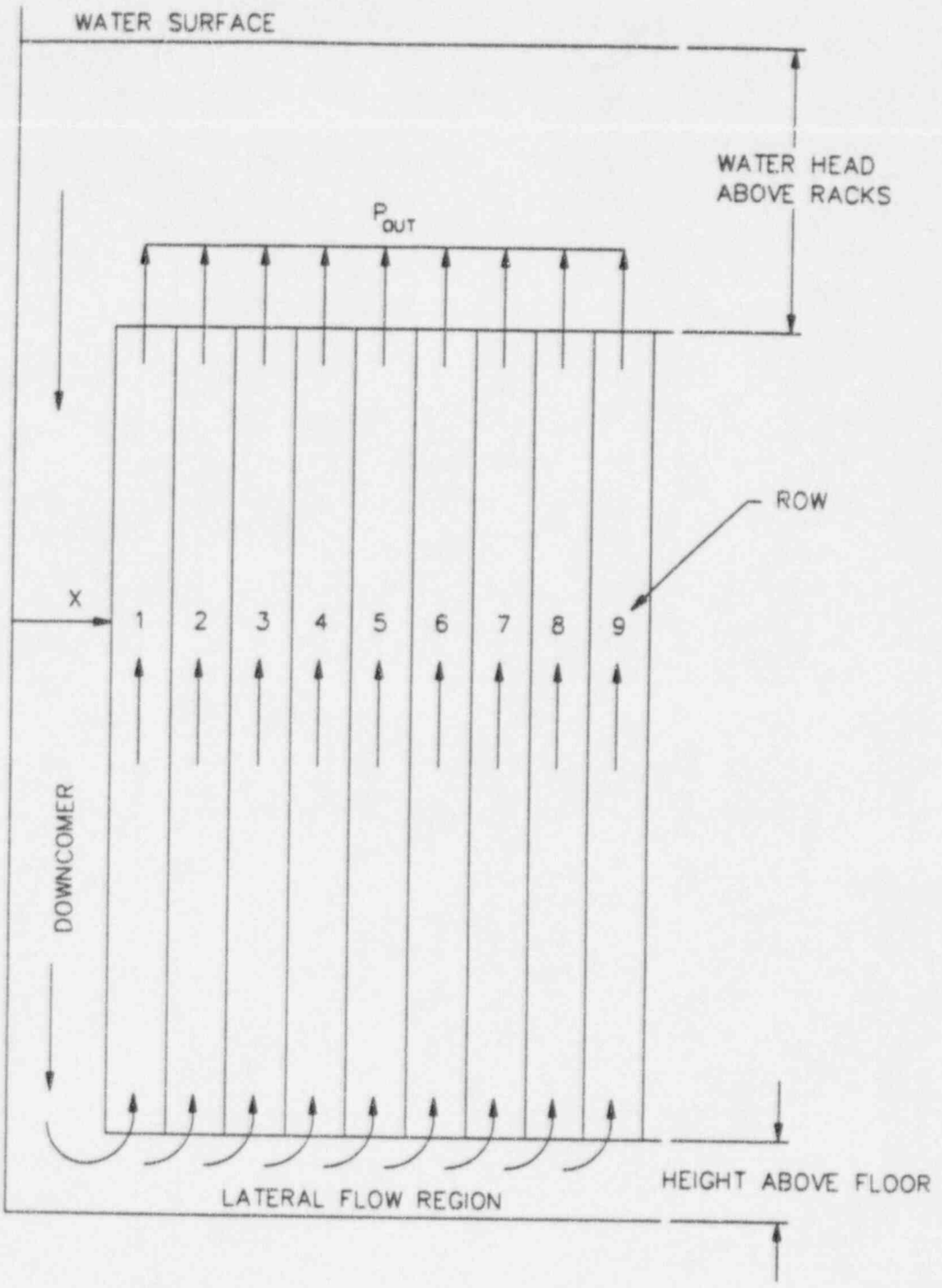

FIGURE 3-10

TYPICAL SFP NATURAL CIRCULATION MODEL

(PLAN VIEW)

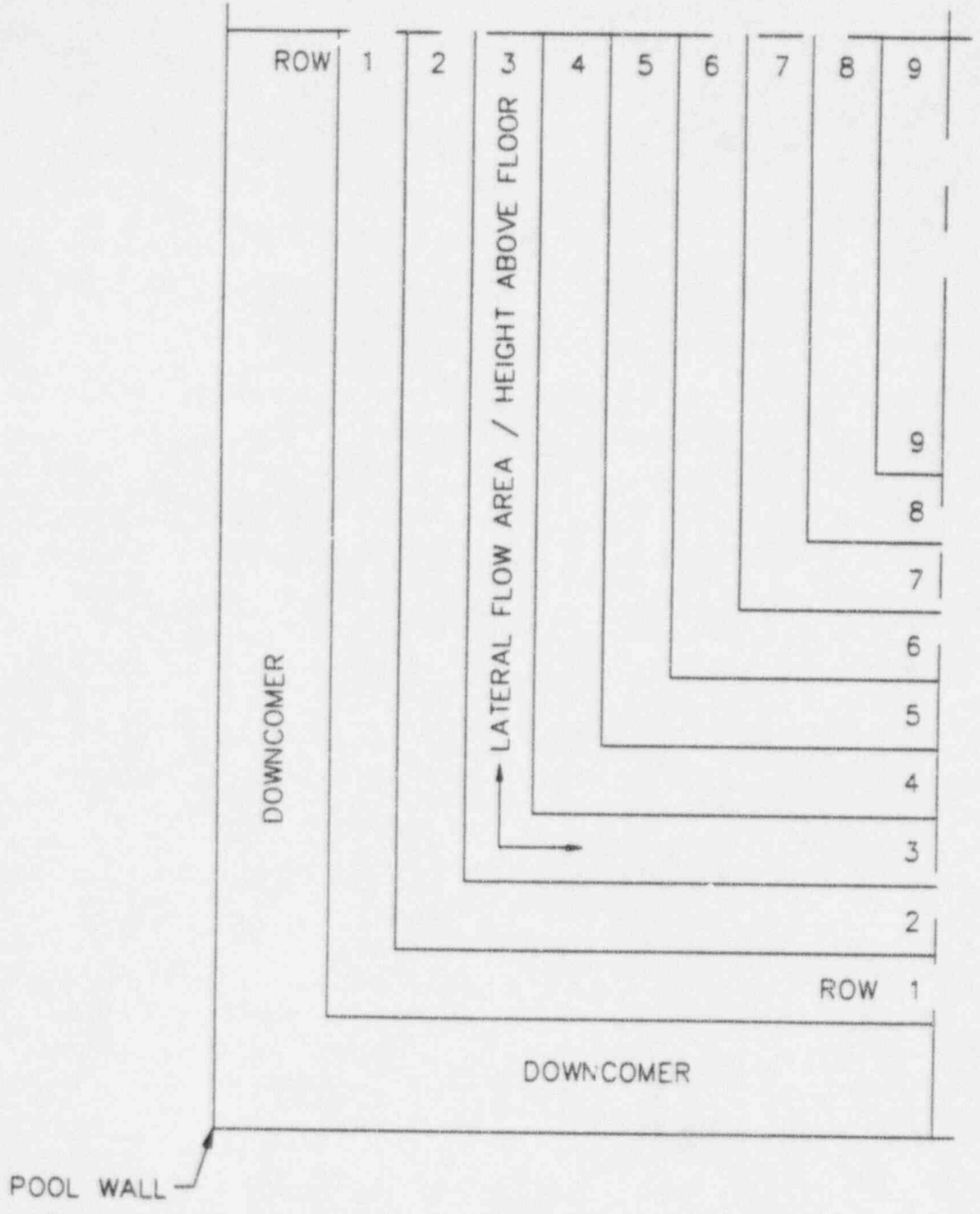

FIGURE 3-11

HIGH DENSITY RACK INLET FLOW MODEL

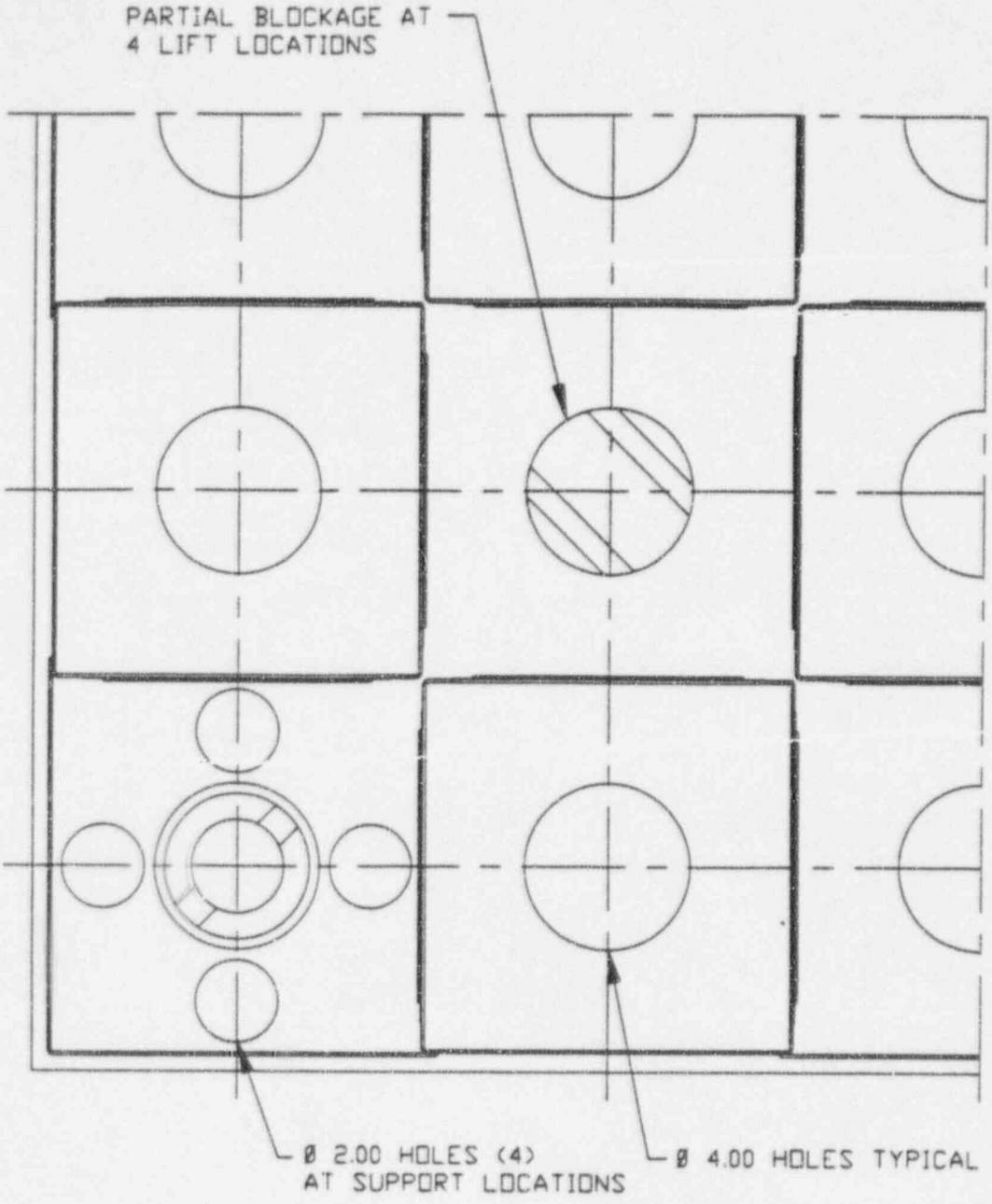

3.4 POTENTIAL FUEL AND RACK HANDLING ACCIDENTS

This section discusses the method for moving the racks into SFP2, changes to fuel handling procedures that will be required by rack installation, and the effects of potential fuel and rack handling accidents . As discussed below, postulated accidents will not cause the neutron multiplication factor in the pool to exceed 0.95 and will not cause loss of cooling for the SFP.

3.4.1 INSTALLATION METHOD

The installation of the new high density racks will be accomplished in accordance with the following considerations and guidelines:

- Movements of the high density racks within the SFP area will be performed using a rack handling crane and special rigging as required. The crane will be safety related and single-failure-proof.

- Rack installation will be performed in SFP2 only. SFP1 contains low density racks and remains unchanged. During rack installation activities, SFP2 will not contain spent fuel or other irradiated material. SFP2 will be dry. However, there will be spent fuel in SFP1 during the SFP2 rack installation.

- Load handling operations in the SFP area will be conducted in accordance with the criteria of NUREG-0612, "Control of Heavy Loads at Nuclear Power Plants," [Ref. 29]. The existing Fuel Building Overhead Crane, which travels in the east-west direction is a single-failure-proof crane but cannot travel over SFP1 or SFP2. This crane will be used to lift the racks from the Fuel Building loading area to the SFP area and place the racks on a temporary platform. A rack handling crane will be installed in the Fuel Building during the rack installation process to move the racks from the platform to SFP2. See Figures 3-12 and 3-13 for the Safe Load Areas for SFP2 rack installation.

3.4.2 RACK HANDLING CRANE AND PLATFORM

The existing fuel handling bridge crane is rated for a lifting load of 4,000 lb, while the heaviest rack weighs approximately 20,600 lb. Therefore the rack installation process will require the use of a rack handling crane for lifting the racks from the temporary platform to the pools. The rack handling crane will be erected, installed, and tested specifically for use during the rack installation process. The crane has been designed for a hoist capacity of 30,000 lb. The crane is safety related and single-failure-proof.

Operational tests will be performed on the rack handling crane prior to installation, and in-place testing will be performed prior to initial use. Rated load tests will be performed at the factory prior to shipment. A full performance test at the rated load will also be conducted at the factory prior to shipment and final field erection. Furthermore, a functional test will be conducted each time the rack handling crane is assembled for use in the rack installation process, after having been disassembled.

Crane operators will be trained in accordance with Chapter 2-3 of ANSI B30.2-1990 [Ref. 27]. The design and operation of the crane complies with Section 5.1.1 of NUREG-0612 [Ref. 29], on general criteria. The operation of the crane also complies with Option 2 of Section 5.1.2 of NUREG-0612, which covers cranes used near SFP areas, by utilizing mechanical stops to prevent the crane from passing a heavy load over a storage rack containing spent fuel.

A temporary platform will be placed over the wet cask transfer area during the rack installation process. The wet cask transfer area is located midway between SFP1 and SFP2 and can be accessed by both the overhead crane and the rack handling crane. The temporary platform provides a working area for the transfer of loads between the fuel building overhead crane and the rack handling crane. The most convenient location for the platform has been determined to be the east side of the wet cask transfer area.

3.4.3 INSTALLATION SEQUENCE

The rack installation will involve only SFP2 and will follow the sequence described in the following paragraphs. The pool will be dry during high density rack installation in SFP2. Safe load areas will be used throughout the rack installation effort as shown in Figures 3-12 and 3-13. The racks will be brought from storage to the Fuel Building loading bay and lifted using the existing Fuel Building Overhead Crane onto the temporary platform. They will then be transferred to the rack handling crane and eventually be placed in the pool. The use of mechanical stops and/or electrical interlocks will prevent loads from being lifted over the fuel transfer canal or SFP1.

The first step in the rack installation process consists of moving the existing fuel handling bridge crane to the south end of the SFP operating deck, placing the temporary platform over the wet cask transfer area, installing the rack handling crane on the existing bridge crane rail for use in the pool area, removing the rail stops at the north end of SFP2, and removing other interferences identified in the Fuel Building. Mechanical stops will be installed on the bridge crane rail south of the wet cask transfer area which will prevent the rack handling crane from moving over SFP1.

The next step in the sequence consists of placing the racks in the pool. A general order needs to be followed because of protrusions extending from the north and south SFP walls, requiring that certain north and south perimeter racks be installed before the installation of adjacent racks. The following identifies the rack quantity and size.

Quantity	Description
3	High Density rack 11 x 14 array
6	High Density rack 12 x 14 array

Three racks (12 x 14) are to be installed along the south wall of SFP2. Three racks (12 x 14) are to be installed along the north wall of SFP2. Finally, three racks (11 x 14) are installed between the 12 x 14 racks in the center of SFP2. The final sequence of installation of the racks is flexible as long as the existing interferences are accounted for in the installation process. After final installation, the spent fuel racks are levelled.

The final step consists of removing the rack handling crane from the SFP area and removing the temporary platform and the mechanical stops on the bridge crane rail to allow movement of the existing fuel handiing bridge crane.

FIGURE 3-12

RACK INSTALLATION SAFE LOAD AREA

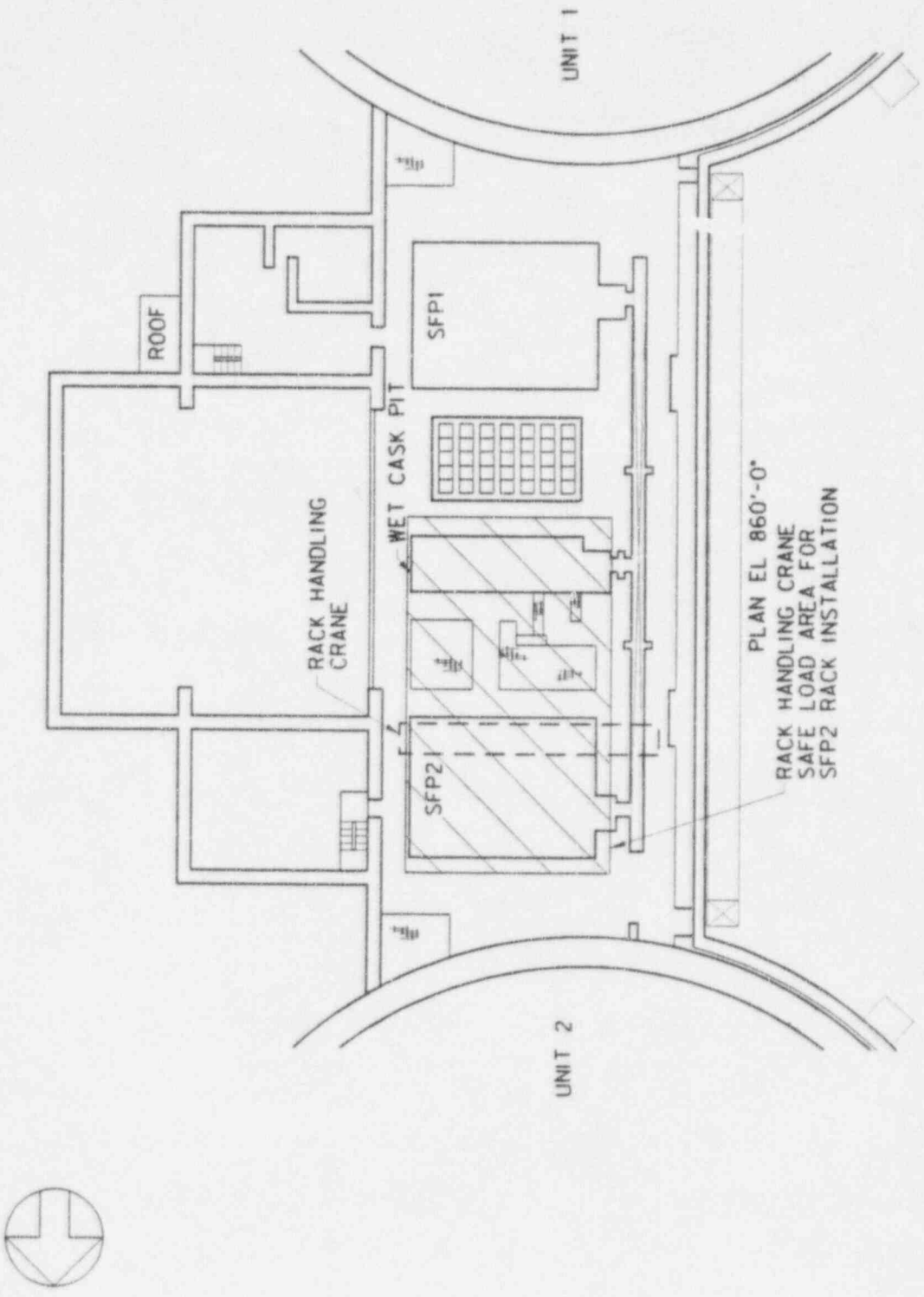

FIGURE 3-13

RACK INSTALLATION SAFE LOAD AREA

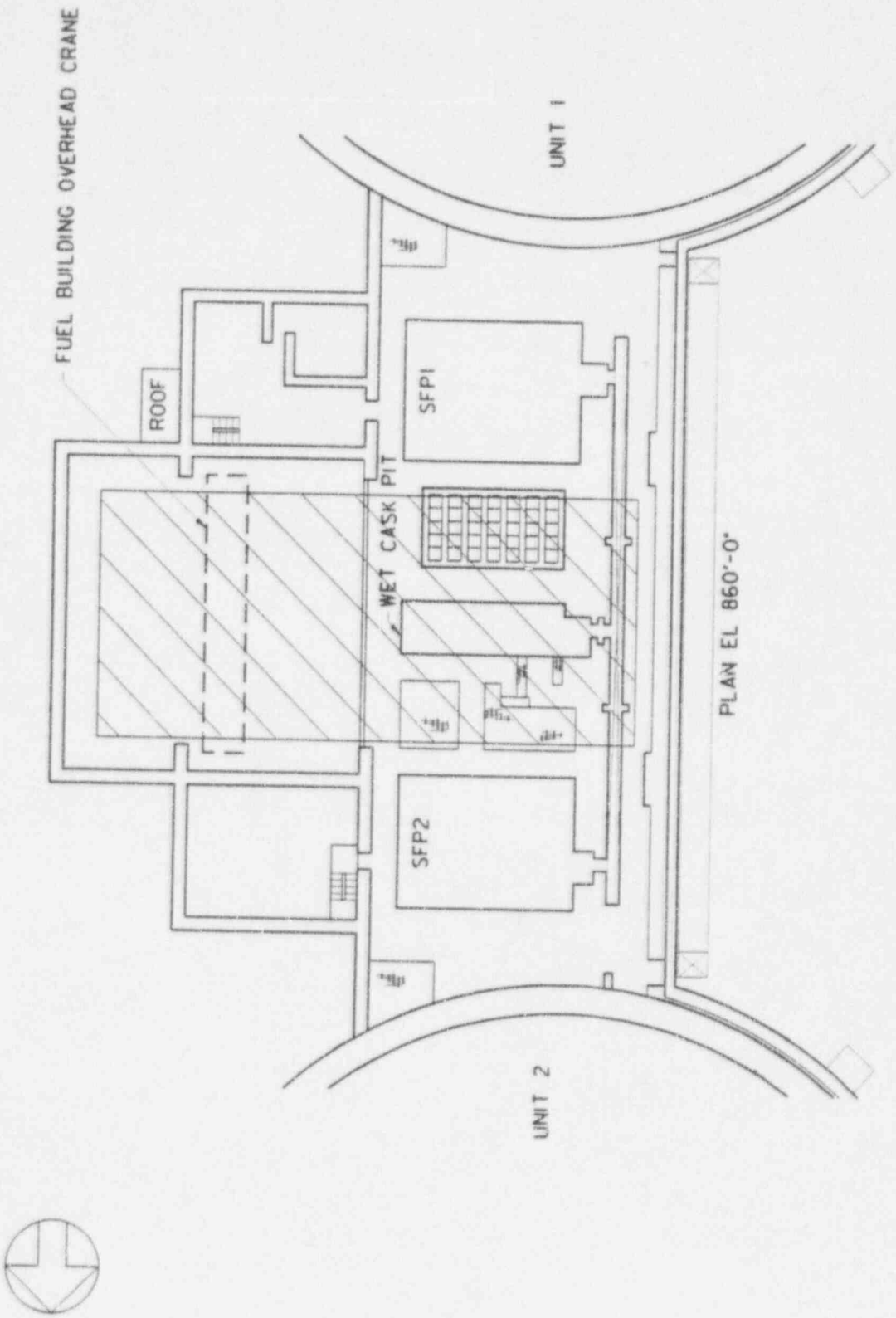

3.4.4 FUEL HANDLING PROCEDURES

The placement of both new and burned fuel in the high density racks in SFP2 will be administratively controlled to satisfy the criticality requirements discussed in this report. A 1 out of 4 (1/4) placement array or a 2 out of 4 (2/4) placement array will be allowed for assemblies based on the initial enrichment and burnup criteria given in Figure 3-3.

The Reactor Engineering group is responsible for the development and review of fuel movement sequence sheets. The refueling procedure which describes the process for preparation, review, and implementation of fuel movements will be revised. The revision will specify limitations and a detailed description of the criticality requirements that must be met for the placement of fuel in SFP2. The Technical Specification figure of minimum burnup versus initial U235 enrichment will be referenced. An independent reviewer familiar with the criticality requirements of this report shall review any proposed fuel movements. No fuel movements are performed without the use of the reviewed and approved sequence sheets.

The refueling procedure which provides the precautions, limitations, and instructions for the handling of fuel assemblies shall also be revised to include the criticality requirements discussed in this report.

Training shall be conducted with personnel involved with fuel movements in SFP2. This shall include the individuals responsible for the development, review, and approval of fuel movement sequence sheets. Training shall also be given to fuel handling personnel responsible for the actual physical movements of fuel in SFP2. Independent verification shall be conducted for any movement and placement of fuel assemblies in SFP2.

The computer program which is utilized to generate the fuel movement sequence sheets and to track fuel movements and fuel storage will be revised to show which storage locations in SFP2 are NOT available for use,

3.4.5 EFFECTS OF RACK HANDLING ACCIDENTS

Installation of the high density racks is scheduled to be completed before any spent fuel is moved into SFP2. However, spent fuel is present in SFP1. Potential fuel transfer and fuel handling accidents are discussed in Section 15.7 of the CPSES FSAR [Ref. 3] and are not affected by rack installation.

The effects of rack handling accidents are limited by the fact that rack installation will occur when SFP2 is dry. At no time will the crane which lifts and positions racks in SFP2 carry a high density rack over SFP1. This restriction will be controlled both administratively and physically. Mechanical stops will be appropriately positioned to prevent the crane from reaching SFP1. With this installation approach, no potential exists for radiological release resulting from a high density rack drop accident during rack installation in SFP2.

As discussed in Section 3.1, the criticality analysis performed for the high density rack design considered the effects of fuel handling accidents involving placement of an assembly between racks or placement of an unirradiated fuel assembly or partially burned fuel assembly into a high density (2/4) or (1/4) controlled storage location. The analysis shows that postulated fuel handling accidents will not cause the neutron multiplication factor in the pool to exceed 0.95.

3.5 TECHNICAL SPECIFICATION CHANGES

Proposed technical specification changes include:

1) description of the high density storage racks and the limitations on their use, and

2) increasing the storage capacity from 1116 to 1291 fuel assemblies.

The use of the new high density racks is limited to either a 2 of 4 checkerboard (2/4) or a 1 of 4 expanded checkerboard (1/4) configuration based on initial fuel enrichment and burnup.

4.0 MECHANICAL, MATERIAL AND STRUCTURAL CONSIDERATIONS

4.1 DESCRIPTION OF STRUCTURE

4.1.1 DESCRIPTION OF FUEL BUILDING

The Fuel Building is a seismic Category I reinforced concrete structure which houses the new fuel storage area and the two spent fuel storage pools. The facilities of the Fuel Building provide common service to both units of CPSES. The building is arranged so that either SFP can be used for storage of fuel assemblies from either or both reactors. A transfer canal on the west side of the building permits movement of spent fuel assemblies between the two pools and the wet cask pit. See Figure 1-1.

The Fuel Building has an overhead electric crane designed for movements of fuel shipping casks between the loading area on the east side of the building and the wet cask pit, which is located between the two SFPs. The Fuel Building arrangement does not permit the overhead crane to pass over either of the SFPs. This crane, which has a hoist capacity of 130 tons, will be used to transport racks between the Fuel Building loading bay area and a temporary platform which will be installed over the wet cask pit during rack installation.

A fuel handling bridge crane is mounted on the operating floor to transport new and spent fuel assemblies between the SFPs, the new fuel storage area, the wet cask pit and the transfer canal. The fuel handling bridge crane can not be used to transport racks. The rack handling crane which will be installed during rack installation will use the fuel handling bridge crane rails. Section 3.4 discusses details of the rack installation process.

4.1.2 DESCRIPTION OF SPENT FUEL POOL

The spent fuel pool (SFP) is a water flooded volume used for storage, shielding, and cooling of spent fuel assemblies. Water maintains the temperature of stored spent fuel within defined limits. The SFP has thick reinforced concrete floors and walls. A liner covering the pool floor and walls provides a water retaining barrier to maintain the water level during plant operation.

The liner consists of 3/16 inch thick butt welded stainless steel plates anchored into the concrete wall with welded studs.

To detect any leakage through the SFP liner welds, a channel is provided in back of the welds to form a leak chase. Concrete troughs are formed under the welds in the floor plate. Sections of any welds which are leaking can be determined by observing which leak chase the water is coming from before the leak chases merge into a common drain header. Once a section of weld has been determined to be leaking, the exact location can be determined with a leak detection device.

4.2 APPLICABLE CODES, STANDARDS AND SPECIFICATIONS

The SFP systems, Fuel Building structure and the high density racks are designed and analyzed in accordance with the applicable provisions of the following codes and standards:

4.2.1 FUEL BUILDING AND SFP

American Institute of Steel Construction, AISC Specification for the Design, Fabrication, and Erection of Structural Steel for Buildings (1969) including Supplements 1, 2 & 3. [Ref. 31]

American National Standards Institute, ANSI N210-1976, "Design Objectives for Light Water Reactor Spent Fuel Storage Facilities at Nuclear Power Stations." [Ref. 27]

American National Standards Institute, N16.1-1975, "Nuclear Criticality Safety in Operations with Fissionable Materials Outside Reactors."[Ref. 32]

American Concrete Institute, ACI 318-71, "Building Code Requirements for Reinforced Concrete."[Ref. 25]

American Concrete Institute, ACI 349-76, "Code Requirements for Nuclear Safety Related Concrete Structures", Appendix A, "Thermal Considerations." [Ref. 26]

American Society of Mechanical Engineers, Boiler and Pressure Vessel Code, Section III, Division 1, Subsection NF. 1980, Summer 1982 Addenda.[Ref.4]

4.2.2 HIGH DENSITY RACKS

The high density racks are designed in accordance with the applicable provisions of the following codes, standards, and regulatory guidance.

NRC "OT Position for Review and Acceptance of Spent Fuel Storage and Handling Applications" dated April 14, 1978 and revised January 18, 1979. [Ref. 5]

NRC Regulatory Guides [Ref. 6]

R.G. 1.13	Spent Fuel Storage Facility Design Basis
R.G. 1.29	Seismic Design Classifications
R.G. 1.44	Control of the Use of Sensitized Stainless Steel
R.G. 1.60	Design Response Spectra for Seismic Design of Nuclear Power Plants
R.G. 1.61	Damping Values for Seismic Design of Nuclear Power Plants
R.G. 1.92	Combining Modal Responses and Spatial Components in Seismic Response Analysis
R.G. 1.124	Service Limits and Loading Combinations for Class I Linear-Type Component Supports

NRC Standard Review Plans [Ref. 8]

SRP 3.7	Seismic Design
SRP 3.8.4	Other Category I Structures
SRP 9.1.2	Spent Fuel Storage
SRP 9.1.3	Spent Fuel Pool Cooling and Cleanup System

Industry Codes and Standards

American Society of Mechanical Engineers, Boiler and Pressure Vessel Code, Section III, Division 1, Subsection NF, 1980, Summer 1982 Addenda. [Ref.4]

American National Standards Institute, ANSI 57.2-1983, "Design Objectives for Light Water Reactor Spent Fuel Storage Facilities at Nuclear Power Stations." [Ref. 7]

American National Standards Institute, ANSI N16.1-1975, "Nuclear Criticality Safety in Operations with Fissionable Materials Outside Reactors. [Ref.32]

4.3 LOAD DEFINITIONS AND COMBINATIONS

4.3.1 FUEL BUILDING AND SPENT FUEL POOL

4.3.1.1 LOAD DEFINITIONS FOR FUEL BUILDING AND SFP

The following loads were considered in the analysis of the Fuel Building and SFPs.

Normal Loads

Normal loads are those which are encountered during normal plant operation and shutdown. They include the following:

D = dead loads and their related moments and forces, including any permanent equipment loads.

L = live loads and their related moments and forces, including any movable equipment loads and other loads which vary with intensity and occurrence.

To = thermal effects and loads during normal operating or shutdown conditions, based on the most critical transient or steady state condition.

Ro = Pipe reactions during normal operating or shutdown conditions, based on the most critical transient or steady state condition.

Severe Environmental Loads

Severe environmental loads are those loads that could be encountered infrequently during the plant life. They include the following:

F_{eqo} = loads generated by one-half the Safe Shutdown Earthquake (SSE) = the Operational Basis Earthquake (OBE)

W = loads generated by the design wind specified for the plant.

Extreme Environmental Loads

Extreme environmental loads are those loads which are credible but highly improbable. They include the following:

F_{eqs} = loads generated by the SSE.

Wt = loads generated by the design tornado specified for the plant: the loads include those caused by the tornado wind pressure, tornado-created differential pressures, and tornado-generated missiles.

Abnormal Loads

Abnormal loads are those loads generated by a postulated high-energy pipe break accident within a building or compartment thereof, or both. They include the following:

Ta = thermal loads under abnormal thermal conditions generated by the postulated pipe break including To.

Pa = pressure-equivalent static load within or across a compartment or building, or both, generated by the postulated break; it includes an appropriate dynamic factor to account for the dynamic nature of the load

Ra = pipe reactions under thermal conditions generated by the postulated break and including Ro

Yr = equivalent static load on the structure generated by the reaction on the broken high-energy pipe during the postulated break; it includes an appropriate dynamic factor to account for the dynamic nature of the load.

Yj = jet impingement equivalent static load on a structure generated by the postulated break; it includes an appropriate dynamic factor to account for the dynamic nature of the load.

Ym = missile impact equivalent static load on a structure generated by or during the postulated break, e.g., pipe whipping; it includes an appropriate dynamic factor to account for the dynamic nature of the load

There are no high energy lines in the Fuel Building. Therefore, abnormal loads are limited to those loads generated by loss of SFP cooling accident and load drop accidents. They include the following:

Ta' = worst thermal loads based on the thermal gradient corresponding to the coldest environmental temperature and the loss of spent fuel cooling accident temperature of the pool walls.

Fd = impact loads resulting from the drop of a fuel assembly from 3.5 feet above the top of the racks onto the fuel pool liner and slab.

Variable Loads

For loads which may vary, the values (within the possible range) which produce the most critical combination of loading are used in the analysis.

4.3.1.2 LOAD COMBINATIONS FOR FUEL BUILDING

The following load combinations are satisfied.

U = the section strength required to resist design loads based on the methods described in ACI 318-71.

Load Combinations for Service Load Conditions

1. $U = 1.4\,D + 1.7\,L$
2. $U = 1.4\,D + 1.7\,L + 1.9\,F_{eqo}$
3. $U = 1.4\,D + 1.7\,L + 1.7\,W$

If thermal stresses due to To and Ro are present, the following combinations are also satisfied:

4. $U = 0.75\,(1.4\,D + 1.7\,L + 1.7\,To + 1.7\,Ro)$
5. $U = 0.75\,(1.4\,D + 1.7\,L + 1.9\,F_{eqo} + 1.7\,To + 1.7\,Ro)$
6. $U = 0.75\,(1.4\,D + 1.7\,L + 1.7\,W + 1.7\,To + 1.7\,Ro)$

L was considered for its full value or for its complete absence.

The following load combinations are also satisfied:

7. $U = 1.2\,D + 1.9\,F_{eqo}$
8. $U = 1.2\,D + 1.7\,W$

Load Combinations for Factored Load Conditions

For these conditions, which represent extreme environmental, abnormal environmental, abnormal/severe environmental, and abnormal/extreme environmental conditions, respectively, the following load combinations are satisfied:

1. $U = D + L + To + Ro + F_{eqe}$

2. $U = D + L + To + Ro + Wt$
3. $U = D + L + Ta + Ta' + Ra + 1.5\ Pa$
4. $U = D + L + Ta + Ta' + 1.25\ F_{eqo} + Ra + 1.25\ Pa + 1.0(Yr + Yj + Ym)$
5. $U = D + L + Ta + Ta' + 1.0\ F_{eqs} + Ra + 1.0\ Pa + 1.0(Yr + Yj + Ym)$

In combinations shown in Items 3, 4, and 5, the maximum values of Pa, Ta, Ra, Yj, Yr, and Ym, including an appropriate dynamic factor, are used, unless a time-history analysis is performed to justify otherwise. Combinations 2, 4, and 5, and the corresponding structural acceptance criteria should be satisfied first without the tornado missile load in 2 and without Yr, Ym, Yj, in 4 and 5. For combinations shown in Items 2, 4, and 5, local stresses caused by the concentrated loads Wt, Yr, Yj, and Ym may exceed the allowables when there is no loss of function of any safety-related system.

L is considered for its full value or for its absence.

4.3.1.3 LOAD COMBINATIONS FOR SPENT FUEL POOL

The elastic working stress design methods of Part 1 of the American Institute of Steel Construction (AISC) Specification [Ref. 31] are used. The following load combinations are satisfied.

S = the required section strength required based on the elastic design methods and the allowable stresses defined in Part 1 of the AISC Specification.

Load Combinations for Service Load Conditions

1. $S = D + L$
2. $S = D + L + F_{eqo}$
3. $S = D + L + W$

If thermal stresses due to To are present, the following load combinations are satisfied:

4. $1.5\,S = D + L + To + Ro$
5. $1.5\,S = D + L + To + F_{eqo} + Ro$
6. $1.5\,S = D + L + To + W + Ro$

L is considered for its full value or for its absence.

Load Combinations for Factored Load Conditions

1. $1.6\,S = D + L + To + F_{eqs} + Ro$
2. $1.6\,S = D + L + To + W_t + Ro$
3. $1.6\,S = D + L + Ta + Ta' + Fd + Ra + Pa$
4. $1.6\,S = D + L + Ta + Ta' + F_{eqo} + Fd + Ra + Pa + 1.0(Yj + Yr + Ym)$
5. $1.7\,S = D + L + Ta + Ta' + F_{eqs} + Fd + Ra + Pa + 1.0(Yj + Yr + Ym)$

In these combinations, thermal loads were neglected when they were secondary and self-

limiting in nature and when the material was ductile.

In combinations shown in Items 3, 4, and 5, of the factored load conditions, the maximum values of Pa, Ta, Ra, Yj, Yr, and Ym, including an appropriate dynamic factor, are used unless a time history analysis is performed to justify otherwise.

4.3.2 HIGH DENSITY RACKS

4.3.2.1 LOAD DEFINITIONS

The definition of loads is the same as in Section 3.8.4 of the SRP with the exception of the following:

Pi = Upward force on the rack caused by a postulated stuck fuel assembly.

Ta = Highest temperature associated with the postulated abnormal design conditions

4.3.2.2 LOAD COMBINATIONS FOR HIGH DENSITY RACKS

The load combinations and acceptance limits are as follows:

Load Combination	Acceptance Limit
1. D + L	Level A service limits of NF
2. D + L + E	Level A service limits of NF
3. D + L + To	Lesser of 2Sy or Su stress range
4. D + L + To + E	Lesser of 2Sy or Su stress range
5. D + L + Ta + E	Lesser of 2Sy or Su stress range
6. D + L + To + Pf	Lesser of 2Sy or Su stress range
7. D + L + Ta + E'	Level D service limits of NF

Notes:

1. The provisions of NF-3300 of ASME Section III, Division I, shall be amended by the requirements of Paragraphs c.2, 3 and 4 of Regulatory Guide 1.124, entitled "Design Limits and Load Combinations for Class A Linear-Type Component Supports." [Ref. 6]

2. For the faulted load combination, thermal loads will be neglected when they are secondary and self-limiting in nature and the material is ductile.

4.4 DESIGN AND ANALYSIS PROCEDURES

4.4.1 FUEL BUILDING AND SPENT FUEL POOL

4.4.1.1 FUEL BUILDING SEISMIC ANALYSIS

The purpose of the seismic analysis of the Fuel Building was to investigate the effects of the change from the current, low-density, bolted-down spent fuel racks to the new, high density, free standing racks. The seismic analyses were performed for a bounding design of 3386 storage locations with consolidated fuel storage. Response spectra at various damping ratios for the OBE and SSE events were generated at major floor elevations of the CPSES Fuel Building using soil-structure interaction analysis.

Two complete analyses were performed. The first, Analysis A, produced raw floor response spectra for the current configurations of the Fuel Building. The second, Analysis B, incorporated modelling changes to represent a bounding configuration of the Fuel Building and the new high density racks.

Fuel Building Model Refinements

The Fuel Building models used in both analyses consist of a lumped mass "stick" model with six active degrees of freedom at each of five elevations.

Analysis A - Licensed Configuration

The structural model for Analysis A incorporated the following features:

- Nodes at six elevations: 805.33', 819.56', 838.75', 860', 899.5' and 918.25' elevations (node at 819.56' used to allow explicit determination of input motion to the racks).

- o Fluid mass was distributed between the 819.50', 838.75', and 860' elevations. A portion of the fluid was modeled as a sloshing mass at the 860' elevation.

- o At each floor, 4 nodes were added to the model at the extreme corners of the building and connected rigidly with the floor center of mass to allow explicit determination of the worst case floor response.

Analysis B - Bounding Configuration

The second analysis was performed using a slightly modified version of the structural model used in Analysis A. The modifications included appropriate changes in the lumped masses to represent the Fuel Building with the bounding racks and additional stored fuel:

- o Additional mass of the new racks and stored fuel. Fuel masses in SFP2 were taken to be 1650 lbm for 224 locations and 2960 lbm for 1470 locations (i.e., conservatively assumes masses of consolidated fuel with 4/4 loading).

- o The combined mass of the racks and fuel was decoupled from the rigid structural floor mass at the 819.56' floor level.

Soil Properties

In the soil structure interaction analyses, the soil was modeled as a horizontally layered viscoelastic system overlying a half-space. The Fuel Building has an irregular basemat in elevation which exhibits a range of embedment from five to thirty feet. The soil properties were adjusted using the technique discussed in the CPSES FSAR, Section 3.7B.2.4.2 [Ref. 3], to account for the embedment of the Fuel Building.

Procedure to Generate Floor Response Spectra

The procedure to generate the floor response spectra can be divided into six steps:

Step 1 - Generate Ground Motion Time History Accelerations

An interactive method was used to compute ground motion time history accelerations using the CPSES FSAR Section 3.7B.1 [Ref. 3] ground motion response spectra at 5% damping as target spectra. In each iteration, the response spectrum was recomputed from the generated time history accelerations and compared to the target response spectra. The iterations continued until a satisfactory match was achieved. Three checks were made to show the validity of the new time history accelerations, which were used to generate the floor response spectra:

1) The three ground motion accelerations were checked for statistical independence.

2) The power spectral densities for the horizontal ground motion accelerations were shown to meet the criteria of the Standard Review Plan.

3) Response spectra for each ground motion acceleration were computed at damping levels of 5, 7 and 10%, then shown to envelop the corresponding design basis spectra of the FSAR in accordance with the Standard Review Plan.

Step 2 - Soil-Structure Interaction Analysis

The modal properties of the Fuel Building such as mode shapes and frequencies were generated for a fixed base condition. These modal properties and modal damping ratios (0.04 for OBE and 0.07 for SSE) were used as input to the soil structure interaction analysis.

The assumptions used in the soil-structure interaction analysis were:

- o surface founded structure (soil properties adjusted to account for embedment)
- o rigid foundation
- o layered soil over a half-space
- o input motions applied at the free-field at surface level
- o vertical and horizontal ground motions correspond to vertically propagating waves, compressional waves for the vertical earthquake and shear waves for the horizontal earthquakes.

The three new ground accelerations developed in Step 1 were applied in the two horizontal directions and in the vertical direction. Analyses were performed for both models for each ground motion acceleration direction, generating floor accelerations at the different locations in three directions for each ground motion application. From the acceleration time history, response spectra for each floor were generated at 1, 2, 3, 4 and 5% damping for OBE analysis, and 2, 3, 4, 5 and 7% damping for SSE analysis.

Step 3 - Combination of Floor Spectra

The floor spectra at every floor location generated in Step 2 for each input direction were combined using the square root of the sum of the squares (SRSS) rule. This is acceptable because of the statistical independence of the ground input time histories.

Step 4 - Enveloping of Floor Spectra

Final floor response spectra were the envelope of response spectra at the four worst location points at that floor. This was performed for each direction for every damping value specified.

Step 5 - PVRC Damping

The final enveloped floor spectra, from Step 4 at 2, 3, 4, and 5% damping were used to generate Pressure Vessel Research Committee (PVRC) damping spectra for the OBE and SSE events for all specified elevations. The development of the PVRC damped spectra was performed according to PVRC Research Committee on Piping Systems, Pressure Vessel Research Committee, Progress Report on Damping Values, 1985 [Ref. 33].

Step 6 - Plotting the Floor Response Spectra

The final enveloped floor spectra of the worst locations from Analysis A and Analysis B were plotted together with the corresponding design basis floor spectra from the FSAR.

4.4.1.2 SPENT FUEL POOL STRUCTURAL ANALYSIS

The SFP structure was analyzed to evaluate the adequacy of the four main components of the pool structure that are affected by the additional mass due to use of high density racks. These pool structures are:

1) Pool Liner
2) Pool Floor Slab
3) Pool Walls
4) Fuel Building Basemat

The evaluation was performed by identifying the components that may be affected by the additional fuel storage loads, reviewing existing design calculations, determining stresses resulting from the additional loads, and evaluating the components' structural adequacy according to their original design criteria. Results from this evaluation are given in Section 4.5.

4.4.2 HIGH DENSITY RACKS

The seismic analysis, which produces the governing loading conditions, yields results which are divided into two types (stresses and displacements).

The stresses were checked against the design limits to ensure the structural adequacy of the design. The horizontal displacement results were checked against the rack clearances to determine whether the racks collide with another rack or the pool wall. The vertical displacements of the support pads, due to rack rocking and lift-off, were evaluated to determine if the racks overturn. The results are given in Section 4.5 and show that the high density racks are structurally adequate to resist postulated stress combinations and the racks have margin against overturning and collision.

4.4.2.1 ANALYSIS OVERVIEW

Spent fuel storage racks are seismic Category I equipment. Therefore, they are required to remain functional during and after an SSE [Ref. 6] . Since the high density racks are free standing (neither anchored to the pool floor, to the pool wall, nor structurally interconnected) and the fuel is free to move inside the cell within the limits of the clearance between the fuel and cell, a nonlinear seismic analysis was performed. To ensure the limiting values have been obtained with a nonlinear analysis, numerous conditions with different combinations of parameters were analyzed in order to identify the combination of parameters which produces the limiting conditions. The parameters within the pool configuration which affect the response of the high density racks are:

- Damping
- Impact between the fuel assembly and cell
- Fluid coupling between the fuel racks and pool wall
- Coefficient of friction between the fuel rack support points and pool floor
- Structural characteristics of the fuel racks

To obtain the rack responses (rigid body motion, structural deformation, loads, stresses, etc.) the analysis was performed on a three (3) dimensional nonlinear dynamic finite element model of a high density rack which was subjected to the simultaneous application of three statistically independent, orthogonal acceleration time histories at the pool floor. The response spectrum from each corresponding time history record are shown in Figures 4-1 through 4-3. The design spectrum is also plotted on each figure to show that the time history spectra enveloped the design spectra. The pool floor acceleration time history data developed for the SSE are shown in Figures 4-4 through 4-6.

The steps in the seismic analysis were:

A. Develop three (3) dimensional nonlinear dynamic finite element models of a high density rack consisting of beam, mass, dynamic gap, and friction elements.

B. Perform time history analyses on the nonlinear dynamic models for the bounding cases using the dynamic capabilities of the nonlinear modal superposition solution technique of the Westinghouse Electric Computer ANalysis (WECAN) Code [Ref. 35, 36].

C. Compute the stresses in the high density rack at the critical structural locations using the loads from the previous step. These stresses were checked against the design limits given in section 4.3.2.2 to ensure the adequacy of the design.

4.4.2.2 SEISMIC MODEL

Since the fuel assembly is not structurally connected to the cell wall and the high density racks are free standing, the seismic model must have the capability to address a wide variety of rigid body motions:

- The fuel moving in the clearance between the fuel and cell with subsequent impact on the cell wall ("fuel rattling condition");
- The rack sliding on the pool floor ("sliding condition");
- One or more support pads momentarily losing contact with the pool floor ("tipping condition");
- Rack rocking onto one support pad and pivoting about that pad ("torsional rotating condition");
- The high density rack may also experience a combination of sliding and tipping conditions.

These mechanical nonlinearities in the high density rack dynamic responses required a strong emphasis on the modeling of both the linear and nonlinear elements.

To determine the dynamic response of a system with multiple nonlinearities, as described above, the analysis must be conducted on a model which realistically represents the dynamic characteristics. That is: the model must have realistic linear stiffness and mass properties as well as the correct number and geometric location of impact points, a realistic value of impact stiffness, and sufficient Dynamic Degrees of Freedom (DDOF) in order to develop the higher modes of response which are associated with impact forces. The linear and nonlinear elements used in the model have the capabilities described in the following paragraphs.

The linear elements represent both the fuel and rack stiffnesses as well as the geometric properties (support pad spacing, fuel grids locations, etc.) with sufficient DDOF to capture the dynamic response of the combined fuel and rack system. More specifically, the number and location of fuel to cell contact points were accurately modeled in order to provide the correct impact force magnitude and location so that the correct modes of response of the fuel and cell were produced. The rack height, mass distribution, and support pad spacing were modeled to provide a representation of the rack rigid body stability characteristics.

The nonlinear elements which model the impacting between the fuel assembly grids and cell included the impact stiffness, impact damping, and gap size. The nonlinear elements that model the support pads which may lift off and impact the floor, or may slide relative to the pool liner, included the impact stiffness, impact damping, and Coulomb friction to appropriately simulate this interface between the high density rack and pool floor.

4.4.2.2.1 MODEL DESCRIPTION

The time history analysis was performed on a 3-D nonlinear finite element model which represents one rack in the pool. The following sections describe in detail the structural model and the nonlinear single rack model.

To compile the finite element model, the properties of the linear elements and nonlinear elements must be calculated. The properties of the linear elements are obtained from a 3-D finite element structural model of the fuel rack. The linear properties, referred to as the effective structural properties, are calculated from the structural model and used as the basis of the nonlinear model. The nonlinear elements, with properties such as impact stiffness, gap, impact damping, and friction coefficient, are added to the effective structural properties to produce the nonlinear model. The details of the structural model, effective structural properties, and the nonlinear model are presented in the following paragraphs.

4.4.2.2.2 STRUCTURAL MODEL

The structural model is a 3-D finite element model of the high density rack. The structural model used in the analysis is shown in Figure 4-7.

The high density rack is composed of the following structural components: support pad assembly, baseplate, cells, and cell to cell connections. These components are attached in a manner which produces an overall rack structure. The structural input properties of each component are discussed in the following paragraphs.

The support pad assembly is composed of a leveling pad assembly, leveling screw, and support block. The structural components in the assembly, leveling screw and support block, are modeled as beams with area and inertia values obtained from cross sectional properties.

The baseplate assembly in the structural model has the effective stiffness values of the baseplate, support blocks, and cells welded to the baseplate. The baseplate is modeled as effective beams which connect the support pads and the cells. Since the cells are welded to the baseplate, the inertia and area of the baseplate effective beams are based upon the cross section which includes a portion of the cell wall.

The cells are square (.075 inch wall thickness) tubular sections which have 0.024 inch thick spacer plates on the four sides. The cells are modeled as beams with area and inertia based upon the cross section of the 0.075 inch thick cell wall and only one spacer plate on the tensile side of the cell. The use of one spacer plate on the tensile side of the cell is based upon the post buckled condition which produces structurally ineffective members of the spacer plates which are loaded in compression. It is noted that the dynamic analysis is based upon section properties which include the spacer plate on the tensile side, but the stress analysis is based upon section properties which do not include the spacer plate, thereby producing a conservative analysis.

The cell to cell connections are the members which form the structural connection between the cells and produce the overall shear connection of the rack assembly. The connection is produced by cell to cell welds at the cell corners. This connection is modeled with effective beams which connect between cells.

The properties of the effective structural model are obtained from the results of the structural model. The effective model shown in Figure 4-8 is composed of elements which represent the cell assembly, cell to cell connection, and support pad/baseplate. The properties of these elements are calculated from the load and displacement results of the structural model, as discussed in the following paragraphs.

A finite element model of the effective structural model is compiled and run, and the mode shapes, including the higher cell modes, of the effective model are compared with those of the structural model to ensure that the effective structural model is an adequate dynamic representation of the structural model and has a sufficient number of modes to produce the higher mode response due to fuel impact loads.

The properties of the cell assembly in the effective structural model are the same as those in the structural model.

The properties of the cell to cell connection in the effective model are rotational stiffnesses (K_θ) in units of in-lb/rad. These values are the ratio of bending moments reacted by the cell to cell connection members divided by the angular rotation of the connection at the cell from the structural model. At each elevation of cell to cell connection, this calculation is performed at each cell location and averaged for the total cross section to obtain the effective rotational stiffness at that elevation. The cell to cell connections, which produce the overall shear connection of the rack, are placed at locations along the length of the cells to produce the required frequency of the rack. As shown in Figure 4-8, there are 3 cell to cell connections (welds) for the high density rack effective structural model. The value of the rotational stiffness between the bottom of the cell and baseplate is calculated by the same method as the cell to cell rotational stiffness values. It is included in the stiffness matrix element, [K], between the bottom of the cell and baseplate.

The effective support pad/baseplate properties are calculated in two stages. The overall baseplate rotational stiffness is calculated from the structural model, and then the combination of rigid beams with vertical spring elements on the ends is used to represent the rotational stiffness while providing the effective vertical stiffness and geometric spacing of the corner support pads. The overall baseplate rotational stiffness is calculated by dividing the rotation of the rack base by the total moment applied to the base. The rotation of the rack base is calculated by dividing the vertical displacement at each cell location on the base by the distance from that point to the rack centerline, and calculating the average for the cell locations in the rack base. This accounts for both the support pad deformation and baseplate deformation at the locations between support pads.

The vertical stiffness of the effective corner pads is calculated by equating the rotational stiffness of the vertical spring/rigid beam assembly to that of the baseplate rotational stiffness (K_θ). Using four support pads, one at each corner, and a spacing of (L) inches between support pads, the effective vertical stiffness per former pad is $K_V = K_\theta/L^2$.

4.4.2.2.3 NONLINEAR SEISMIC MODEL

The nonlinear model, shown in Figure 4-9, is a 3-D model composed of effective properties from the structural model, to account for the rack structure, with additional elements to account for the fuel assembly, fuel to cell gap, fuel hydrodynamic mass, support pad boundary conditions of a free standing rack, and the hydrodynamic mass between the fuel rack and the pool wall or between fuel racks. A better illustration of the elements of a 2-D view of the 3-D model is shown in Figure 4-10.

The effective components/properties from the structural model are:

- The cell assembly represented by 3-D beam elements with effective stiffness properties and mass density;

- Cell to cell connections represented by rotary stiffness elements in both horizontal axes;

- Cell to base connection represented by a stiffness matrix element with rotary stiffness in both horizontal axes, lateral stiffness in both horizontal axes, and rigid connection in the vertical axis;

- Support pad corner spacing represented by rigid 3-D beam elements connecting the center and the four corners;

- The effective support pad/baseplate vertical stiffness represented by a 3-D friction element which has the nonlinear capability to slide on the horizontal plane or lose contact in the vertical direction (support pad lift-off) and impact upon contact.

The fuel assembly is represented by a combination of 3-D beam elements and rotational stiffness elements. The beam elements have properties of inertia, area, and mass density. The area and inertia values are based upon the fuel rod cladding and fuel skeleton cross section. The rotational stiffness elements have rotational stiffness about both horizontal axes to account for the connection of the fuel rods at the fuel grid locations. The connection between the fuel base and high density rack baseplate is modeled with a 3-D friction element which has the nonlinear capability to allow the fuel assembly to lift-off the baseplate and produce impact forces.

The fuel to cell gaps are modeled by 3-D dynamic elements with gaps, impact stiffness, and impact damping values to represent the gap between the fuel and cell. The fuel assembly impact stiffness and damping values for the 17 x 17 fuel assemblies were used in the analysis. The maximum value of the gap between the fuel and cell is conservatively used in the model. This is done by using the tolerances to produce the minimum fuel grid dimension and maximum cell opening. The gap is input as a concentric gap where the fuel is initially in the center of the cell and can impact any of the four sides of the cell. The impact stiffness between the fuel and cell is based upon the series combination of the fuel grid impact stiffness and the local stiffness of the cell wall. The fuel grid impact stiffness is supplied by the fuel vendor, and the local cell wall stiffness is calculated from the displacements of the cell wall, modeled as a flat plate, due to loads applied at the corners of the fuel grid. The impact damping of the fuel grid is based upon values supplied by the fuel vendor. There are 9 gap elements located along the length of the fuel assembly to represent 8 intermediate grids and one top fitting.

The hydrodynamic mass between the fuel assembly and cell is modeled by a 3-D mass matrix element in both horizontal directions. Since the fuel assembly is an open array of rods, the proximity effect of the cell wall on the rods only affects the edge row of rods and does not produce a significant hydrodynamic mass on the fuel assembly. Thus, the flow around the rods is the condition which produces the governing hydrodynamic mass. The calculation of the hydrodynamic mass due to flow around the fuel rods is based upon the kinetic energy of the fluid [Ref. 37]. The hydrodynamic mass elements are modeled at 8 locations along the length of the fuel with values proportional to the effective fuel length at each location.

The hydrodynamic mass between the high density rack and the pool wall is modeled by 3-D mass matrix elements in both horizontal directions. The hydrodynamic mass elements are modeled at 9 locations along the length of the cell with values proportional to the effective cell length at each location. The values of hydrodynamic mass for the high density rack are based upon potential flow theory and are calculated by evaluating the effects of the gap between the rack and the pool wall or between racks by using the method outlined in the paper by R. J. Fritz [Ref. 41]. A more detailed discussion on hydrodynamic mass is presented in Paragraph 4.4.2.2.5 Fluid Coupling.

4.4.2.2.4 DAMPING

There are two types of damping present in the dynamic response of a nonlinear structure such as the fuel rack. These are structural damping and impact damping.

The structural damping values used for the seismic analysis of high density rack structures are 2% for OBE and 4% for SSE. These values are in accordance with Regulatory Guide 1.61 [Ref. 39] for welded steel structures.

The damping which occurs during impact is produced by the small amount of local plastic deformation which takes place. The two types of locations in the high density rack which have impacts are the fuel grid to cell wall and the support pad to the pool floor. The damping value used for the fuel grid impact, which was supplied by the fuel vendor, is 25%. The damping value used for the support pad impact is based upon steel on steel impact. The range of coefficient of restitution for steel on steel is 0.5 to 0.8 [Ref. 40]. Thus, conservatively using a value of 0.85 coefficient of restitution produces an effective impact damping of 4% for the support pads.

4.4.2.2.5 FLUID COUPLING

The effect of water on the dynamic response of a submerged structure is significant, and was included in the modeling. If one body of mass (m_1) vibrates adjacent to another body of mass (m_2), and both bodies are submerged in a frictionless fluid medium, then Newton's equations of motion of the two bodies have the form:

$$(m_1 + M_{11})\ddot{X}_1 - M_{12}\ddot{X}_2 = \text{applied forces on mass } m_1$$

$$-M_{21}\ddot{X}_1 + (m_2 + M_{22})\ddot{X}_2 = \text{applied forces on mass } m_2$$

$\ddot{X}_1, \ddot{X}_2$ denote absolute accelerations of mass m_1 and m_2, respectively.

Fluid coupling coefficients, M_{11}, M_{12}, M_{21}, and M_{22}, depend on the shape of the two bodies, their relative disposition, etc. Fritz [Ref. 38] gives data for M_{ij} for various body shapes and arrangements. It is noted that the above equations indicate that the effect of the fluid is to add a certain amount of mass to the body (M_{11} to body 1), and an external force which is proportional to the acceleration of the adjacent body (mass m_2),. Thus, the acceleration of the one body affects the force field on another. This force is a strong function of the interbody gap, reaching large values for very small gaps. This inertial coupling is called fluid coupling. It has an important effect in rack dynamics. The motion of the rack as well as the lateral motion of a fuel assembly inside the storage location will encounter this effect.

The hydrodynamic coupling between the fuel and cell and between the high density rack and pool wall is represented in the models by mass matrix elements. The hydrodynamic mass between the fuel assembly and the cell walls is based upon the fuel rod array size and cell inside dimensions using the technique of potential flow and kinetic energy. The hydrodynamic mass is calculated by equating the kinetic energy of the hydrodynamic mass with the kinetic energy of the fluid flowing around the fuel rods. The concept of kinetic energy of the hydrodynamic mass is discussed in a paper by D. F. Desanto [Ref. 37].

The hydrodynamic mass between the high density racks and pool wall was calculated by evaluating the effects of the gaps between the racks and the pool wall using the method based upon potential flow theory outlined in the paper by R. J. Fritz [Ref. 38]. To account for the flow in three dimensions, the hydrodynamic masses for flow in the horizontal direction around the racks and for flow in the vertical direction up over the top of the racks and down below the bottom of the racks are calculated independently, and combined to produce an overall hydrodynamic mass value.

4.4.2.2.6 FRICTION COEFFICIENT

Since the high density racks are free standing, the frictional resistance at the interface between the support pads and pool floor is the only horizontal constraint. Thus, the value of friction coefficient must be accurately represented in a manner to conservatively calculate the displacements of the fuel rack. The values used in the analysis are based upon tests performed by Rabinowicz [Ref. 41]. According to Rabinowicz, the results of 199 tests performed on austenitic stainless steel plates submerged in water show a mean value of friction coefficient to be 0.503 with a standard deviation of 0.125. The upper and lower bounds (based on two standard deviations) are 0.753 and 0.253 respectively. In order to address the upper and lower bounds of friction, two separate analyses are performed on the rack model with friction coefficient values of 0.8 and 0.2. The results of these analyses showed that different dynamic behavior was produced for each coefficient, thus producing the bounding response.

4.4.2.3 TIME HISTORY EVALUATION

The seismic analysis of a free standing fuel rack is a time history analysis preformed on a 3-D nonlinear finite element model subjected to the simultaneous input of three statistically independent acceleration time histories at the pool floor elevation. The analysis was performed on the Westinghouse Electric Computer Analysis (WECAN) Code [Ref. 35, 36] using the dynamic capabilities of the nonlinear modal superposition method.

The nonlinear model was run for the bounding cases which account for the variation of parameters such as friction coefficient (0.2 and 0.8). The results from these runs include the fuel to cell impact loads, support pad loads, fuel rack structure internal loads and moments, support pad lift-off, fuel rack sliding and structural displacements. Since the seismic analysis was conducted on a single rack model, the absolute (where absolute is the displacement of a rack with respect to the pool floor) displacements at the bottom and top of the racks were obtained, but the relative (where relative is the displacement of the rack with respect to an adjacent rack) displacement between racks is not calculated by the model. To obtain the relative displacement between racks it was conservatively assumed that the adjacent racks respond 180° out-of-phase, thus producing a relative displacement equal to twice the absolute displacement of one rack.

The values of these results were searched through the 20 seconds duration of the time history to obtain the maximum values. The maximum values of the loads and moments were used in the stress analysis, and the displacement results were used to show that significant separation margin against collision with an adjacent rack or the pool wall remains and that there is ample margin against overturn.

A number of conservatisms have been incorporated in the analysis and are listed below.

A. All fuel assemblies are treated as if they respond in phase which results in the maximum rack response.

B. Friction coefficients of 0.8 maximum and 0.2 minimum are used in the analysis.

C. Adjacent fuel racks respond 180° out-of-phase.

D. Hydrodynamic mass is based upon constant gaps. As the gap decreases the hydrodynamic mass restoring force increases; but since the analysis is based upon constant gaps, the displacements which close the gaps are conservative because the restoring forces increase.

E. No friction is used in support pad swivel joints to resist rotation when the rack rocks onto one pad.

F. Gaps between fuel and cell were maximized and produce the maximum impact forces.

4.5 STRUCTURAL ACCEPTANCE CRITERIA AND RESULTS OF ANALYSIS

4.5.1 STRUCTURAL ACCEPTANCE CRITERIA AND ANALYTICAL RESULTS FOR THE FUEL BUILDING AND SPENT FUEL POOL

Allowable loads on the Fuel Building and SFP structural components were determined in accordance with the limitations of the ACI and AISC Specifications [Ref. 25, 26, 31]. The elastic working stress design methods of Part 1 of the AISC Specification [Ref. 31] were used. Concrete thermal loads were evaluated according to ACI 349, Appendix A [Ref. 26].

4.5.1.1 FUEL BUILDING SEISMIC ANALYSIS

As discussed in section 4.4.1.1 above, two complete seismic analyses (Analysis A and Analysis B) were performed. The results of the two analyses allowed a direct evaluation of the impact of the use of high density racks on the Fuel Building's seismic response. This evaluation was made from a set of three overlaid results from Analysis A and Analysis B compared to the design basis floor response spectra for Fuel Building. A separate plot was prepared for each location, damping value and seismic event.

The response spectra plots show that the effect of the use of high density racks on the seismic response of the Fuel Building is insignificant. The only noticeable effect was that peak acceleration responses in the horizontal directions were slightly reduced. This effect was attributed to the fact that the lower frequency of the new racks reduced mass participation in the higher modes of Fuel Building.

The floor spectra from Analysis B were also compared to the design basis floor spectra. The zero period acceleration (ZPA) of the Analysis B floor spectra are consistently below design basis floor spectra values. Peak spectral accelerations from Analysis B are lower than the peak spectral accelerations of the design basis floor spectra in all cases. In the frequency range extending from the peak spectral acceleration up to the ZPA, the design basis floor spectra are substantially higher and thus conservative.

In the low frequency range, the design basis floor spectra envelop the new spectra in all cases except at localized zones where the exceedance ranges from 0.0 to 0.1G. Also, for the 1% damped spectra in the East-West direction at the upper two elevations, a 10% exceedance occurs at 7 Hz. This exceedance is localized and therefore does not indicate increased seismic response of Fuel Building equipment, since the Analysis B response is substantially lower at all high frequencies. At worst, response would be underestimated in a single mode of a component under consideration. It is also to be noted that the input ground motions used in the present analysis have response spectra that conservatively envelop the FSAR spectra by an average of 10% in the above discussed frequency range. Therefore, the actual response would not exceed the design response.

In conclusion, the seismic analysis verified that the design basis floor response spectra of the Fuel Building remain adequate and conservative for the design of equipment in the Fuel Building with the new racks and increased storage loads.

4.5.1.2 SPENT FUEL POOL

To evaluate the effects of the use of high density racks on the SFP structure, structural components affected by the high density racks were re-evaluated.

Pool Liner Integrity

The pool floor is lined with 3/16 inch thick stainless steel plates. These plates are connected to each other by continuous welds and are attached to the SFP concrete floor by embedded plates. Continuous welds protrude above the top of the plates.

To protect these welds and maintain a full contact area between the leveling pad assemblies and the pool floor, 2 inch thick free standing stainless steel bridge plates will be used. Where rack pads are located over liner welds, grooves will be milled in the bridge plate to prevent it from bearing directly on the weld. These bridge plates will be configured in a way that the original contact area is still maintained or exceeded.

The only appreciable load on the liner walls is attributable to fluid pressure.

The loads on the liner walls will not significantly change due to the use of high density racks, since bearing stresses caused by fluid pressure will not change. Therefore, the previous analysis is still valid.

The SFP liner floor is subjected to rack and fluid loads and, therefore, was analyzed accordingly. The liner floor was evaluated for worst case factored loads, using the service load condition allowable stresses. The liner was shown to be acceptable as follows:

Item	Actual Stress	Allowable Stress	Factor of Safety
Bearing Stress	2,077 psi	20,835 psi	10.0
Axial Stress	10,090 psi	13,890 psi	1.4
Weld	935 lb/in	2,784 lb/in	2.9

Building Load Capacity

The SFP structure consists of reinforced concrete walls and slab. The SFP floor slab is integral with the Fuel Building mat foundation, which is resting on top of soil.

The high density racks are fully supported by the floor slab (mat foundation) and there is no interface between the racks and walls. Maximum rack displacements for the SSE event (approximately 0.2 inch at the top of the racks) are small compared to the minimum water gap between the racks and walls (5 inch nominal). As a result, additional loads imparted to the SFP walls by fluid coupling effects can be neglected; therefore, the previous evaluation of static and hydrodynamic loads on the concrete walls is still valid.

The floor slab (mat foundation) will be affected by the higher loads imposed by the new racks. The SFP walls and slab will also be affected by the increase in thermal gradients.

The SFP walls were re-evaluated by obtaining the thermal loads from the previous analysis of a half-model of the SFP1 side of the Fuel Building, multiplying them by an appropriate factor to account for the change in thermal gradient, and adding them to the dead load, live load and seismic loads. The total loads were compared to the capacities of the walls.

The SFP slab was re-evaluated by obtaining the dead load, live load and seismic loads from the previous half-model analysis and multiplying them by an appropriate factor to account for the change in rack weights, then obtaining the thermal loads and multiplying them by an appropriate factor to account for the new thermal gradient. The new loads were added, and the total loads were compared to the capacity of the slab.

Based on the magnitude of increase in loadings to the Fuel Building caused by additional spent fuel storage, and on review of the existing analyses, it is concluded that the Fuel Building is structurally adequate to sustain the additional loadings created by the high density racks.

Specifically, the worst case load combinations (which include load factors) for each type of concrete element surrounding the SFP, for service load conditions, are as follows:

	Axial Force *(k)	Moment (k-ft)	Moment Capacity at Axial Force (k-ft)	Safety Margin
East Wall	-325.1	-698.7	-2401.0	3.44
West Wall	-10.3	-481.9	-1090.3	2.26
North Wall	+31.8	-309.8	-938.8	3.03
South Wall	+197.6	-503.1	-511.8	1.02
Slab	-35.2	-878.5	-1345.3	1.53

* a negative axial force is compressive

For factored load conditions, temperatures in the concrete are increased only negligibly (from 250.0°F to 250.5°F). Since there is no direct contact between the racks and walls, and the additional loads on the pool walls due to fluid coupling effects are also negligible, the only structural element subjected to appreciably increased loads is the concrete slab underneath the SFPs. The worst case load combination for the slab, considering the increased dead weight and seismic loads, was:

	Axial Force *(k)	Moment (k-ft)	Moment Capacity at Axial Force (k-ft)	Safety Margin
Slab	-34.4	-718.2	-1342.1	1.87

It may be noted that for the structural element "Slab", the normal loads are greater than the accident loads. This is due to the difference in load factors involved in the load combination.

Soil Bearing Pressure Evaluation

The deadweight increase due to the new racks and spent fuel is 6.8% of the total Fuel Building deadweight. The additional weight of the new racks and spent fuel will create additional loading to the underlying soil.

The high density racks and additional stored fuel will increase the maximum static soil bearing pressure from 10 ksf to 10.7 ksf, which is still much less than the allowable static soil pressure of 20 ksf. Similarly, the dynamic soil pressure is estimated to increase from 13.9 ksf to 14.8 ksf, which is also much less than the allowable dynamic soil pressure of 30 ksf.

It is concluded that the increased soil bearing pressures caused by additional loads from the new high density racks are acceptable.

Rail Integrity

The rail and the concrete slab were analyzed for the increased crane wheel loads, including seismic loads, and determined to be acceptable.

4.5.2 STRUCTURAL ACCEPTANCE CRITERIA AND ANALYTICAL RESULTS FOR HIGH DENSITY RACKS

4.5.2.1 CRITERIA

There are two sets of criteria to be satisfied by the racks:

A. Kinematic Criterion

This criterion seeks to ensure that the rack is a physically stable structure. The racks are evaluated for margin against overturning and also for rack displacement to ensure that rack to rack and rack to pool wall impact does not occur.

B. Stress Limits

The stress limits of the ASME Code, Section III, Subsection NF are used since this code provides the most appropriate and consistent set of limits for various stress types and various loading conditions.

4.5.2.2 STRESS LIMITS FOR SPECIFIED CONDITIONS

The structural analysis of the high density racks is an elastic type analysis of linear type supports per ASME Code, Section III, Subsection NF. The Load Combination and Acceptance Limit table is shown in section 4.3.2.2 and repeated below.

Load Combination	Acceptance Limit
1. D + L	Level A service limits of NF
2. D + L + E	Level A service limits of NF
3. D + L + To	Lesser of 2Sy or Su stress range
4. D + L + E + To	Lesser of 2Sy or Su stress range

5.	$D + L + E + Ta$	Lesser of 2Sy or Su stress range
6.	$D + L + To + P_f$	Lesser of 2Sy or Su stress range
7.	$D + L + Ta + E'$	Lever D service limits of NF

Margins to Allowable shown in Table 4-1 are for the limiting load combinations 2, 5 and 7. The Margin to Allowable (MA) is calculated, as shown in equation form below, by comparing the acceptance limit with the applied stress. It can be seen in the table above that there are three different acceptance limits: one for load combinations 1 and 2, another for load combinations 3 through 6, and a third for load combination 7. Thus, it is possible to meet the requirements of the load combinations by addressing the three limiting combinations. Load combination 7 is limiting because it is the only combination involving the SSE condition. Load combinations 2 and 5 are the limiting combinations of combinations 1 through 6 as shown in the following paragraphs.

Load combination 2 envelops load combination 1 .

Load combination 5 envelops load combinations 3 and 4. Since stresses caused by the stuck fuel assembly load condition (Pf) are much lower than stresses caused by the OBE [Ref. 38], load combination 5 also envelops load combination 6.

The MA shown in Table 4-1 is defined as:

$$MA = \frac{\text{Allowable Stress}}{\text{Applied Stress}} - 1$$

4.5.2.3 RESULTS FOR HIGH DENSITY RACK ANALYSIS

Table 4-1 shows the minimum margin to allowable for the various components and welds on the racks. There is adequate margin in each case, which shows that the racks meet the structural requirements of the ASME Code.

In addition, the impact loads on the fuel assemblies due to the interaction with the rack during a seismic event have been determined. The maximum calculated seismic impact load is 289 pounds. The loads are within the allowable limits of the fuel rack module materials and fuel assembly materials. Therefore, there is no damage to the fuel assembly or fuel rack module due to impact loads.

4.5.3 FUEL HANDLING CRANE UPLIFT ANALYSIS

An analysis was performed to demonstrate that a rack can withstand an uplift load of 5000 pounds produced by a jammed fuel assembly. The stresses resulting from this load were calculated and compared to the acceptance limits. The stresses were within the acceptance limits. This loading condition was determined not to be a governing condition and is covered by the results reported for the limiting loading combinations. In addition, since the gross stresses remained within the elastic regime, there is no change of rack cell geometry of a magnitude sufficient to cause the criticality acceptance criterion to be violated.

4.5.4 FUEL ASSEMBLY DROP ACCIDENT ANALYSIS

The objectives of this analysis are to ensure that, in the unlikely event of dropping a fuel assembly, accidental deformation of the rack will not cause sufficient deformation to result in violation of the criticality acceptance criterion, or the SFP liner to be perforated.

Three accident conditions are postulated. The first accident condition assumes that the weight of a fuel assembly and control rod assembly impacts the top end fitting of a stored fuel assembly or the top of a storage cell from a drop height of 3.5 feet in a straight attitude. The second accident condition is similar to the first except the impacting mass is at an inclined attitude.

The third accident condition assumes that the dropped assembly falls straight through any empty cell and impacts the rack baseplate from a drop height of 3.5 feet above the top of the rack, which is the maximum height possible given the features of the fuel handling equipment.

For fuel drop accident conditions, the double contingency principle of ANSI N16.1-1975 [Ref. 32] is applied. This states that one is not required to assume two unlikely, independent, concurrent events to ensure protection against a criticality accident. Thus, for accident conditions, the presence of soluble boron in the storage pool water can be assumed as a realistic initial condition since not assuming its presence would be a second unlikely event.

The presence of boron in the pool water will decrease reactivity by about 20 to 30 percent k_{eff}. With boron in the pool water there is no deformation that could be achieved by the drop of a fuel assembly that would cause the criticality acceptance criterion to be exceeded. Therefore, the requirement for the drop accident conditions that the fuel be maintained below 0.95 k_{eff} has been satisfied due to the presence of the boron in the water.

In addition to performing the evaluation to ensure that the rack does not deform enough to affect the criticality analysis, an evaluation has been performed to demonstrate that the pool liner would not be perforated for the condition of a dropped fuel assembly passing through an empty cell. For this evaluation, it is assumed that when the fuel hits on the baseplate at the bottom of the cell, the baseplate welds or a local region of the baseplate fails and allows the fuel assembly to travel to the pool floor. The strain energy absorbed by the failed baseplate or the welds is neglected. The energy due to the falling fuel assembly is assumed to be absorbed by crushing the baseplate and the fuel assembly lower end fitting.

The fuel drop energy is the product of the total dropped weight times the drop height. By equating the strain energy to the fuel drop energy, the value of strain and in turn stress and impact force are determined. Using these methods, the stress on the pool liner was calculated and was found to be 30% of the Code allowable limit for Faulted Conditions, thus ensuring that the liner will not be perforated.

4.5.5 HIGH DENSITY RACK SLIDING AND OVERTURNING ANALYSIS

The racks were evaluated for overturning and sliding displacement due to earthquake conditions.

The nonlinear model described above was used in this evaluation to account for fuel-to-rack impact loading, hydrodynamic forces, and the nonlinearity of sliding friction interfaces. From the nonlinear time history analysis, the maximum rack displacement (absolute displacement) was determined to be 0.28 inches in the east-west direction and 0.24 inches in the north-south direction. The remaining rack to pool wall gap is calculated by taking the minimum initial clearance between the rack and the pool wall and then subtracting the installation tolerance (0.25 inches), total thermal growth of one rack (0.09 inches), and the seismic displacement of the rack. The minimum remaining rack to pool wall gap is determined to be 4.84 inches and is based on the nominal initial rack to wall gap of 5.46 inches in the east-west direction and the seismic displacement of 0.28 inches.

The most limiting relative displacement between racks is determined by conservatively doubling the absolute displacement of one rack. Using the appropriate minimum initial clearance between racks of 1.87 inches and then subtracting the thermal growth of two racks (0.18 inches total due to 0.09 inches per rack), and the seismic relative displacement between racks (2 x 0.28 inches), the remaining rack to rack gap is determined to be 1.13 inches.

From these results it is concluded that the racks are spaced with sufficient clearance so that rack to rack and rack to pool wall impact does not occur. Additionally, because the bridge plate is much larger than the levelling pad, the levelling pad assembly will not slide off the bridge plate.

Also extracted from the time history results is the maximum support pad vertical displacement (lift-off). The maximum support pad lift-off is found to be 0.003 inches. For this magnitude of pad lift-off the factor of safety against rack overturning is determined to be greater than 50 which satisfies the requirements of Section 3.8.5.II.5 of the Standard Review Plan.

4.6 MATERIAL CONSIDERATIONS FOR THE HIGH DENSITY RACKS

Construction materials for the racks conform to the requirements of ASME Boiler and Pressure Vessel Code, Section III, Subsection NF [Ref. 4]. The materials used in the construction are compatible with the storage pool environment. The racks are constructed from Type 304 stainless steel except the leveling screws which are type 17-4 PH stainless steel.

TABLE 4-1

HIGH DENSITY RACKS

MINIMUM MARGIN TO ALLOWABLE

	OBE[a]	SSE[b]
Support Pads	0.54	0.89
Cells	0.17	0.43
Welds:		
Cell to base plate	0.96	0.94
Cell to Cell	0.22	0.59
Cell Seam	0.40	0.78
Cell to Spacer	0.25	0.30

a - Load combination D + L + E

b - Load combination D + L + Ta + E'

FIGURE 4-1

DESIGN VS TIME HISTORY RESPONSE SPECTRA

NORTH-SOUTH SSE 4% DAMPING

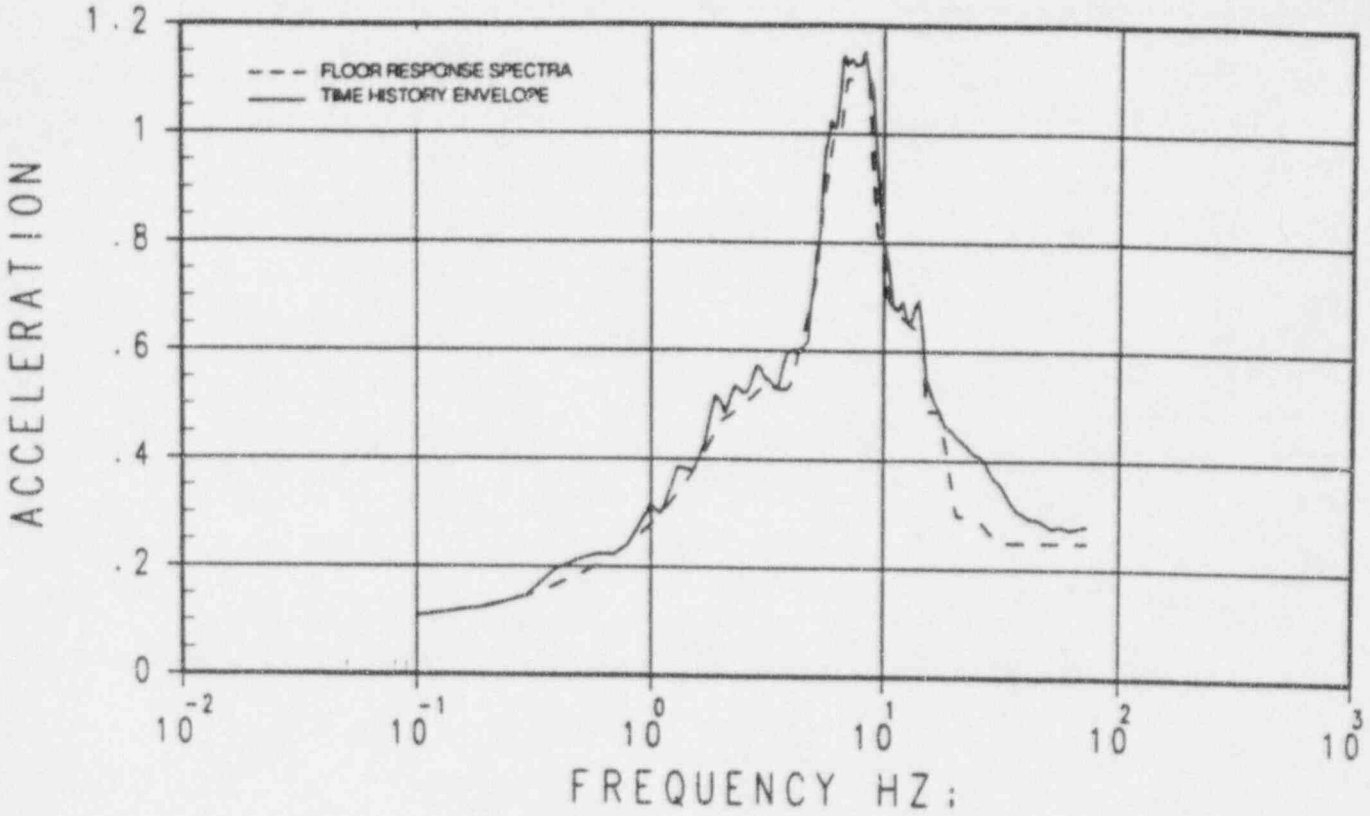

FIGURE 4-2

DESIGN VS TIME HISTORY RESPONSE SPECTRA

EAST-WEST SSE 4% DAMPING

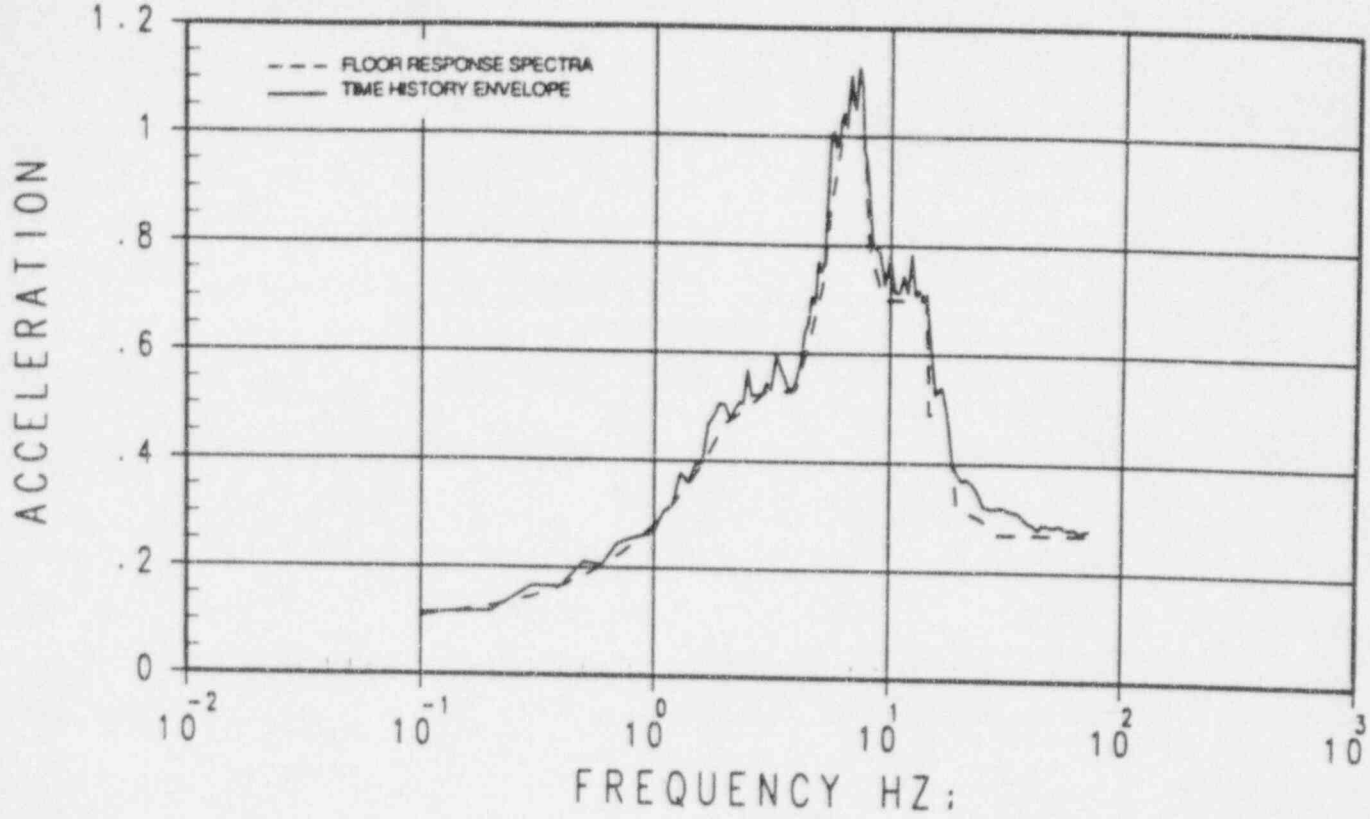

FIGURE 4-3

DESIGN VS TIME HISTORY RESPONSE SPECTRA

VERTICAL SSE 4% DAMPING

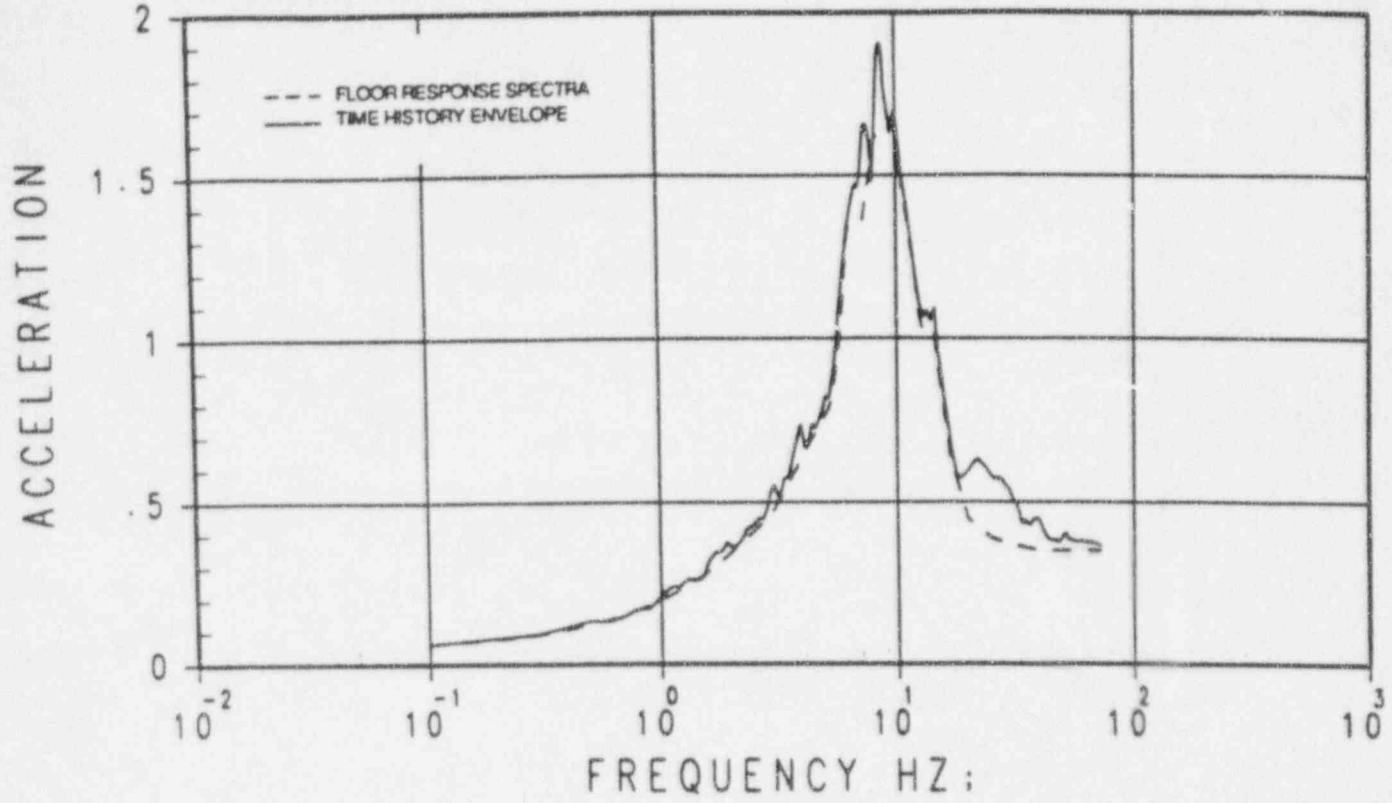

FIGURE 4-4

ACCELERATION TIME HISTORY

NORTH-SOUTH SSE

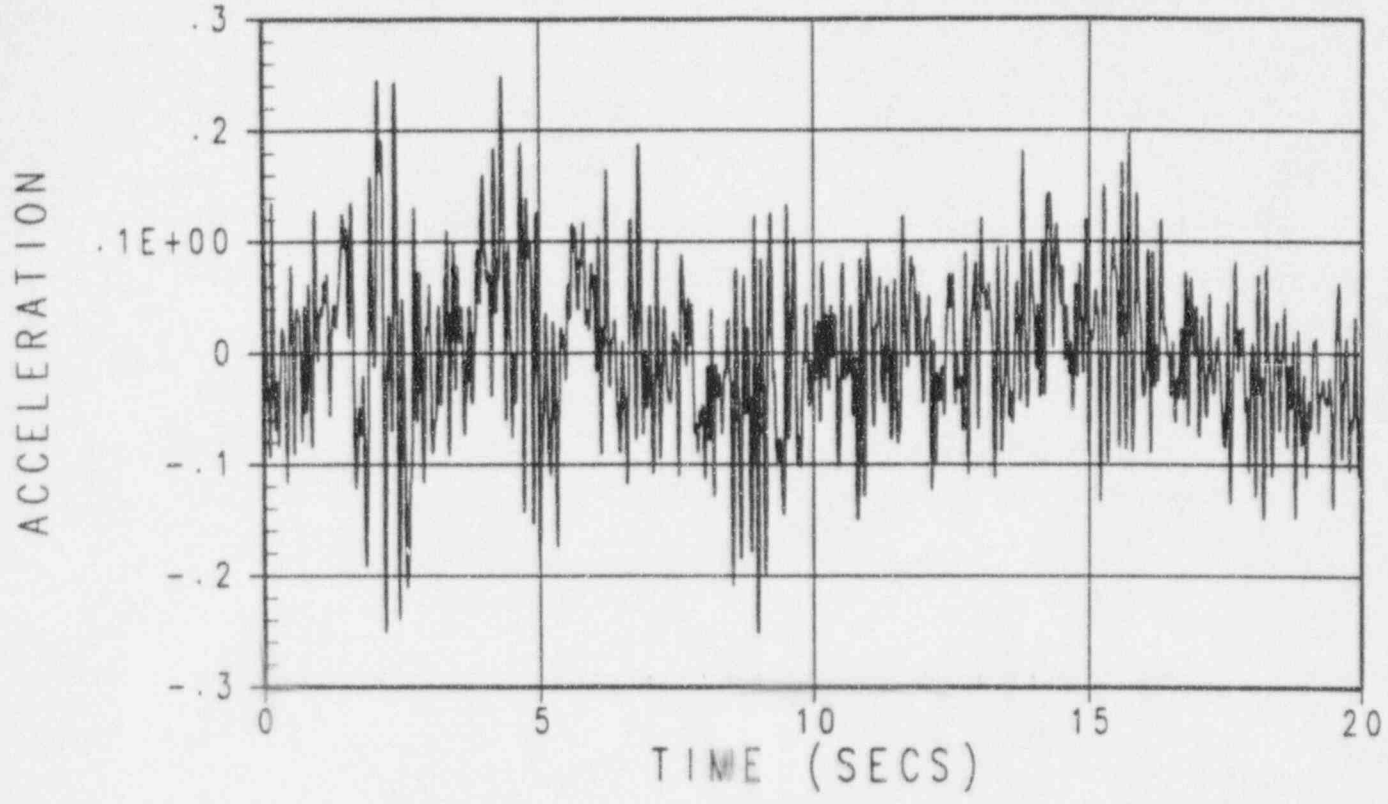

FIGURE 4-5

ACCELERATION TIME HISTORY

EAST-WEST SSE

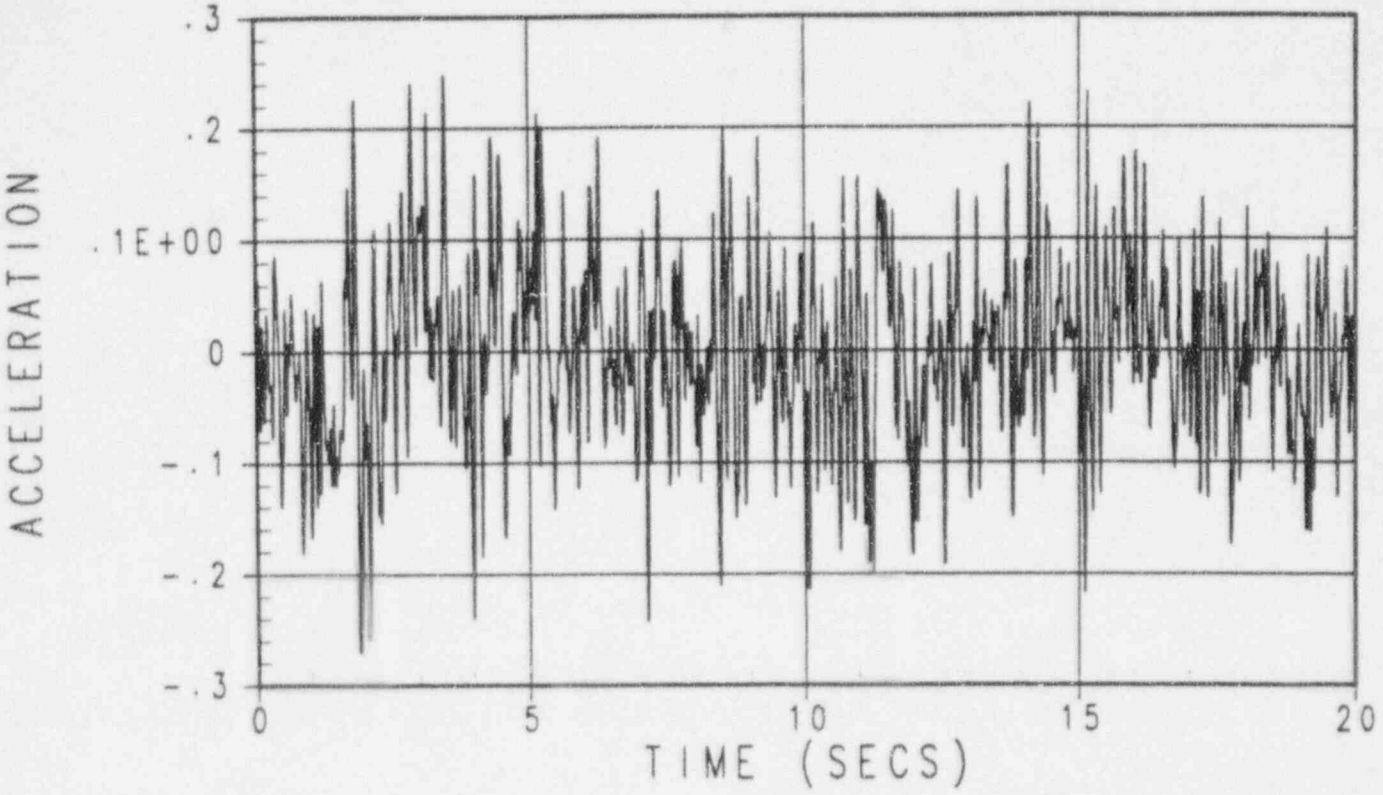

FIGURE 4-6

ACCELERATION TIME HISTORY

VERTICAL SSE

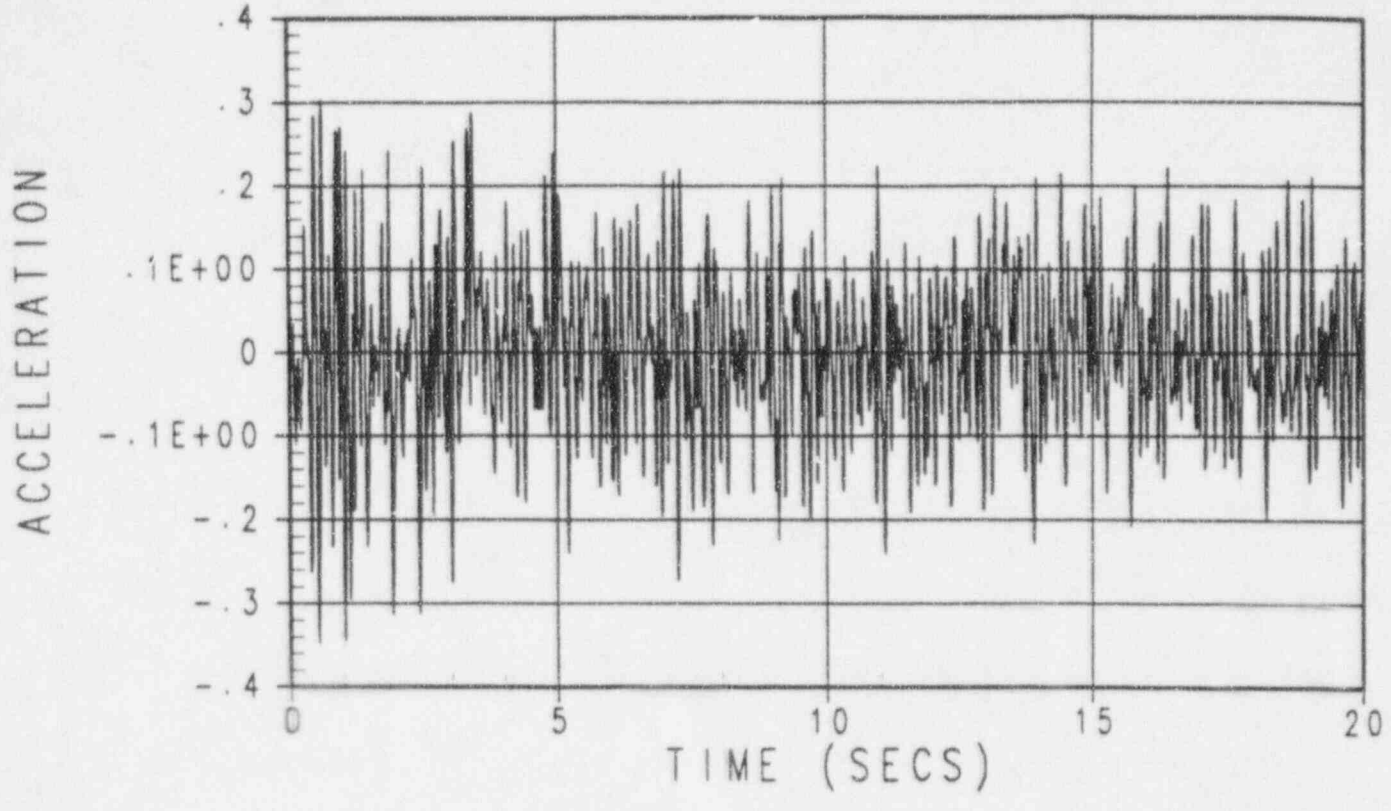

FIGURE 4-7

STRUCTURAL MODEL

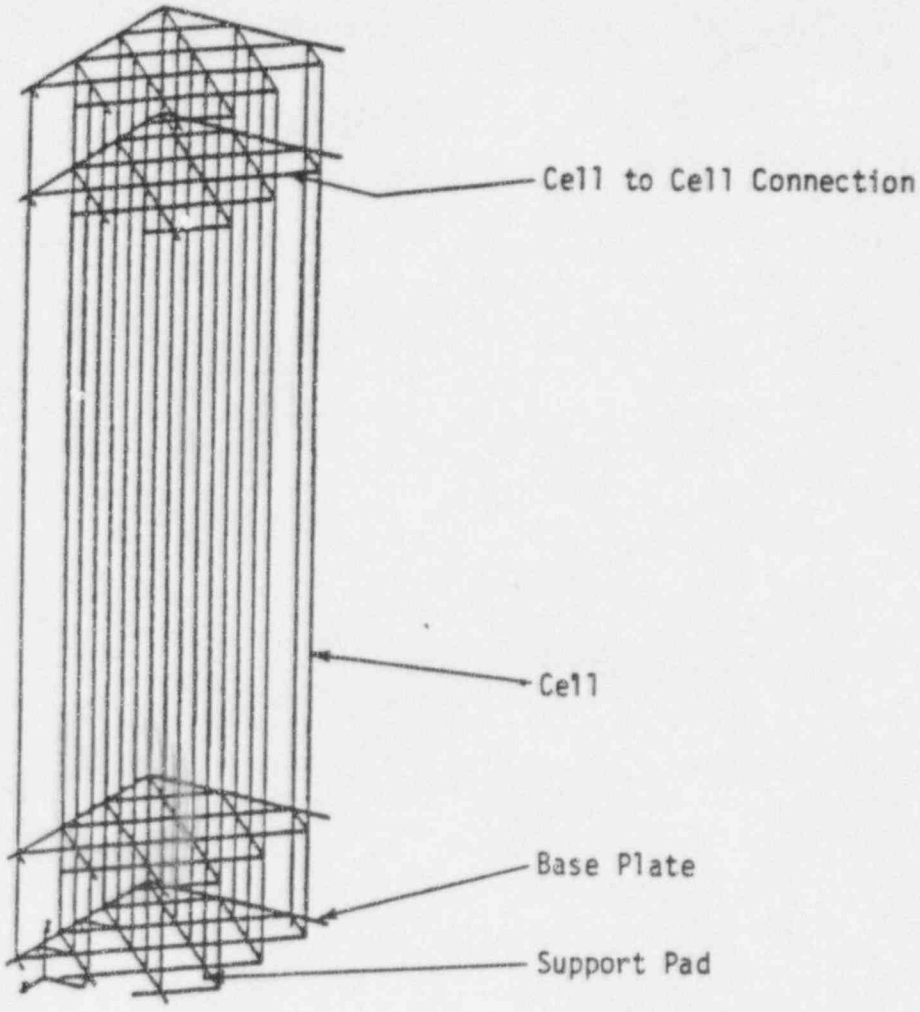

FIGURE 4-8

EFFECTIVE STRUCTURAL MODEL

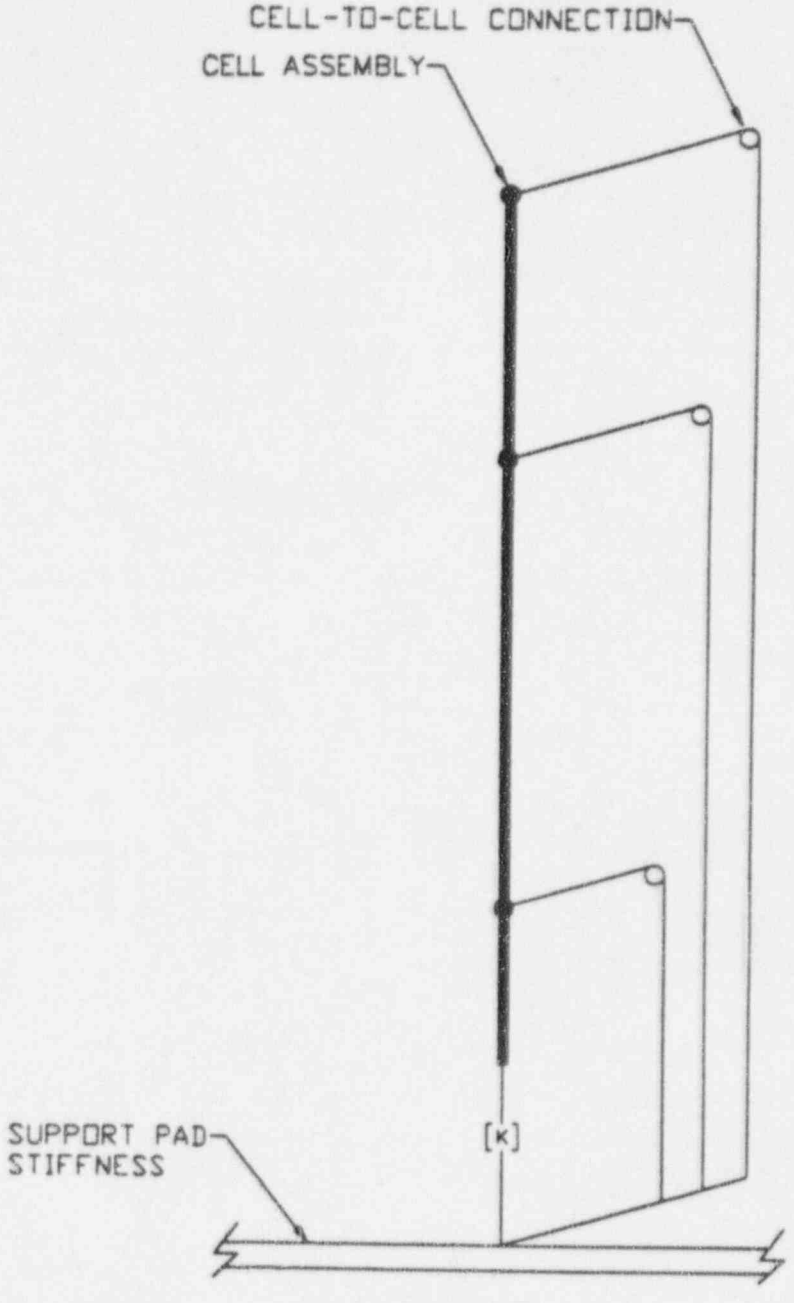

FIGURE 4-9

HIGH DENSITY RACK, 3-D NONLINEAR SEISMIC MODEL

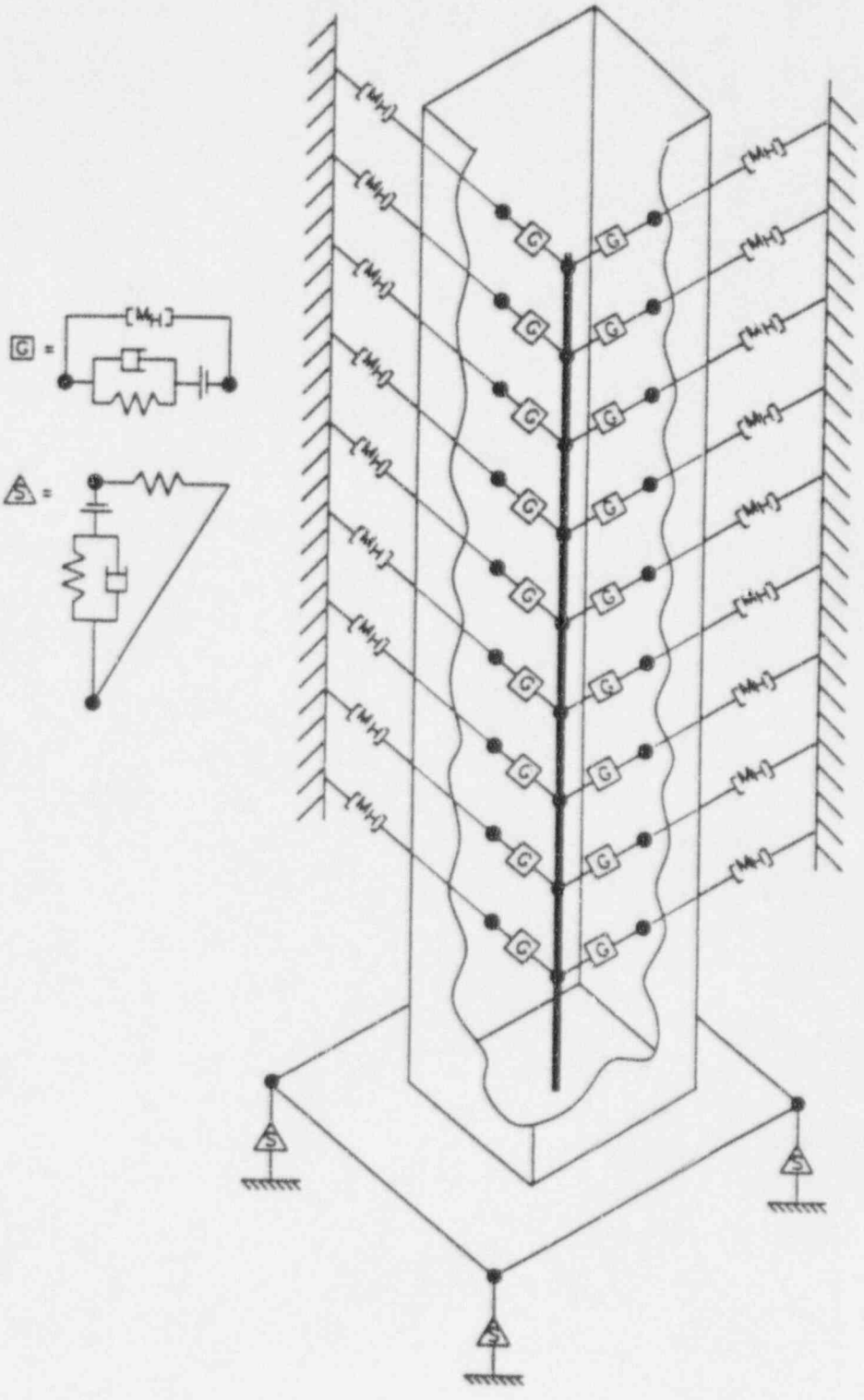

FIGURE 4-10

HIGH DENSITY RACK, NONLINEAR SEISMIC MODEL

(2-D VIEW OF 3-D MODEL)

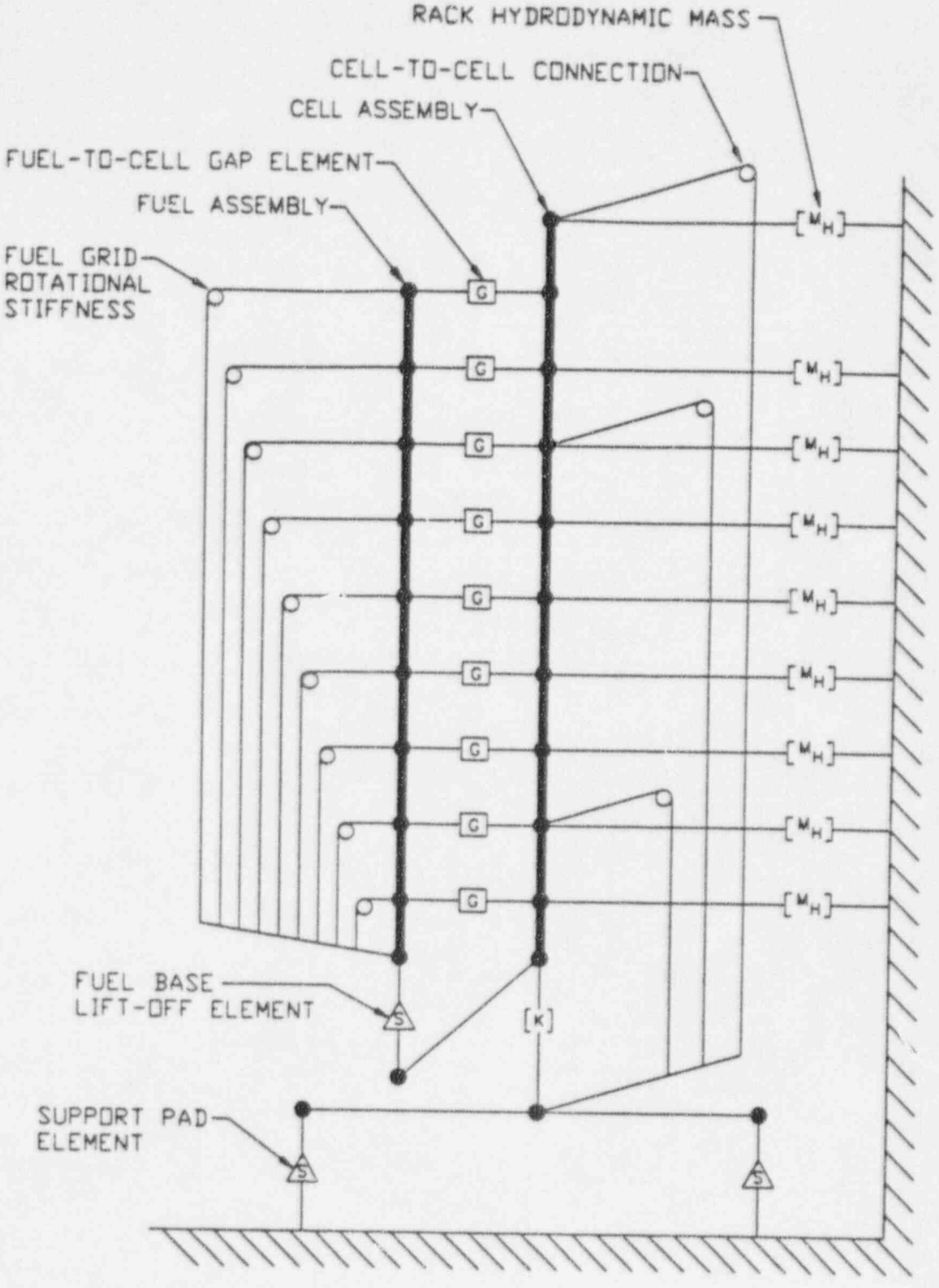

5.0 COST/BENEFIT AND ENVIRONMENTAL ASSESSMENT

5.1 COST/BENEFIT

As demonstrated below, the use of high density racks is the most advantageous means of storing spent fuel, considering the needs of TU Electric customers for a dependable source of electric power.

5.1.1 NEED FOR INCREASED STORAGE CAPACITY

In accordance with Public Law 97-425, Nuclear Waste Policy Act of 1982, TU Electric has a contract with the Department of Energy (DOE) for the disposal of spent fuel. The services to be provided under the contract are for DOE to begin to accept delivery of spent fuel from contract holders no later than January 31, 1998. Subsequently, the scheduled acceptance date by DOE for spent fuel to a repository was postponed until 2003. Furthermore, in 1989 DOE officially estimated that the operation of the repository would not begin until 2010, and the NRC estimates that it may not begin operation until even later.

When DOE does begin to accept delivery of spent fuel from the contract holders, DOE will not be accepting Comanche Peak spent fuel in the first year. Reactors with a longer operating history have priority. It is estimated that once the DOE facility actually begins operations, it will begin taking delivery of the Comanche Peak spent fuel in the tenth year.

TU Electric is seeking to provide additional spent fuel storage capacity for spent fuel assemblies generated at CPSES. Table 5-4 presents expected refueling schedules for both Unit 1 and Unit 2, and the expected number of fuel assemblies that will be transferred into the SFPs at each refueling. No contractual arrangements exist for the interim storage or reprocessing of spent fuel from CPSES.

5.1.2 ESTIMATED COSTS

The total cost for increasing the licensed fuel storage capacity from 1116 to 1291 and the installed capacity from 556 to 1291 fuel assemblies is approximately $6.5 million.

5.1.3 CONSIDERATION OF ALTERNATIVES

TU Electric has considered various alternatives to the proposed on-site spent fuel storage. These alternatives are discussed in the following subsections.

5.1.3.1 SHIPMENT OF FUEL TO A REPROCESSING DISPOSAL FACILITY

No commercial spent fuel reprocessing facilities are presently operating in the United States. While commercial reprocessing is available in Europe, the reprocessing of CPSES spent fuel is impractical for two reasons. First, the use of mixed oxide fuels that result from reprocessing is not authorized in the United States, and no market exists for the use or sale of mixed oxide fuel. And second, CPSES does not have a license to store the high level radioactive waste, which the reprocessor would return with recycled fuel materials. The DOE facility for spent fuel disposal is not currently scheduled to be providing spent nuclear fuel and other high level nuclear waste disposal services until 2010 and additional delays beyond 2010 are likely. With the assumptions shown in Table 5-4, the maximum storage based on the existing installed capacity will be exceeded in 1996. Spent fuel acceptance and disposal by the DOE is not, therefore, a viable alternative to increased on-site pool storage capacity.

5.1.3.2 SHIPMENT OF FUEL TO ANOTHER SITE

Shipment of CPSES spent fuel to another site, if authorized, could provide short-term relief to the storage capacity problem. However, transshipment of spent fuel merely serves to transfer the problem to another site and does not result in any additional net long-term storage capacity. Further, any such transshipment would have to be inter-company (i.e., to a nuclear station operated by a utility other than TU Electric since CPSES is the only nuclear power station within the TU Electric system). Due to logistics, scheduling, cost, available storage capacity, and licensing problems, it is doubtful that another company would accept responsibility for spent fuel from CPSES.

Accordingly, transshipment of spent fuel to another site is not a viable alternative to high density spent fuel storage at CPSES. Furthermore, shipment to another site could result in greater environmental impacts to society as a whole, due to the radiological impacts (though relatively insignificant) of fuel movement and shipment.

5.1.3.3 DEVELOPMENT OF ONSITE INDEPENDENT STORAGE FACILITY

Development of an independent dry fuel storage facility was deemed undesirable since the cost per stored assembly is higher than the costs associated with installing high density racks. It is more economical to install high density racks at this time than pursue alternate storage techniques. Additionally, the environmental impacts associated with construction and operation of an independent storage facility are similar to or potentially greater than those associated with the expansion of the capacity of the SFPs.

5.1.3.4 CEASING OPERATION AFTER THE CURRENT SPENT FUEL STORAGE CAPACITY IS EXHAUSTED

If CPSES is not operated after the current spent fuel storage is exhausted, it will be necessary to generate electric energy with alternative generating capacity. As discussed in the CPSES Environmental Report Volume 1, Section 1, such alternative means of generation would not present environmental advantages and/or would have greater cost.

The prospective expenditure of approximately $6.5 million for the installation of high density racks in SFP2 is small, even when compared to the estimated incremental cost of replacement power for one year of a single unit's energy output. The total estimate for incremental fuel and capacity costs is $235 million for one year for each unit. Based on these facts, not operating the plant or shutting down the plant after exhaustion of spent fuel discharge capacity is not a viable alternative to high density storage in the SFP.

5.1.4 RESOURCES COMMITTED

High density rack installation and use in the SFPs will not result in any irreversible and/or irretrievable commitments of water, land, or air resources since the expansion will not result in any increase in gaseous or water effluents and will not require the use of significant amounts of additional water. The land area now used for the SFPs will be utilized more efficiently by safely increasing the density of spent fuel storage.

The materials used for new rack fabrication are discussed in Section 4.1.3. The required primary resources for rack fabrication are estimated as follows:

- Stainless steel - 200,000 lbs

These expenditures are insignificant with respect to the availability of stainless steel in the United States and will not foreclose alternative uses of these resources.

5.1.5 THERMAL IMPACT ON ENVIRONMENT

The heat rejection to the environment from operation of CPSES is approximately 2280 MWt or 7800 X 10^6 BTU/hr per unit. Therefore, the current heat rejection is on the order of 15,600 X 10^6 BTU/hr. In contrast, assuming storage of 3386 assemblies, the maximum coincident spent fuel heat load is only 17 X 10^6 BTU/hr, which is insignificant in comparison. Furthermore, the addition of 175 cells (1291-1116) to the spent fuel storage capacity adds less than 1 X 10^6 BTU/hr to the total heat rejected to the environment from spent fuel storage at CPSES. Therefore, the stored spent fuel assemblies will have an insignificant incremental impact on the environment.

5.2 RADIOLOGICAL EVALUATION

Installation of high density racks at CPSES will increase the storage capacity of the SFPs. The radiological consequences have been evaluated with the objective of determining if there is significant on-site or off-site incremental impact relative to previous evaluations. In addition, radiological impact to operating personnel has been evaluated to ensure exposure remains as low as reasonably achievable (ALARA).

5.2.1 SOLID RADIOACTIVE WASTE

The volume of solid radioactive waste generated by operation of the spent fuel pool clean up system is dependent upon general system cleanliness and the rate of core component replacement. Solid radioactive waste volume is not affected by the capacity of the spent fuel storage racks. The frequency of refueling is determined by operational considerations and fuel design. In general, system cleanliness and frequency of core component replacement are both governed by plant operations, component design, and materials of construction, not by the amount of stored assemblies. Operational experience demonstrates that required replacement of SFP clean-up demineralizer resins and filters and fuel building ventilation system high-efficiency particulate air (HEPA) filters and charcoal beds results primarily from buildup of non-radioactive impurities such as dust, dirt, airborne debris, resin fines, etc. These components are rarely replaced as a result of radiological considerations. Table 5-1 shows the amount of filter media used from 1991 to September 1994.

No significant increase in the volume of solid radioactive waste is expected due to the increased storage capacity of the new racks. Increases in the amount of spent resin from the SFP cleanup system from the new racks will be negligible.

TABLE 5-1

FILTER MEDIA USAGE

(Units in ft^3)

	1991	1992	1993	1994
Resin	67	0	0	0
Filters	1.77	5.31	1.77	3.54
Charcoal	not tracked	not tracked	915	219

5.2.2 GASEOUS EFFLUENT

Gaseous radioactive effluents are produced by the evaporation of SFP water and by leakage from defective spent fuel assemblies. Evaporation of SFP water will not increase significantly as a result of the increase in storage capacity. Aged spent fuel associated with the expanded capacity contains insignificant amounts of radioiodines and short-lived gaseous fission products because most noble gas and radioiodine activity will significantly decrease within a few weeks after shutdown due to radioactive decay. The exception is Krypton-85 (Kr-85) which has a half-life of 10.72 years. However, the expanded capacity of the SFPs should not result in any significant increase in the amount of Kr-85 released to the environment. Leakage from fuel assemblies occurs due to fuel failure which, in general, occurs as a result of operation, not as a result of storage. Because leakage from fuel failure occurs over a relatively short period of time, long-term storage is not expected to result in significant increases in leakage. Therefore, storage of additional aged fuel should not result in significant increases in releases of Kr-85. This conclusion is supported by existing CPSES data on Kr-85 releases. Since CPSES does not have a fuel building ventilation effluent release point, any Kr-85 effluent will be released through the common plant ventilation system. Kr-85 has never been detected during routine continuous effluent release from the common plant ventilation system for the period of 1992 through September 1994. This has been previously documented in the CPSES Radioactive Effluent Release Reports. Although the number of assemblies stored during this period has increased, there has been no detectable Kr-85 released. This data supports the conclusion that expanded storage will not significantly increase the quantity of gaseous radioactive effluent.

5.2.3 PERSONNEL EXPOSURE

5.2.3.1 EXPOSURE OVER THE LIFE OF THE PLANT

Radiological impact to operating personnel has been evaluated to ensure exposure remains ALARA. Personnel exposure over the life of the plant is a function of the normal operational source term. The source term in this case refers to radioactivity that is accessible and available for release. As discussed in Section 3.2.6, increased spent fuel storage will not have a significant effect on the radiological source term.

External exposure is primarily a function of water-borne activity and is essentially independent of the number of stored fuel assemblies. The stored fuel assemblies are covered by at least twenty-three feet of water for normal storage and ten (10) feet of water for spent fuel movement. This situation affords more than adequate shielding to individuals who may be in the vicinity of the SFP. Therefore, there will not be a significant increase in personnel exposure.

Table 5-2 shows typical gamma radionuclide analyses of the SFP water during normal storage conditions and during spent fuel movement.

TABLE 5-2

TYPICAL RADIONUCLIDE CONSTITUENTS OF SFP WATER

(Units in microcuries/milliliter)

	SFP1 ACTIVITY
Sample Date	10/5/94
Radionuclide ▼	
CR-51	**
MN-54	2.44E-06
CO-57	2.41E-06
CO-58	5.41E-05
CO-60	8.48E-04
FE-59	**
ZN-65	**
ZR-95	**
NB-95	**
AG-110M	**
SB-124	**
SB-125	9.09E-06
CS-134	1.18E-05
CS-137	1.52E-05

**denotes < Minimum Detectable Activity (MDA)

Since the SFP water activity will not change significantly due to increased spent fuel storage, the increase in exposure rate will be minimal. Accordingly, current survey data from the SFP area should reflect the anticipated dose rates with the proposed increased spent fuel storage capacity. These dose rates are shown in Table 5-3.

TABLE 5-3

SFP AREA DOSE RATE

(Units in mrem/hour)

Edge of SFP1	Over water on bridge	General Area
2	3	<1

Due to the insignificant increase in radiological source term, there will be no noticeable increase in internal exposure from the airborne radionuclides in the vicinity of the SFP or at the site boundary.

The primary reason for replacement of demineralizer resins and filters is due to build-up of non-radioactive impurities which are largely independent of the number of stored assemblies. Therefore, the increase in the annual person-rem burden will be negligible.

The SFP clean-up system has an installed skimmer designed to recirculate and clean the surface water. The turnover rate is currently sufficient to preclude the build-up of crud on the sides of the pool. As discussed in Section 3.2.6, the increased storage capacity of the SFPs will not affect the filtration capacity of the SFP clean up system. The expansion in storage capacity will produce an insignificant increase in water-borne activity and therefore will result in a negligible buildup of crud along the sides of the pool.

In summary, the SFP radiological source term is a function of fuel handling activities. The concentration of radioactive materials and other impurities in the SFP water reaches a maximum during refueling activities as a result of initial fuel movement after shut-down. It is not affected by the number of assemblies being stored. Airborne radioactivity levels in the fuel building are highest during initial fuel movement after shut-down because most gaseous fission products are relatively short-lived and tend to escape from any defective fuel soon after shutdown. Aged spent fuel releases relatively insignificant quantities of gaseous fission products. Since increases in water and air activity will be negligible as a result of the expanded storage capacity, the increase in the total effective dose equivalent (TEDE) in the areas of the SFPs is insignificant.

The original CPSES licensing review considered radiological consequences resulting from 40 years of operation for both units. The additional fuel storage capacity contributes little to the concentration of radionuclides in either the SFP water or fuel building atmosphere. Therefore, increasing the storage capacity for aged spent fuel will not significantly influence the radiological source term and resulting radiation doses.

5.2.3.2 EXPOSURE DURING HIGH DENSITY RACK INSTALLATION

All work in the Radiologically Controlled Area will be performed in accordance with station procedures for radiation work control. Work will be controlled and guided by a specific Radiation Work Permit and by appropriate ALARA planning as determined by the requirements of station procedures. The new racks will be installed in a pool that is dry and has never contained any spent fuel. Therefore, installation activities will result in insignificant personnel exposure.

5.2.4 RACK DISPOSAL

There are no racks installed in SFP2. Therefore, there will be no rack disposal.

5.3 ACCIDENT EVALUATION

5.3.1 SPENT FUEL HANDLING ACCIDENTS

In Section 3.1 the criticality concerns of accidents were evaluated. Section 3.1 demonstrates that an accident will not result in a k_{eff} which exceeds 0.95, including uncertainties.

A previous evaluation of the radiological impact from a dropped fuel assembly is discussed in the CPSES FSAR, Section 15.7.5 [Ref. 3]. Only the dropped assembly is damaged, so there is no change in the existing FSAR accident evaluation from the new racks. The proposed rack modifications will not increase the radiological consequences of a fuel handling accident.

5.3.2 LOSS OF SPENT FUEL POOL COOLING

Section 3.2.3 describes the effect of loss of cooling. In the event of a loss of cooling event, CPSES would have sufficient time before the onset of pool boiling to start the makeup system and to restore forced cooling with at least one train of safety related cooling. Even without forced cooling, the makeup system can provide a sufficient rate of water to the SFPs to maintain the pool levels and therefore to maintain the spent fuel assemblies in a cooled and safe condition.

5.3.3 HANDLING OF HIGH DENSITY RACKS

The rack handling crane which will be installed in the Fuel Building during rack installation is the only crane capable of lifting heavy loads over spent fuel. It will not be necessary for the rack handling crane to pass over SFP1 to complete the rack installation. Furthermore, mechanical stops will be provided ch will prevent the rack handling crane from travelling over SFP1 or the new fuel storage vault. Because of the installation approach, the use of a safety related and single-failure-proof rack handling crane, and the safe load restrictions, the radiological consequences of a rack drop need not be evaluated.

TABLE 5-4

PROJECTED SPENT FUEL DISCHARGE

Year/Unit	Discharged Assemblies	Total Discharged Assemblies Following Refueling	Remaining Storage Capability
1991 U1	56	56	500
1992 U1	61	117	439
1993 U1	88	205	351
1994 U2	88	293	263
1995 U1	96	389	167
1996 U2	96	485	* 806
U1	92	577	714
1997 U2	92	669	622
1998 U1	96	765	526
1999 U2	96	861	430
U1	92	953	338
2000 U2	92	1045	246
2001 U1	96	1141	150
2002 U2	96	1237	**

* Use of high density racks in SFP2.

** SFP capacity exceeded if provision for full core offload is maintained. Additional storage capacity required.

6.0 REFERENCES

1. Comanche Peak Steam Electric Station Unit 1 Facility Operating License NPF-87, Docket No. 50-445.

2. Comanche Peak Steam Electric Station Unit 2 Facility Operating License NPF-89, Docket No. 50-446.

3. Comanche Peak Steam Electric Station Final Safety Analysis Report, Docket No.s 50-445 and 50-446.

4. American Society of Mechanical Engineering Boiler and Pressure Vessel (ASME Boiler and Pressure Vessel) Code:

   Section III, Division 1, Subsection NF, 1980, Summer 1982 Addenda

5. Nuclear Regulatory Commission, Letter to All Power Reactor Licensees, from B. K. Grimes, April 14, 1978, "OT Position for Review and Acceptance of Spent Fuel Storage and Handling Applications," as amended by the NRC letter dated January 18, 1979.

6. USNRC Regulatory Guides:

RG 1.13	Spent Fuel Storage Facility Design Basis, Rev.1, 1975
RG 1.29	Seismic Design Classifications, Rev.2, 1976
RG 1.44	Control of the Use of Sensitized Stainless Steel, Rev.0, 1973
RG 1.60	Design Response Spectra for Seismic Design of Nuclear Power Plants, Rev.1, 1973
RG 1.61	Damping Values for Seismic Design of Nuclear Power Plants, Rev.0, 1973
RG 1.92	Combining Modal Responses and Spatial Components in Seismic Response Analysis, Rev. 1, 1976

RG 1.124 Service Limits and Loading Combinations for Class I Linear-Type Component Supports, Rev.1, 1978

7. ANSI/ANS 57.2-1983, Design Requirements for Light Water Reactor Spent Fuel Storage Facilities at Nuclear Power Plants

8. NUREG-800, Standard review Plan:

SRP 3.7 Seismic Design (Rev. 1)
SRP 3.8.4 Other Category I Structures (Rev. 1)
SRP 9.1.2 Spent Fuel Storage (Rev. 3)
SRP 9.1.3 Spent Fuel Pool Cooling and Cleanup System (Rev. 1)
NRC Branch Technical Position ASB 9-2, Residual Decay Energy for Light Water Reactors for Long Term Cooling.(Rev.2)

9. ANSI/ANS 8.1-1983, Nuclear Criticality Safety in Operations with Fissionable Materials Outside Reactors.

10. N. M. Greene, NITAWL-II: SCALE System Module for Performing Resonance Shielding and Working Library Production, NUREG/CR-0200, Vol. 2, Section F2, June 1989.

11. L. M. Petrie and N. F. Landers, KENO Va--An Improved Monte Carlo Criticality Program With Supergrouping, NUREG/CR-0200, Vol. 2, Section F11, November 1993.

12. W. E. Ford III, CSRL-V: Processed ENDF/B-V 227-Neutron-Group and Pointwise Cross-Section Libraries for Criticality Safety, Reactor and Shielding Studies, ORNL/CSD/TM-160, June 1982.

13. Strawbridge, L. E. and Barry R. F., "Criticality Calculations for Uniform Water-Moderated Lattices," Nucl. Sci. & Eng. 23, pp 58-73, 1965.

14. Baldwin, M. N., and Stern, M. E., "Physics Verification Program Part III, Task 4: Summary Report," BAW-3647-20, March 1971.

15. Baldwin, M. N., "Physics Verification Program Part III, Task 11: Quarterly Technical Report January-March, 1974," BAW-3647-30, July 1974.

16. Baldwin, M. N., "Physics Verification Program Part III, Task 11: Quarterly Technical Report July-September 1974," BAW-3647-31, February 1975.

17. M. N. Baldwin, Critical Experiments Supporting Close Proximity Water Storage of Power Reactor Fuel, BAW-1484-7, July 1979.

18. S. R. Bierman and E. D. Clayton, Criticality Separation Between Subcritical Clusters of 2.35 w/o 235U Enriched UO2 Rods in Water with Fixed Neutron Poisons, PNL-2438, October 1977.

19. S. R. Bierman and E. D. Clayton, Criticality Separation Between Subcritical Clusters of 4.29 w/o 235U Enriched UO2 Rods in Water with Fixed Neutron Poisons, PNL-2615, August 1979.

20. S. R. Bierman and E. D. Clayton, Criticality Experiments with Subcritical Clusters of 2.35 w/o and 4.31 w/o 235U Enriched UO2 Rods in Water at a Water-to-Fuel Volume Ratio of 1.6, PNL-3314, July 1980.

21. ANSI N18.2-1973, "Nuclear Safety Criteria for the Design of Stationary Pressurized Water Reactor Plants".

22. Melehan, J. B., Yankee Core Evaluation Program Final Report, WCAP-3017-6094, January 1971.

23. Nguyen, T. Q. et. al., Qualification of the PHOENIX-P/ANC Nuclear Design System for Pressurized Water Reactor Cores, WCAP-11597-A, June 1988.

24. England, T. R., CINDER - A One-Point Depletion and Fission Product Program, WAPD-TM-334, August 1962.

25. American Concrete Institute, ACI 318-71, "Building Code Requirements for Reinforced Concrete."

26. American Concrete Institute, ACI 349-76, "Code Requirements for Nuclear Safety Related Concrete Structures", Appendix A, "Thermal Considerations."

27. ANSI N210-1976 (ANS-57.2), Design Objectives for Light Water Reactor Spent Fuel Storage Facilities at Nuclear Power Stations

28. NUREG 75/087, Standard Review Plan
BTP APCSB 9.5-1, Appendix A, August 23,1976

29. NUREG-0612, "Control of Heavy Loads at Nuclear Power Plants"

30. ASME B30.2-1990, "Overhead and Gantry Cranes"

31. AISC Specification for the Design, Fabrication, and Erection of Structural Steel for Buildings (1969) including Supplements 1, 2 & 3).

32. ANSI N16.1-1975, "Nuclear Criticality Safety in Operations with Fissionable Materials Outside Reactors."

33. PVRC Research Committee on Piping Systems, Pressure Vessel Research Committee, Progress Report on Damping Values, 1985 (incorporated into ASME P&V Code, Code Case N-411, Rev. 1).

34. D. E. Mueller, W. A. Boyd, and M. W. Fecteau (Westinghouse NFD), Qua. ation of KENO Calculations with ENDF/B-V Cross Sections, American Nuclear Society Transactions, Volume 56, pages 321-323, June 1988.

35. WECAN - "Documentation of Selected Westinghouse Structural Analysis Computer Codes," WCAP-8252.

36. WECAN - "Benchmark Problem Solution Employed for Verification of the WECAN Computer Program," WCAP-8929.

37. D. F. DeSanto, "Added Mass and Hydrodynamic Damping of Perforated Plates Vibrating in Water", ASME Journal of Pressure Vessel Technology, May 1981.

38. R. J. Fritz, "The Effects of Liquids on the Dynamic Motions of Immersed Solids," Journal of Engineering for Industry, Trans. of the ASME, February 1972, pp 167-172.

39. USNRC Regulatory Guide 1.61, "Damping Values for Seismic Design of Nuclear Power Plants," Rev. 1, 1973.

40. A. Higdon and W. B. Stiles, "Engineering Mechanics, Vector Edition", Prentice-Hall, Inc., Engelwood Cliffs, N. J., 1962, p.639.

41. "Friction Coefficients of Water Lubricated Stainless Steels for a Spent Fuel Rack Facility", Prof. Ernest Rabinowicz, MIT, a report for Boston Edison Company, 1976.

42. N. M. Greene, XSDRNPM-SI: SCALE System Module for Performing Resonance Shielding and Working Library Production, NUREG/CR-0200, Vol. 2, Section F3, June 1989.

43. D. B. Owen, Factors for One-Sided Tolerance Limits and for Variables Sampling Plans, Sandia Corporation, SCR-607, March 1963.

44. ANSI N16.9-1975, "Validation of Calculational Methods for Nuclear Criticality Safety".